Linköping Studies in Science and Technology.
Dissertations No. 1068

Hydraulic Power Steering System Design in Road Vehicles

Analysis, Testing and Enhanced Functionality

Marcus Rösth

Division of Fluid and Mechanical Engineering Systems
Department of Mechanical Engineering
Linköping University
SE–581 83 Linköping, Sweden

Linköping 2007

Hydraulic Power Steering System Design in Road Vehicles

Analysis, Testing and Enhanced Functionality

Linköping Studies in Science and Technology. Dissertations
No. 1068

Hydraulic Power Steering System Design in Road Vehicles

Analysis, Testing and Enhanced Functionality

Marcus Rösth

INSTITUTE OF TECHNOLOGY
LINKÖPING UNIVERSITY

Division of Fluid and Mechanical Engineering Systems
Department of Mechanical Engineering
Linköping University
SE–581 83 Linköping, Sweden

Linköping 2007

ISBN 978-91-85643-00-4 ISSN 0345-7524

Department of Mechanical Engineering
Linköping University
SE-581 83 Linköping, Sweden

Printed in Sweden by LTAB Linköpings Tryckeri AB, 2007.445

To my wife

Jennifer

Mängden tror att allt svårfattligt är djupsinnigt, men så är det icke. Det svårfattliga är det ofullgångna, oklara, och ofta det falska. Den högsta visdomen är enkel, klar, och går rakt genom skallen i hjärtat.

August Strindberg, 1908, "En ny blå bok"

Abstract

Demands for including more functions such as haptic guiding in power steering systems in road vehicles have increased with requirements on new active safety and comfort systems. Active safety systems, which have been proven to have a positive effect on overall vehicle safety, refer to systems that give the driver assistance in more and less critical situations to avoid accidents. Active safety features are going to play an increasingly important roll in future safety strategies; therefore, it is essential that sub systems in road vehicles, such as power steering systems, are adjusted to meet new demands.

The traditional Hydraulic Power Assisted Steering, HPAS, system, cannot meet these new demands, due to the control unit's pure hydro-mechanical solution. The Active Pinion concept presented in this thesis is a novel concept for controlling the steering wheel torque in future active safety and comfort applications. The concept, which can be seen as a modular add-on added to a traditional HPAS system, introduces an additional degree of freedom to the control unit. Different control modes used to meet the demands of new functionality applications are presented and tested in a hardware-in-the-loop test rig.

This thesis also covers various aspects of hydraulic power assisted steering systems in road vehicles. Power steering is viewed as a dynamic system and is investigated with linear and non-linear modeling techniques. The valve design in terms of area gradient is essential for the function of the HPAS system; therefore, a method involving optimization has been developed to determine the valve characteristic. The method uses static measurements as a base for calculation and optimization; the results are used in both linear and the non-linear models. With the help of the linear model, relevant transfer functions and the underlying control structure of the power steering system have been derived and analyzed. The non-linear model has been used in concept validation of the Active Pinion. Apart from concept validation and controller design of the active pinion, the models have been proven effective to explain dynamic phenomena related to HPAS systems, such as the chattering phenomena and hydraulic lag.

Acknowledgements

The work presented in this thesis has been carried out at the Division of Fluid and Mechanical Engineering Systems at Linköping University and has been financed by ProViking and Volvo Car Corporation. There are a great number of people that I would like to mention. First of all, I would like to thank my supervisor and head of the division, Prof. Jan-Ove Palmberg, for his support and outstanding ability to come up with new ideas. I would also like to give special thanks to my industrial supervisor and co-author of the three appended papers Dr. Jochen Pohl, Volvo Car Corporation, for inspiring discussions and optimism. I do not want to forget Prof. Karl-Erik Rydberg, who is always available for short intensive discussions, which are of great importance.

Many thanks to all members and former members of the Division of Fluid and Mechanical Engineering Systems for more and less serious discussions in between work, which are an important part of the research process called brainstorming. I owe many thanks to Anders Zachrison for his invaluable help throughout the research process. Many other people have also been involved in research not necessarily presented in this thesis: Pär Degerman, Andreas Johansson, Ronnie Werndin, Johan Ölvander, Andreas Renberg, Cristian Dumbrava and Sten Ragnhult.

I would also like to mention the technical staff at the Department of Mechanical Engineering and thank them for invaluable help with the prototype design and the manufacturing of the Active Pinion and Power Steering Test Rig; a special thanks to Ulf Bengtsson, Thorvald "Tosse" Thoor and Magnus "Mankan" Widholm.

Finally, I would like to thank my wife Jennifer, who has held my hand throughout the entire process and put up with my on occasion absent-mindedness, and my family, Leif, Siv and Kristina, for their great support during the years.

Linköping in December, 2006

Marcus Rösth

Papers

The following six papers are appended and will be referred to by their Roman numerals. All papers are printed in their originally published state with the exception of minor errata and changes in text and figure layout.

In papers [II, IV, V], the first author is the main author, responsible for the work presented, with additional support from other co-authors. In paper [III, VI], the work is equally divided between the first two authors, with additional support from other co-authors. Paper [I] is submitted for publication at the 10th Scandinavian International Conference on Fluid Power, SICFP'07, in the Tampere, Finland.

[I] Rösth M. and Palmberg J-O., "Robust Design of a Power Steering Systems with Emphasis on Chattering Phenomena" Submitted and accepted to *The 10th Scandinavian International Conference on Fluid Power, SICFP'07,* Tampere, Finland, 21th–23th May, 2007.

[II] Rösth M. and Palmberg J-O., "Modeling and Validation of Power Steering System With Emphasis on Catch-Up Effect," in Proc. of *The 9th Scandinavian International Conference on Fluid Power, SICFP'05,* (Eds. J-O Palmberg), CD publication, Linköping University (LIU) Print, Linköping, Sweden, 1st–3rd June, 2005.

[III] Rösth M., Pohl J. and Palmberg J-O., "Modeling and Simulation of a Conventional Hydraulic Power Steering System for Passenger Cars," in Proc. of *The 8th Scandinavian International Conference on Fluid Power, SICFP'03,* (Eds. K.T. Koskinen and M. Vilenius), pp. 635–650, vol. 1, Tampere University of Technology (TUT) Print, Tampere, Finland, 7th–9th May, 2003.

[IV] Rösth M., Pohl J. and Palmberg J-O., "Active Pinion - A Cost Effective Solution for Enabling Steering Intervention in Road Vehicles," Submitted and accepted to *The Bath Workshop on Power Transmission & Motion Control, PTMC'03*, Bath, United Kingdom, 10th-12th September, 2003.

[V] Rösth M., Pohl J. and Palmberg J-O., "Increased Hydraulic Power Assisted Steering Functionality Using the Active Pinion Concept," in Proc. of *5th International Fluid Power Conference Aachen, IFK2006*, Aachen, Germany, 20th-22nd March, 2006.

[VI] Rösth M., Pohl J. and Palmberg J-O., "Parking System Demands on the Steering Actuator," in Proc. of *ASME 2006 International Design Engineering Technical Conferences & Computers and Information in Engineering Conference, ESDA 2006*, Torino, Italy, 4th-7th July, 2006.

Papers not included

The following papers are not included in the thesis but constitute an important part of the background. Paper [X] is a working paper.

[VII] Degerman P., Rösth M. and Palmberg J-O., "A Full Four-Quadrant Hydraulic Steering Actuator Applied to a Fully Automatic Passenger Vehicle Parking System," in Proc. of *Fluid Power Net International - PhD Symposium , 4th FPNI-PhD 2006*, CD-Publication, Sarasota, FL, USA, 13th-17th July, 2006.

[VIII] Zachrison A., Rösth M., Andersson A. and Werndin R., "Evolve – A Vehicle-Based Test Platform for Active Rear Axle Camber and Steering Control" in Journal of *SAE TRANSACTIONS*, pp 690–695, vol. 112, part 6, USA, 2003.

[IX] Rösth M., Pohl J. and Palmberg J-O., "Linear Analysis of a Conventional Power Steering System for Passenger Cars," in Proc. of *The 5th JFPS International Symposium on Fluid Power,* (Eds. S. Yokota), pp. 495–500, vol. 2, Nara, Japan, 12th–15th November, 2002.

[X] Rösth M., Pohl J. and Palmberg J-O., "A Modular Approach to Steering Actuator Design in Road Vehicles – Implementation stages with respect to associated customer functions," working paper, intended for submission to Journal of *Automobile Engineering, IMechE.*

Contents

Appended papers

Nomenclature

α_{AP}	Actuation valve angle generated by the pilot motor	$[rad]$
α_v	Angular displacement of the valve	$[rad]$
β_e	Bulk modulus	$[Pa]$
δ	Steering wheel angle	$[rad]$
δ_{opt}	Optimal steering angle in the LKA system	$[rad]$
$\dot{x}_{p0}$	Break speed for the column friction	$[m/s]$
γ	Angle of the bevel in the valve	$[rad]$
ρ	Oil density	$[kg/m^3]$
τ	Exponential constant for the column friction	$[-]$
A	Connection to cylinder chamber A	
$A[\pm T_{sw}]$	Valve area opening	$[m^2]$
$A_{1,2}$	Area openings within the valve	$[m^2]$
$A_{1,2}$	Valve area opening	$[mm^2]$
A_p	Cylinder area	$[m^2]$
b	Width of the valve bevel on the spool	$[m]$
B	Connection to cylinder chamber B	
b_1	Total width of grove in valve body	$[m]$
b_2	Total width of land on the spool	$[m]$
B_{sw}	Viscous damping in the steering wheel	$[Ns/m]$
B_w	Lateral viscous damping in the	$[Ns/m]$
C	Hydraulic Capacitance	$[m^5/N]$
c	Stiffness on the torsion bar in the valve	$[Nm/rad]$
c_q	Flow coefficient	$[-]$
D	Disturbance	$[Pa]$
dp_{ECA}	Pressure drop over the ECA	$[Pa]$
dp_{valve}	Pressure drop over the valve	$[Pa]$
F_{assist}	Assisting Force applied on the steering rack	$[N]$
F_{manual}	Manual Force applied on the steering rack	$[N]$
F_{Obj}	Object function in the optimization	
F_{tot}	Total force applied on the steering rack	$[N]$
F_{Weight}	Weight function in the optimization	
F_A	Assisting force ratio	$[-]$

F_j	Pretension of the joke	$[N]$
F_L	Maximal external load	$[N]$
F_L	External load acting on the steering rack	$[N]$
F_M	Manual force ratio	$[-]$
h_0	Clearance between spool and valve body	$[m]$
$K_{0,1,2,3,4}$	Coefficient in the polynomial area function	
K_c	Linearized flow–pressure coefficient	$[m^5/Ns]$
K_p	Pressure gain	$[Pa/mm]$
K_q	Flow gain	$[m^2/s]$
K_t	Equivalent spring coefficient in the torsion bar	$[N/m]$
K_w	Lateral spring coefficients in the tire	$[N/m]$
L	Length of the land in on the spool	$[m]$
m_{sw}	Mass of the steering wheel	$[Kg]$
$m_{w,i}$	Mass of the wheels f–front, r–rear	$[Kg]$
m_b	Mass of the body	$[Kg]$
m_r	Mass of the rack	$[Kg]$
m_s	Mass of the sub-frame	$[Kg]$
P	Connection to supply line	
P_{ECA}	Energy loss in the ECA	$[w]$
$P_{Loffset}$	Change in load pressure to generate T_{offset}	$[Pa]$
P_{LN}	Nominal load pressure, undist. valve characteristic	$[Pa]$
P_{pump}	Energy loss in the pump unit	$[w]$
P_{valve}	Energy loss in the valve unit	$[w]$
p_L	Load pressure	$[Pa]$
p_p	Maximal pump pressure	$[Pa]$
p_s	System pressure, pressure before the valve	$[Pa]$
q	Load flow normalized with system flow	$[-]$
q_{ECA}	Flow consumed during pressurization of the ECA	$[m^3/s]$
q_{leak}	General leakage in the valve unit and the piston	$[m^3/s]$
q_p	Flow delivered by the pump	$[m^3/s]$
q_{shunt}	Flow shunted back to the suction side of the pump	$[m^3/s]$
q_L	Load flow due to motion of the cylinder	$[m^3/s]$
q_S	System flow entering the valve	$[m^3/s]$
R_{valve}	Radius of the spool	$[m]$
r_r	Gear radius of the pinion	$[m]$
T	Connection to tank line	
$T_{assistance}$	Assisting torque generated by the load pressure	$[Nm]$
T_{offset}	Offset torque due to the actuation of the pilot motor	$[Nm]$
T_{sw}	Steering wheel torque	$[Nm]$

T^*_{sw}	Nominal torque, undisturbed valve characteristic	$[Nm]$
T_{tot}	Total torque sum of $T_assistance$ and T_{sw}	$[Nm]$
w	Area gradient	$[m]$
V_0	Total volume in cylinder	$[m^3]$
V_v	System Volume, volume between pump and valve unit	$[m^3]$
X	Parameters optimized in the optimization	
$x_{A_{1,2}}$	Equivalent linear displacement of the valve	$[m]$
x_{AP}	Valve displacement of the valve due to the actuation of the pilot motor	$[rad]$
x_{sw}	Displacement of the steering wheel	$[m]$
x_b	Displacement of the body	$[m]$
x_r	Rack position	$[m]$
x_r	Displacement of the rack	$[m]$
x_v	Linear displacement of the valve	$[m]$
x_w	Displacement of the wheel	$[m]$

1
Introduction

1.1 Background

Safety is a predominant issues today; therefore, a great deal of research concerns safety issues. Safety in cars can be divided into two categories, passive and active safety. Passive safety refers to functions that help mitigate the severity of accidents when such as seat belts, airbag etc. Active safety features refer to functions that assist the driver to avoid an accident such as anti-lock brakes, traction control [1], and active yaw control. Wilfert proposed a definition of passive and active safety where he also suggested a classification [2]. A more resent work concerning active safety was performed by E. Donges, [3], who divides active safety functions and driver assisting functions into four levels, Information, Warning, Vehicle Dynamic Control and Action Recommendation. The effect of active safety functions has been proven successful for overall vehicle safety. A. Tingvall et al. stated that the dynamic yaw control system increases safety up to 38%, especially on winter road conditions [4]. Several other investigations have reached similar conclusions, see for instance [5–8]. The active yaw control system was the first active safety system on the market, where the potential for the systems was visible. New systems are entering the market such as Adaptive Cruise Control, ACC, which is a system that helps the driver in the longitudinal control of the car, thereby keeping a safe distance to the vehicles ahead, [9].

The systems mentioned above use the brakes, the drive-train or a combination of both to enable active safety functions. Power steering systems have not been involved in active safety system with the exception of the newly introduced variable ration power steering system, Active steering, which is described by P. Köhn, [10, 11]. When implemented in the vehicle, the system does not effect active safety but could be used for active yaw control. Research concerning dynamic yaw control utilizing the power steering system has been carried out by J Ackermann et al., [12–14].

Active safety features are going to play a more important roll in future safety strategies; therefore, it is essential that vehicle sub systems are adjusted to meet new demands. Next generation active safety might also involve the steering system in guiding the driver out of a safety critical situation such as Lane Keeping Aid, LKA. LKA systems help the driver keep the lateral position of the vehicle, thereby reducing the risk for road departure accidents; this can be compared to the ACC system, which is a longitudinal control. The LKA system has been investigated by different researchers and with different actuation. Franke et al. enable the system by adding a correction to the driver's input steering, [15]; whereas Pohl and Ekmark added a guiding torque to the steering wheel, thereby enabling a haptic communication with the driver, [16]. The last example can be seen as an action recommendation that guides the driver out of a safety critical situation. There are also other safety functions that can utilize enhanced functionality in the steering system, which will be discussed further in the thesis.

There are a number of feasible concepts to enable steering intervention ranging from additional actuators applying torque to the steering column to Electric Power Assisted Steering, EPAS, systems, [17]. The latter has recently entered the market, mainly in order to meet future requirements on emission and fuel consumption, as the efficiency of traditional hydraulic power assisted steering, HPAS, systems, especially for highway driving, is quite low. However, unless 42V technology is available, the application of EPAS systems will be restricted to smaller and medium sized vehicles, [18]. This thesis concerns hydraulic actuator design in HPAS systems to support and enable active safety functions that demand haptic communication with the driver.

1.2 Limitation

This thesis focuses on enhancing the functionality of a traditional hydraulic power steering unit. In the development of this project, different simulation environments have been developed and used to support the design process regarding performance prediction, controller development and prototype design. These models has also been proven effective to analyze, predict and explain different problems related with the hydraulic power steering, such as the chattering phenomena and hydraulic lag. This thesis describes the design process of power steering systems in a general manner with no intension of develop or contribute to important areas such as energy consumption; noise, vibration, and harshness, NVH, problems or improving handling characteristics. The active safety and comfort functions that are to use the increased functionality of the hydraulic power steering system are described to give a background for the different control strategies and are not a focus in this thesis. In the project, different existing dynamic vehicle models have been used as tools but should not be considered to be a part of the research project.

1.3 Contribution

The main contribution of this thesis is the concept for enhancing functionality in traditional hydraulic power assisted steering systems. This project is a novel approach to enhance the functionality of HPAS systems to meet the demands of future active safety systems. The development of the enhanced power steering unit includes simulation and testing of different control strategies that can be used in both active safety systems and comfort systems. This project has resulted in a new concept called Active Pinion, which is can be seen as a modular add-on to a traditional hydraulic power steering system. The focus of the active pinion concept is to enable a haptic communication with the driver, which can be used for guiding and easing the driver when performing different driving tasks.

In addition to the concept, different controller designs are developed to meet future demands for active safety and comfort systems such as LKA systems and automatic parking systems. Apart from concept validation and controller design of the active pinion, the models have been proven effective to explain dynamic phenomena related to HPAS systems, such as the chattering phenomena and hydraulic lag.

2
Power Steering Systems

2.1 History

Power steering systems are probably the most used servo* system by the common man, even though most users never give it a second thought. The first power steering unit was invented by Francis W. Davis in the mid 1920's [19], but was not introduced in passenger cars until 1951. A figure of the system can be seen in Figure 2.1. This system was of the type: ball and nut, and is still in use in vehicles with higher steering forces, typically larger trucks.

The predominant system used today is of the type: rack and pinion, which was introduced in the late 1960's in medium performance sports cars. There are several different power assisted steering, PAS, solutions for passenger cars on the market today. The most common is the rack and pinion solution with a constant flow controlled pump, *Hydraulic Power Assisted Steering - HPAS system*. More recently an *Electric Power Assisted Steering, EPAS system*, was introduced in smaller cars.

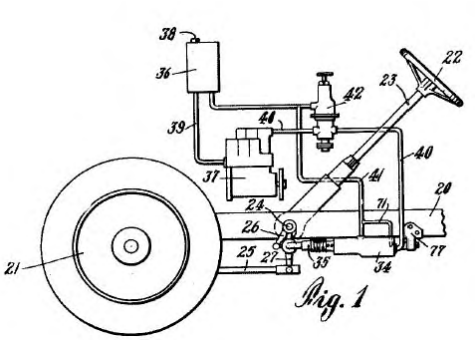

Figure 2.1 *Figure from one of the first patents by Francis W. Davis [20].*

*Latin: servio -ire (with dat.), [to be a slave, to serve, help, gratify].

2.2 Working Principle of Hydraulic Power Assisted Steering Systems

The main task of a power steering system in passenger cars is to decrease the steering effort of the driver in certain situations such as low speed maneuvering and parking. Power steering has become a necessary component in modern cars of all sizes due to high axel weight, larger tire cross-sections and front wheel drive. In most medium and larger cars, the reduction of steering effort is accomplished by using a hydraulic system, which produces an additional torque to the torque applied by the driver.

The basic principle of a hydraulic power steering system is an ordinary hydromechanical servo parallel to a pure mechanical connection. A hydromechanical servo is a system that copies an operator applied movement, normally with the possibility to cope with higher forces or torque. In a normal configuration of a follower servo, the force fed back to the driver is minimal.

2.2.1 Influence of steering property on vehicle handling characteristics

The main task of the power steering system is to reduce, not remove, the steering effort of the driver by adding a certain amount of torque to the driver's torque, while at the same time supplying the driver with a relevant amount of road feel through the steering wheel torque. Assistance torque and road feel are an inherent compromise in conventional hydraulic steering systems due to the system's architecture, which will be discussed later. Car companies have spent a great deal of effort in balancing these two characteristics.

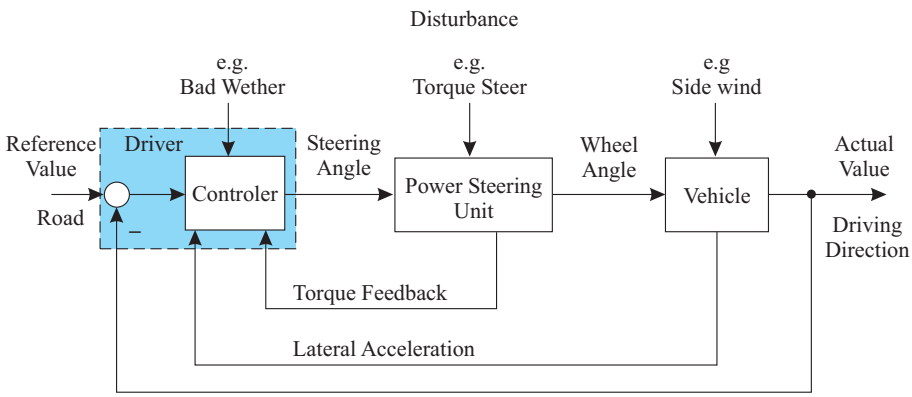

Figure 2.2 *The power steering system is part of the vehicle's closed loop [21]*

Driving a car is really a closed loop system, where the driver is the controller

and the steering unit is the actuator. The steering system transfers the steering wheel angle to the wheel angle, where the action changes the heading of the vehicle. As the main reference, the driver uses the visual information to place the car on the road, he/she also uses the lateral acceleration and the torque fed back via the steering wheel to ensure that the steering command is performed in the intended way. This closed loop system is described in Figure 2.2, where it can be seen that different instances are subjected to disturbances, which will affect the driving performance. In Chapter 5, this figure will be used to discuss the possibility to reduce the effect of the disturbance. In the loop, it is noticeable that the power steering unit is closest to the controller, which means that the first feedback concerning the commanded steering wheel angle is from the steering wheel.

L. Segel researched torque feedback in the 1960's and found that the relationship between lateral acceleration and steering wheel torque plays an important role in safely placing the car on the road [22]. This work was continued by F. Jaksch in the 1970's and F.J. Adams and K.D. Norman in the 1980's [23], [24], [25]. Car manufactures use these results today to design power steering systems. To have a specified relationship between the build-up in steering wheel torque and lateral acceleration is essential for the driver to make the road feel fed back to the driver as consequent as possible. In Figure 2.3, a typical specification of the relationship between the lateral acceleration and steering wheel torque is displayed, notice the steep gradient in steering wheel torque at low lateral acceleration to ensure a good torque feedback on center handling. In order to obtain the specified relationship between the lateral acceleration and the steering wheel torque, the assistance ratio of the power steering can be used together with the layout of the front wheel suspension. However, this assistance ratio is a trade off between different requirements not just the relationship discussed above. Normal driving requires steering wheel torque values of 0-2Nm, [26].

One of the most important characteristics of the power steering unit is the relationship between the manually applied torque and the the assisting torque generated by the power steering unit, which is often visualized in the so-called boost curve. The boost curve shows the static characteristic of the power steering unit and is determined by the shaping of the valve.

2.2.2 Static characteristic of the PAS-system

The shaping of the static characteristic is always a trade-off between assistance and road feel. The reason for this trade-off lies in the nature of the system, and that the vehicle is used in different driving situations. In Figure 2.4, a boost curve is displayed where the characteristic is given by the static relationship between steering wheel torque and load pressure. Also displayed in the figure is three different driving scenarios, highway driving, city driving and parking.

As seen in this figure, the load pressure or assistance is kept minimal at low

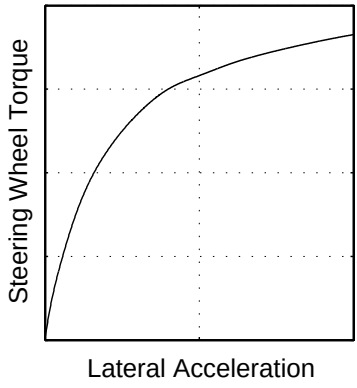

Figure 2.3 *Steering wheel torque as a function of lateral acceleration.*

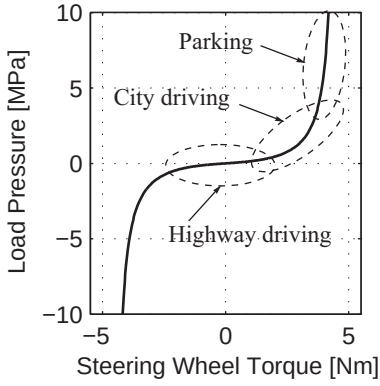

Figure 2.4 *Boost Curve with different working areas depending on the driving envelope.*

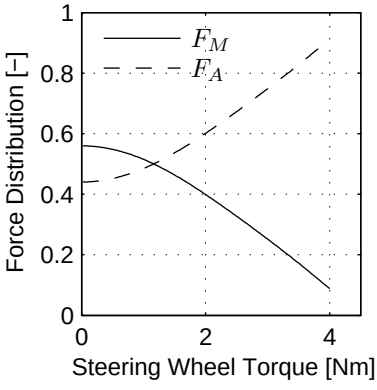

Figure 2.5 *Force distribution between manual force, F_M, and assisting torque, F_A, depending on applied steering wheel torque. Defined by Equation 2.1.*

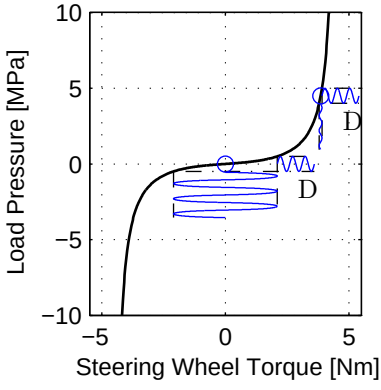

Figure 2.6 *Disturbance propagation when controlling the system at a working point of high torque and low torque.*

torque; at the same time, this implies a low gain, and a high road feel. When demands increase and the driver applies more torque to the steering wheel, the assisting load pressure increases almost exponentially, which reduces the haptic feel fed back to the driver.

Due to the shape of the boost curve, the balance between manual force and assisting force changes with applied torque. In Figure 2.5, the relationship between assisting force and manual force is shown as a factor of the total generated force, Equation 2.1. In the figure, it is shown that at low torque, the manual force is dominant to ensure good road feel. At higher torque, the assisting torque is increased, which also leads to less haptic interference with the road. However, this is not critical during low speed maneuvering.

$$\begin{aligned} F_{tot} &= F_{manual} + F_{assist} \\ F_M &= \frac{F_{manual}}{F_{tot}} \\ F_A &= \frac{F_{assist}}{F_{tot}} \end{aligned} \tag{2.1}$$

In Figure 2.6, road disturbance is simulated with a sinusoidal input at two different working points. The disturbance is held constant at both of the working points. It can be seen that haptic feedback varies depending on which working point the disturbance has initiated. As mentioned earlier, the higher torque areas support the driver during parking and slow city driving when haptic feedback is not important. Unfortunately, high performance driving eases demands on steering wheel torque in the higher region. This means that the driver will not be able to sense the road, no haptic feedback, at a working point with high steering wheel torque. Additional technical solutions to reduce this problem will be discussed in section 2.4.

2.3 General Design of Power Steering Systems

There are basically two different types of power steering units on the market today, hydraulic power assisted steering, HPAS, systems and electric power assisted power steering, EPAS, systems. EPAS systems have been on the market for a few years and are installed in small and medium sized cars, due to its limitation to cope with higher steering forces. However, the functionality of these systems is greater than a traditional power steering unit, which will be discussed in Chapter 5. In this chapter, the EPAS system will not be discussed further; basic information regarding layout and performance can be found in an article written by R. Backhaus, [27].

HPAS system layout is basically the same from car to car, see Figure 2.7. This figure shows the power steering unit in a more detailed view. As seen in this figure, the steering wheel is connected to the steering rack via the valve, which

is the controlling element in the steering unit. The displacement of the valve together with the hydraulic system modulates the pressure in the cylinder such that appropriate assistance is added to the steering rack. The haptic feeling of the forces acting on the steering rack is essential to the driver, which is one reason why the hydraulic system is parallel to a mechanical connection. The assistance generated by the hydraulic system is in relation to the torque applied by the driver on the steering wheel, earlier mentioned as the boost curve, Figure 2.4.

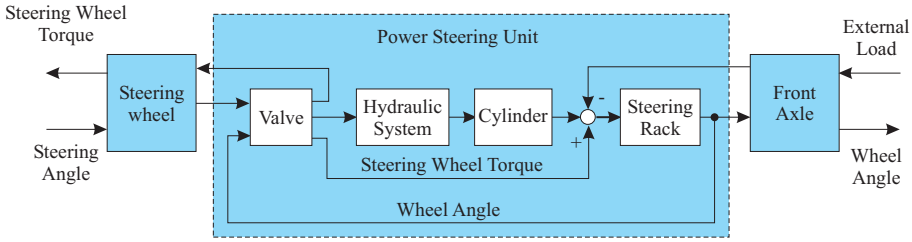

Figure 2.7 *The power steering system is a part of the vehicle's closed loop [21].*

.

Since the valve is the controlling element in the HPAS system, the shaping and design will affect the characteristic of the system deeply. Most of the power steering systems used in cars today utilize an open center valve solution instead of a closed center solution. The reason for this is that the open center valve is an inherit pressure control valve together with a constant flow. A specific valve displacement will result in a specific load pressure when neglecting the motion of the controlled cylinder, pumping motion, where a closed center valve is more suitable for velocity control. A specific valve displacement will result in a specific cylinder velocity, when neglecting the variation in load. Based on this knowledge, it is natural that most power steering units utilize an open-center valve over a closed-center valve. However, some researchers and car manufactures are considering closed-center valves, due to the fact that a valve based on closed-center technology will have the possibility to reduce energy consumption. Energy consumption in power steering systems will be discussed further in section 2.5.

In Figure 2.8, a cut-through sketch of a HPAS system including pump, valve assembly, rack and the hydraulic cylinder is shown. The interesting part of this figure is the valve assembly with the torsion bar in the core of the valve. In Figure 2.9, a photo of a separated valve unit, showing the pinion, torsion bar, spool and valve body is shown. The function of the torsion bar is to activate the valve and at the same time transfer the applied manual force down to the pinion. The top part of the torsion bar is attached to the spool and the lower part is attached to the pinion. Since the valve body is also solidly attached to the pinion, a displacement of the torsion bar will create an angular displace-

ment between the spool and the valve body. When torque is applied to the steering wheel, the torque will be transferred down to the valve via the steering column. When torque is applied to the torsion bar it will twist. The twisting of the torsion bar is linear to the applied torque. This means that the valve displacement is proportional to the applied torque. When the valve is activated or displaced, the valve will modulate the pressure within the chambers of the hydraulic cylinder in order to assist the driver. Figures 2.8, 2.10 and 2.11 show the different modes of the valve.

- In Figure 2.8, the cut-through view of the valve displays the valve in a neutral position, which means that the pressure is equal in both chambers A and B, thereby not assisting the driver.
- In Figure 2.10, a cut-through is made of the valve when counter clockwise torque is applied to the steering wheel. As seen in the figure, the valve is twisted such that the A side of the cylinder chamber is opened to the pump and the B side of the chamber is opened to the tank outlet. Due to the change in metering orifice area, the pressure in the hydraulic cylinder is modulated to assist the driver.
- Figure 2.11 shows the valve when the torque is applied in a clockwise direction, which will displace the valve in the opposite direction, thereby changing the direction of the assisting pressure.

2.3.1 Characteristic defined by the valve

When it comes to defining the characteristic of the HPAS system, the valve is the most important component. As mentioned earlier, the traditional power steering system is based on an open center valve and a flow controlled pump. The main reason for using an open center valve is that the system's main task is to perform pressure control to generate assistance to the driver. In an open center solution, the valve displacement is directly related to a generated load pressure. This means that the main task of the system is built into the concept. In the valve solution shown in Figure 2.8, the torsion bar will work as a translation from applied steering wheel torque to valve displacement. This means that there will be a function that statically defines the relationship between the load pressure generated by the hydraulic system and the applied torque, see Equation 2.2. In order to meet the desired function, the area openings of the valve have to be designed.

The system can be simplified by lumping the multiple orifices in the valve, normally 3-4 multiples, into a Wheatston bridge representation, Figure 2.12. Based on Figure 2.12, it is possible to calculate the load pressure as a function of opening areas, which in turn is related to the applied steering wheel torque, T_{sw}. Equations 2.3 and 2.4 refer to the calculations made by H.D. Merritt [29],

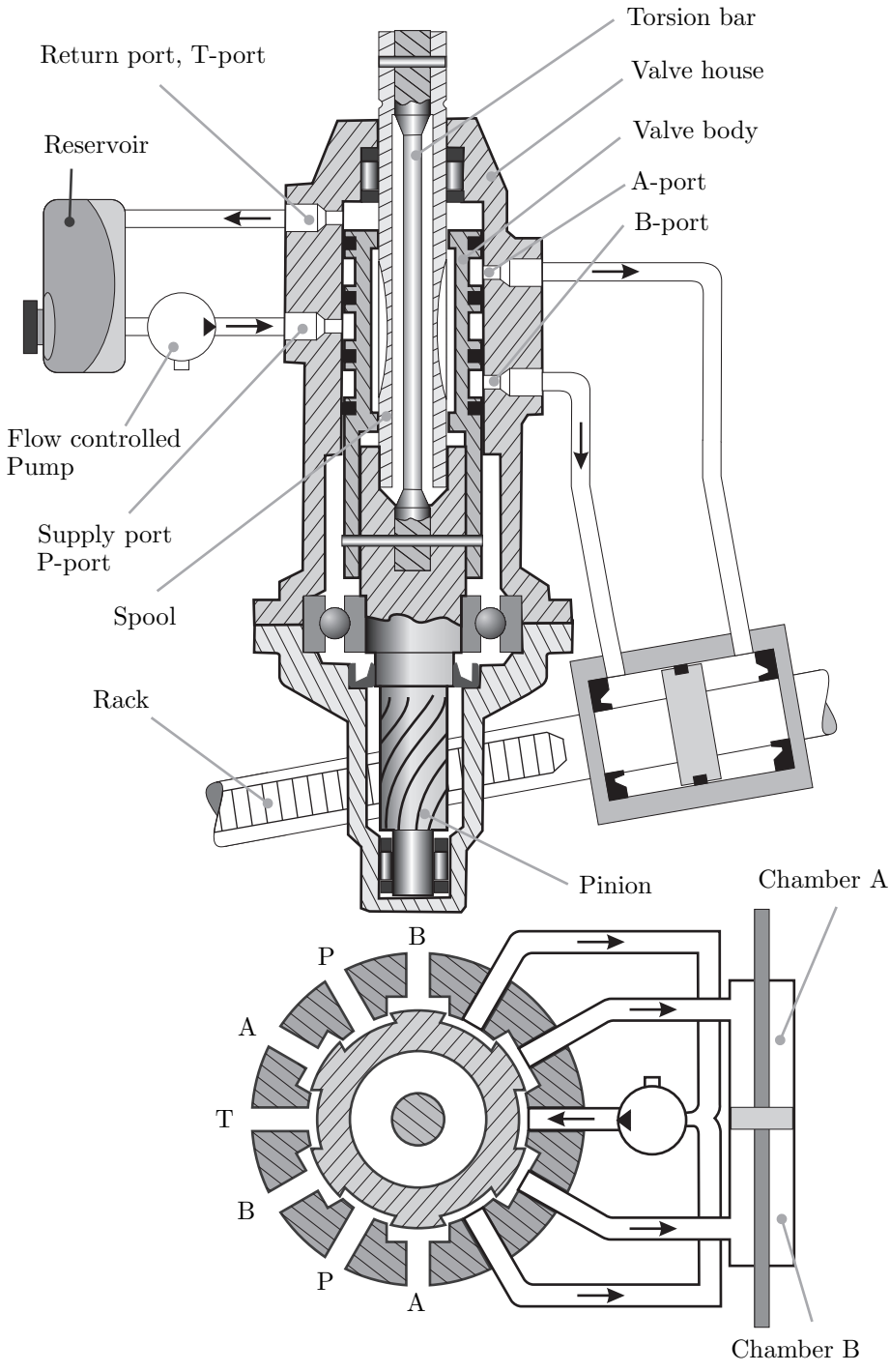

Figure 2.8 *HPAS system including, pump, cylinder and valve assembly. Valve is displayed in neutral position.* Figure is inspired by [28].

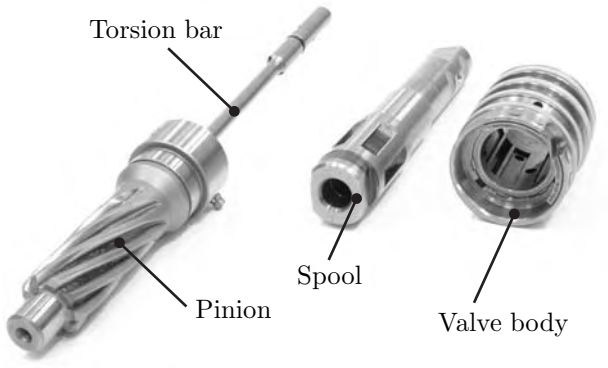

Figure 2.9 *Photo of the valve when separated, notice the pin in the pinion, which is used to connect the valve body to the pinion.*

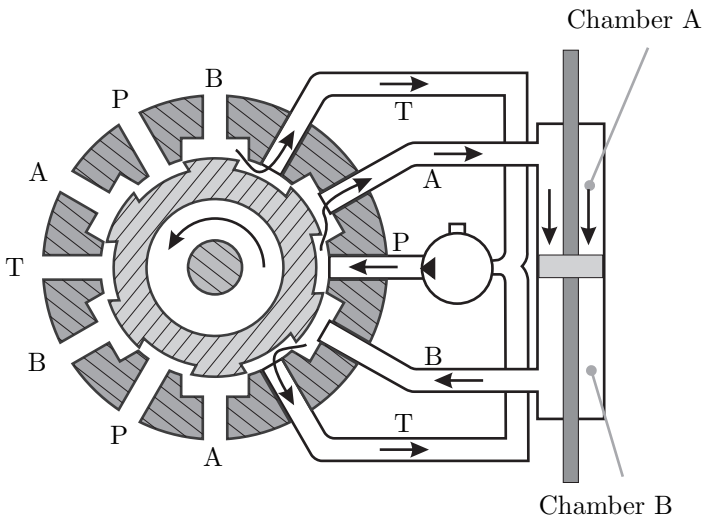

Figure 2.10 *Valve displacement in a counterclockwise direction, metering P to A and B to T.*

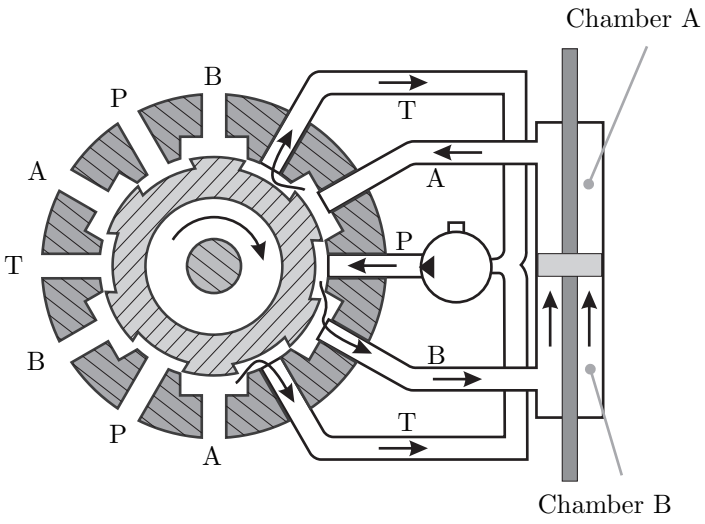

Figure 2.11 *Valve displacement in a clockwise direction, metering P to B and A to T.*

which establish the load flow and system flow depending on the system pressure, load pressure and the area openings.

$$p_L = f\left(T_{sw}\right) \tag{2.2}$$

$$q_S = c_q A\left[-T_{sw}\right]\sqrt{\frac{p_S - p_L}{\rho}} + c_q A\left[T_{sw}\right]\sqrt{\frac{p_S + p_L}{\rho}} \tag{2.3}$$

$$q_L = c_q A\left[-T_{sw}\right]\sqrt{\frac{p_S - p_L}{\rho}} - c_q A\left[T_{sw}\right]\sqrt{\frac{p_S + p_L}{\rho}} \tag{2.4}$$

Based on these equations, establishing q_S and q_L, make it possible to establish the flow relationship, which in turn is used to resolve the load pressure and system pressure depending on the area opening and induced load flow. The displacement of the valve is related to the applied steering wheel torque; therefore, the area openings are a function of the applied steering wheel torque, $A[-T_{sw}]$ and $A[T_{sw}]$. Notice that the system flow, q_s, is used rather than the pump flow, q_p. The reason to differentiate between system flow and pump flow is that they can differentiate dynamically; in a static view, they will be equal, see Figure 2.12. Equations 2.3 and 2.4 can be reformulated and described as Equations 2.5 and 2.6, which in turn can be reformulated and described as

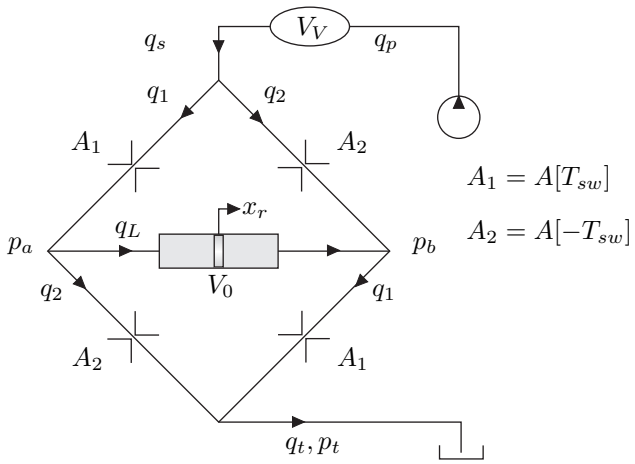

Figure 2.12 *Valve configuration of the power steering unit. Wheatstone bridge representation, where the multiple orifices are lumped together.*

Equations 2.7 and 2.8.

$$q_s + q_L = 2c_q A\left[-T_{sw}\right]\sqrt{\frac{p_S - p_L}{\rho}} \tag{2.5}$$

$$q_s - q_L = 2c_q A\left[T_{sw}\right]\sqrt{\frac{p_S + p_L}{\rho}} \tag{2.6}$$

$$p_S - p_L = \frac{\rho}{4}\left(\frac{q_s}{c_q A\left[-T_{sw}\right]}\right)^2\left(1 + \frac{q_L}{q_s}\right)^2 \tag{2.7}$$

$$p_S + p_L = \frac{\rho}{4}\left(\frac{q_s}{c_q A\left[T_{sw}\right]}\right)^2\left(1 - \frac{q_L}{q_s}\right)^2 \tag{2.8}$$

From Equations 2.7 and 2.8, the load pressure and system pressure can be resolved, Equations 2.11 and 2.12. The difference between load pressure and system pressure is also of interest as it gives a good indication on how effective the valve is, Equation 2.7. High differences between load and system pressure result in high losses over the valve. As seen in Equations 2.7-2.12, the quota of load flow and system flow is defined. This can be simplified to a normalized flow, q. Normalized flow, $q = 1$, defines the limit of the rack speed, $\dot{x}_{r_{max}}$, with maintained ability to generate assisting pressure.

$$q = \frac{q_L}{q_S} \tag{2.9}$$

$$\dot{x}_{r_{max}} = \frac{q_s}{A_p} \tag{2.10}$$

$$p_L(T_{sw}, q) = \frac{\rho q_S^2}{8c_q^2}\left(\left(\frac{1-q}{A[T_{sw}]}\right)^2 - \left(\frac{1+q}{A[-T_{sw}]}\right)^2\right) \quad (2.11)$$

$$p_S(T_{sw}, q) = \frac{\rho q_S^2}{8c_q^2}\left(\left(\frac{1-q}{A[T_{sw}]}\right)^2 + \left(\frac{1+q}{A[-T_{sw}]}\right)^2\right) \quad (2.12)$$

In Equation 2.11, load pressure is shown as a function of the opening areas of the valve; when equal, the generated load pressure is zero and no assisting force will be produced. Notice also that the valve opening areas are functions of the applied steering wheel torque, T_{sw}. Other variables that affect the load pressure are the flow delivered by the pump down to the valve, system flow, q_s, and load flow, q.

Vehicle and system data

Vehicle weight	1600	kg
Front axle weight	950	kg
Controlled pump flow	8.20	l/min
Maximal pump pressure	11	MPa
Cylinder area	8.26	cm^2

In this chapter, the following graphs will be based on a fictive vehicle. The basic information of the vehicle and system are presented above. In Figure 2.13, the valve area openings are shown as a function of applied steering wheel torque. In reality, the increased area is limited by the orifices in the valve body and levels off between 20 and 30 mm^2. This does not affect the analysis and will be discussed further in Chapter 4. The static characteristic of the power steering system is displayed in Figure 2.14; this curve will later be referred to as the boost curve. However, this graph is only valid when the steering rack velocity is low. As discussed earlier, the generated load pressure is also quasi statically affected by the load flow, which in turn is a result of the motion of the rack. Depending on the direction of the motion in relation to the generated pressure, the assistance will increase or decrease.

Figure 2.15 shows the effect of the load flow, q. The curve in the middle represents the static curve when the load flow is zero. The lower curve represents a load flow of $q = 0.8$. A positive value means that the assistance and the rack velocity are acting in the same direction, see Figure 2.16. This case is probably the most common when the driver needs assistance to perform a maneuver. As seen in Figure 2.15, assistance is reduced with increased rack speed and will eventually result in loss of assistance; this phenomena is called catch-up and is discussed in paper [II]. The second scenario is when the assisting pressure and the rack motion are acting in the opposite direction of each other, which results in an increase of the generated assistance, Figure 2.17. In order for the rack motion and the generated assistance to act in opposite directions, the rack

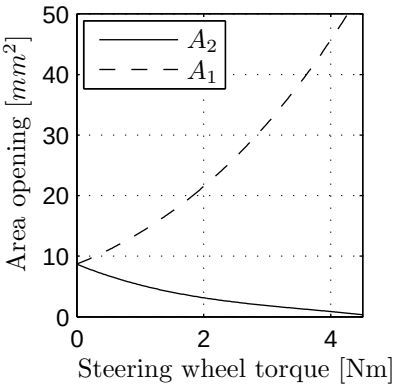

Figure 2.13 *Area opening as a function of applied steering wheel torque.*

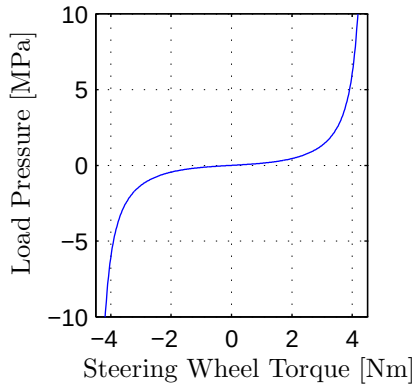

Figure 2.14 *Generated load pressure as a function of applied steering wheel torque. Related to the area openings in Figure 2.13.*

has to be driven by an external load, which can be the case when exiting from cornering. The external load is then the aligning torque, which is a result of the front suspension geometry. The increase of assistance can be a problem in a dynamic perspective; an increase in assistance means that the system gain also increases. Since the system is a closed loop system, the gain will lead to low amplitude or phase margin and result in instability. This is discussed in paper [I].

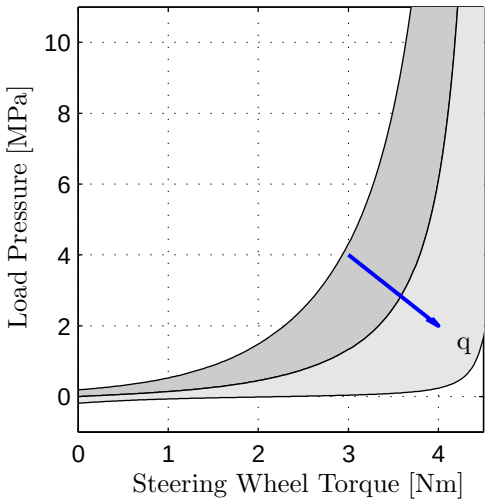

Figure 2.15 *Quasi static plot of the boost curve. Outer limits in the graph are defined by different load flow values, $q = \pm 0.8$. The curve in the middle represents the static boost curve with no load flow applied.*

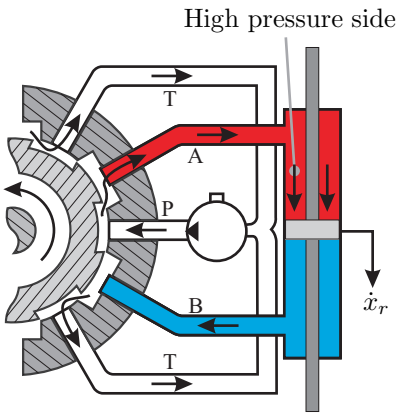

Figure 2.16 *Pressure and rack velocity in the same direction. This will reduce the assistance, refer to Figure 2.15 with positive load flow, q.*

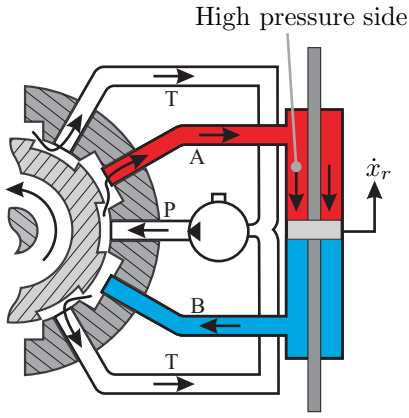

Figure 2.17 *Pressure and rack velocity in the opposite direction. This will increase the assistance, refer to Figure 2.15 with negative load flow, q.*

2.3.2 Design aspects and internal system dependencies

In this subsection, the design process or sizing of a HPAS system will be briefly discussed. The focus of the discussion is mainly on the hydraulic part; mechanically the system also has demands depending on structure problems, gear ratio etc, which are not treated in this thesis.

The dimension of the HPAS system depends primarily on the front axle weight of the vehicle. Based on the expected power steering load, the system can be sized statically. The components that have to be sized are listed in the box below.

Components concerning the hydaulic

- Hydraulic cylinder
- Pump
- Valve
- **E**xpansion **C**hamber **A**ttenuator, ECA
- Cooler

The internal dependencies between the ingoing components are described and discussed below. These dependencies have an impact on the sizing of the components.

Hydraulic cylinder

The sizing of the cylinder depends mainly on the load in which it has to overcome during different driving scenarios. The load is in turn dependent mainly on the front axle weight, but also on the tires and the geometry of the suspension. The size of the maximal load indirectly gives the size of the hydraulic cylinder when the maximal pump pressure level, $p_{p_{max}}$, is set between $110-130$ Bar, Equation 2.13.

$$A_p = \frac{F_{L_{max}}}{p_{p_{max}}} \tag{2.13}$$

Hydraulic cylinder design requires external information regarding:

- Gear ratio steering wheel to wheel
- Pinion gear ratio
- Front axle weight
- Maximal pump pressure

Pump

The system is an open center system, which relies on a constant flow source, a flow controlled pump. The normal pump configuration is a fixed displacement pump directly driven by the vehicle's engine, and a flow control valve, see Figure 2.18. Other pump configurations can also be used such as a variable displacement pump and a directly driven electric pump. Choicing the pump technology is mainly related to the energy consumption of the system, which will be discussed later in section 2.5. The required maximal steering rack speed decides the flow that has to be delivered and controlled by the pump, this can be seen as a function requirement, which is independent from the choice of the pump solution. Therefore, the pump size, or the controlled flow delivered by the pump, is mainly dependent on the performance demand set by the manufacture regarding maximal rack speed. In order to be able to assist the driver, the pump has to deliver at least the flow amount that the hydraulic cylinder is demanding at required maximal speed, Equation 2.14.

$$q_p = A_p \dot{x}_{r_{max}} \tag{2.14}$$

The relation discussed above, gives the static layout of the pump without leakage, which has to be compensated for. The flow pressure characteristic of the pump, which varies with pressure and temperature, has to be considered. In Figures 2.19 and 2.20, the flow pressure characteristic of a power steering pump is shown; notice that the variation in delivered flow varies greatly when the pump speed is 850 rpm. In Figure 2.19, the characteristic is dominated by the characteristic of the pump core or pumping elements; whereas in Figure 2.20, the characteristic of the flow controller is visible.

There is also leakage in the valve unit depending on the geometry of the valve, which means that none of the orifices in the valve can be assumed to be fully closed, Equation 2.15. Another thing that has to be considered is the dynamic effect of the same problem called the hydraulic lag, which is an affect of the oil compressibility and the expansion of ingoing components, such as the **E**xpansion **C**hamber **A**ttenuator, ECA. The ECA expands during pressurization. The catch-up effect and hydraulic lag are discussed in more detail in appended paper [II].

$$q_p = A_p \dot{x}_{r_{max}} + q_{leak} + q_{ECA} \tag{2.15}$$

Pump design requires information regarding:

- Hydraulic Cylinder
- ECA
- Valve due to leakage

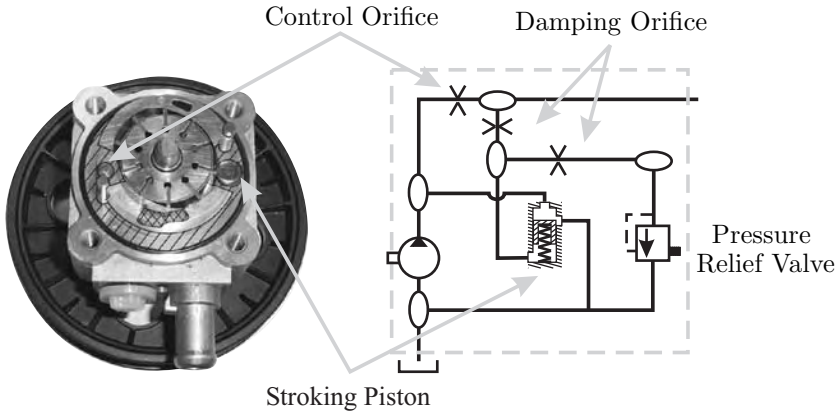

Figure 2.18 *Pump including flow compensator. Dashed area in the picture represents the high pressure side of the pump. Double dashed area represents the low pressure side, only one of two is visible.*

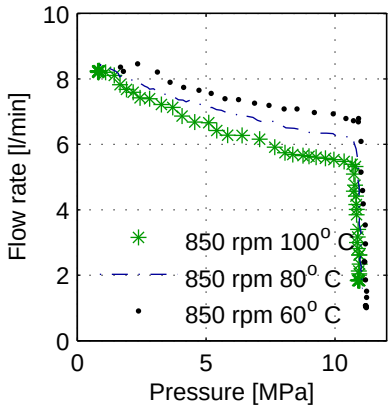

Figure 2.19 *Measurement on the pump characteristic at 850 rpm with variation in working temperature. In the graph, the flow controller in the pump is not controlling. The visible characteristic represents the pumping part of the pump concerning leakage due to pressure and temperature.*

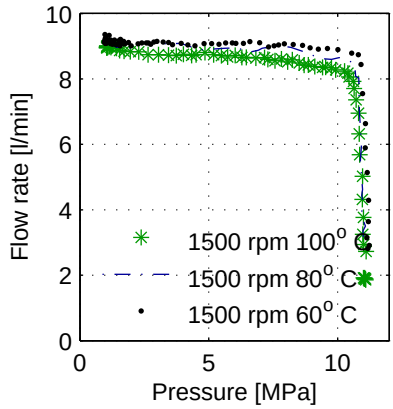

Figure 2.20 *Measurement on the pump characteristic at 1500 rpm with variation in working temperature. In the graph, the flow controller in the pump is controlling. The visible characteristic represents the flow controller in the pump.*

Expansion Chamber Attenuator

The function of the **E**xpansion **C**hamber **A**ttenuator, ECA, is to reduce the noise level in the system. It is mounted between the pump and the valve. The component that generates the most noise in the system is the pump, which causes the ECA's dependency. The function of the ECA is to work as a hydraulic filter and dampen the pulsation emitted by the pump. The difficulty in the automotive industry is that the pump is often driven directly by the engine, which implies that the undesired frequency spectrum varies with the pump speed. Attenuator technology in industrial applications is often easier to design when the spectrum of frequency is fixed. In this research, the function of the ECA is not studied in detail; the focus has rather been on the drawbacks with the attenuator, which will reflect on the overall system layout [30].

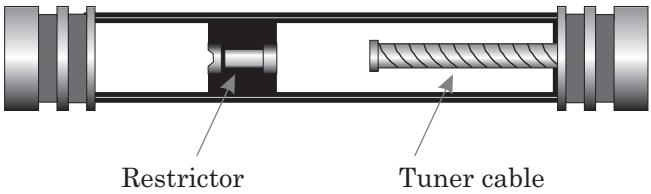

Figure 2.21 *Expansion Chamber Attenuator, ECA, including two expansion chambers, tuner cable and restrictor.*

There are some drawbacks with the ECA that have to be considered during the design process. There are different design solutions to the ECA, but the ECA used in this project includes two chambers and an orifice in between the chambers, see Figure 2.21. This means that introducing an ECA will lead to increased system pressure, which in turn generates losses both in the ECA and the pump. Due to the function of the ECA, it will reduce the effective bulk modulus of the system, which can result in hydraulic lag or dynamic catch-up. The effect of the hydraulic lag is loss of assistance. This occurs when the pressure rises rapidly in the system, which leads to an expansion of the ECA. The expansion will result in less effective flow to the valve and assistance is reduced. This effect will be mentioned later in Chapter 4, but can also be found in paper [II]. Positive effects of the ECA that are not often mentioned are added dampening to the system dynamic, as well as reducing the noise level it. This is due to the fact that it softens out the pressure peaks generated by the system dynamics; this can be seen as soft pressure feedback.

ECA design requires external information regarding:

- Pump

Valve

The function of the valve is to modulate the pressure such that it assists the driver while driving and eases the steering effort during parking maneuvers. As discussed earlier, the shaping of the valve defines a large part of the characteristic of the steering unit. However, the characteristic is not only dependent on the valve, but also on the flow delivered by the pump, q_p, and piston area of the cylinder, A_p. This can be seen in Equations 2.16 and 2.17. As mentioned earlier, the torque pressure characteristic also depends on the load flow.

$$p_L(T_{sw}, q) = \frac{\rho q_p}{8c_q^2}\left(\left(\frac{q-1}{A_2(T_{sw})}\right)^2 + \left(\frac{q+1}{A_1(T_{sw})}\right)^2\right) \tag{2.16}$$

$$F_{assist} = p_L A_p \tag{2.17}$$

Valve design requires external information regarding:

- Pump
- Cylinder

Cooler

Due to the system layout, some systems will need a cooler to keep the system's temperature down. The temperature in the system is mainly due to losses in the system and, therefore, depends on the efficiency of the ingoing component. In some cases, the cooler also has to be designed to handle external effects, such as heat radiation from the exhaust manifold. In the power steering system, the component that generates the most losses, heat, in the system is the pump, due to the fact that it normally produces excessive flow that has to be shunted back to the suction side of the pump. There will also be losses due to the pressure drop of the valve and the ECA.

Cooler design requires external information regarding:

- Pump
- Valve
- ECA
- External heat sources

Each component has its problems and in depth design aspects. A few of these component's characteristics and design will be studied in more detail in the chapters concerning modelling, Chapters 3 and 4.

2.4 Speed Dependent Assistance

In order to increase handling, the power steering system can be equipped with a valve that changes the characteristic depending on the velocity of the car. In low speed maneuvering, the system has a higher assistance ratio compared with high speed maneuvering, see Figure 2.22. HPAS systems with speed dependent assistance, progressive steering, have been on the market for some time and are standard in sports cars and high-end models today. Progressive steering increases the road feel transferred to the driver via the steering wheel at higher vehicle speeds. There are different ways of realizing this, to name a few:

- Reduce flow delivered to the valve
- Change stiffness of the torsion bar
- Variable geometry in the valve

The traditional way of accomplishing progressive steering is to reduce the flow to the valve, thereby decreasing the assisting torque generated by the hydraulic power steering system, [31]. Another way is to change the layout of the valve and make the valve body move axial on the spool, where the spool has variable geometry. This will make the area opening of the spool not only depend on the twisting of the torsion bar, but also the axial position of the valve body [32]. Since the twisting is dependent on the stiffness of the torsion bar, it is obvious that an increase in stiffness will reduce the assistance produced by the hydraulic power steering system due to the reduction in the movement of the valve. The system that is preferable from a road feel point of view is the variable torsion bar, where assistance is reduced simotaniously as the pure mechanical connection between the steering wheel and rack stiffens.

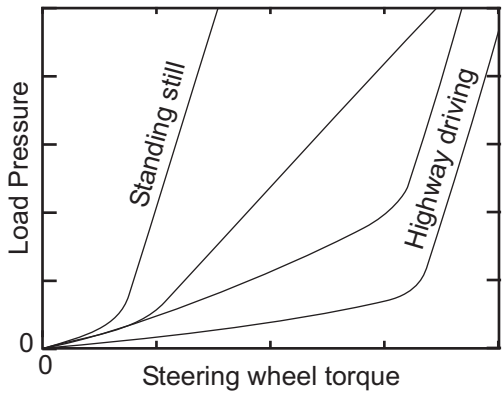

Figure 2.22 *Vehicle dependent assistance to increase road feel and handling. Change in assistance depending on vehicle speed.*

2.5 Energy Aspects of Hydraulic Power Assisted Steering Systems

Until recently, hydraulic power steering was the only technology available on the market to ease the steering effort of the driver, and energy consumption was not an issue. When the EPAS system was introduced a few years ago, the main benefit of the system was low energy consumption. This addressed energy consumption as a total for the power steering system including the HPAS system.

The advantages of the EPAS system are mainly in the area of energy consumption. However, due to the design concept of the EPAS system, there are many other built-in advantages. One of the features that is quite convenient is the possibility to adjust the assisting torque continuously during driving. The energy saving in EPAS systems, compared to HPAS systems, is done by more or less shutting down the power steering system during highway driving as assistance is less needed, which is also one of the reasons for low energy consumption. According to R. Herkommer, [33], fuel consumption can possibly be reduced up to 0.25 liters of fuel per 100 km when EPAS systems are introduced in cars; whereas, traditional HPAS systems consume approximately 0.3 liters of fuel per 100 km. However, these numbers are hazy, as energy consumption is strongly dependent on the driving scenario and the size of car, which is one thing that Breitfeld, [18], showed in his study between traditional HPAS and EPAS systems, see Figure 2.23. In this study, the HPAS system was more efficient during parking maneuvers, but power losses in straight driving were more than the double; the number is based on a middle class car. The relatively low losses in the EPAS system are due to the capability to shut down parts of the system. Whereas, the HPAS system has full capability in the system due to the low controllability of the pump. Based on this fact, the EPAS system seems to be superior to the traditional HPAS system which is partly true. The drawbacks to the EPAS system are its ability to only be used in small and medium sized cars due to the fact that it can not handle the forces associated with larger and luxury cars. Another problem with the EPAS system is the fail safe mode, which is a strong argument for the HPAS system.

Energy consumption in HPAS systems is dependent on the delivery of oil. Normally, hydraulic pumps are fix-mounted on the engine; since the engine speed of the vehicle will change during the drive, the flow delivered by the pump will also vary. The pumps are normally dimensioned to deliver full flow at engine idle, which consequently leads to the production of surplus oil when the engine does not run at idle, see Figure 2.24. This surplus oil is responsible for most of the losses, energy consumption, associated with hydraulic power steering, [34]. The valve is also a source of loss as oil continually flows through restrictions in the valve unit. Both of these losses are aspects being looked into. Reduction of losses in the system, including the valve, ECA, cooler and return line will result in reduction in losses associated with the pump. This

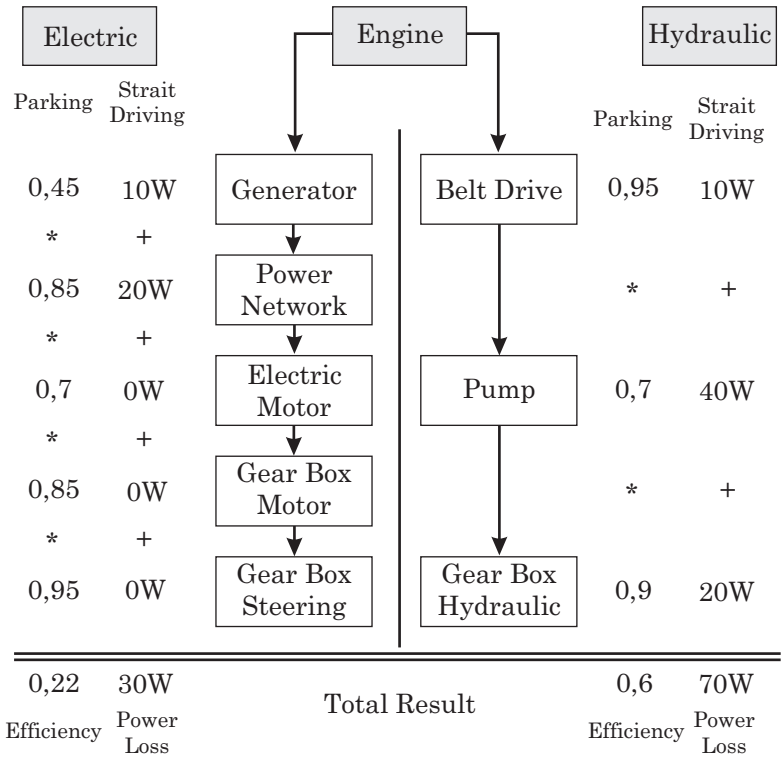

Figure 2.23 *Efficiency and energy loss comparison for hydraulic and electric power steering systems. Figures and numbers from [18].*

is due to the fact that a reduction in system pressure will definitely benefit losses related to the pump. The simplified equations describe the relationship, Equations 2.18–2.20. Notice that the flow delivered by the pump affects the total loss significantly. Reducing this will reduce the total system pressure and, thereby the total losses. However, reduction in the controlled pump flow, q_p, will affect the characteristic of the system, as discussed earlier, but in ceratin circumstances this can be accepted, speed dependent assistance.

$$P_{pump} = q_{sh}p_{sys} = q_{sh}(dp_{ECA} + dp_{Valve}\ldots) \quad (2.18)$$

$$P_{ECA} = q_p dp_{ECA}(q_s) \quad (2.19)$$

$$P_{valve} = q_p dp_{valve}(q_s) \quad (2.20)$$

To understand the losses of a hydraulic power steering system, the graph displayed in Figure 2.25 can be used, which gives an overview of the hydraulic losses associated with the pump and the valve unit. The graph is divided into three different graphs. The two small graphs, to the left and on top, display

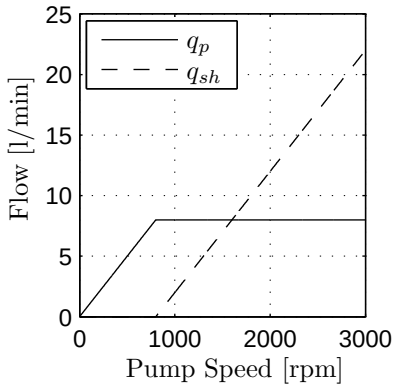

Figure 2.24 *Flow delivered from the pump depends on the pump speed. q_p represents the controlled flow delivered by the pump and q_{sh} represents the excessive flow that has to be directed back to the suction side of the pump.*

the likelihood for a certain system pressure and the likelihood for a certain engine speed. These two graphs help in the understanding of the likelihood of a certain working point and estimating the associated hydraulic losses. The third and main graph is divided into two parts; the left part displays energy consumption and losses associated with the valve unit, the X-axis in this part is the speed of the rack in percentage. The right part of the main graph visualizes losses associated with the surplus discharge flow; the engine speed is on the X-axis. As previously mentioned, the pump delivers full flow at idle speed, which is set at 600 rpm in this graph. The area of the main graph is then the hydraulic energy consumption and losses of the system.

In the graph in Figure 2.25, two scenarios are visualized; one scenario could be highway driving with small steering corrections and low torque demands. The losses in the valve unit are roughly 40W and the losses due to the surplus oil created by the pump are approximately 160W. Even when the demand is fairly low, the losses associated with the pump are dominant. The second driving scenario could be city driving at low speeds, where the demands on the power steering system increase.

2.5.1 Methods to reduce energy consumption

There are different ways to reduce energy consumption in traditional HPAS systems. The reason for using the term ”reduction in energy consumption” instead of ”increase in efficiency” is that energy consumption can be reduced without a significant improvement in efficiency. According to the graph in Figure 2.25, energy consumption can be lowered by a decrease in system pressure or flow, linear relation between flow and engine speed.

The surplus oil produced by the pump stands for most of the losses in the

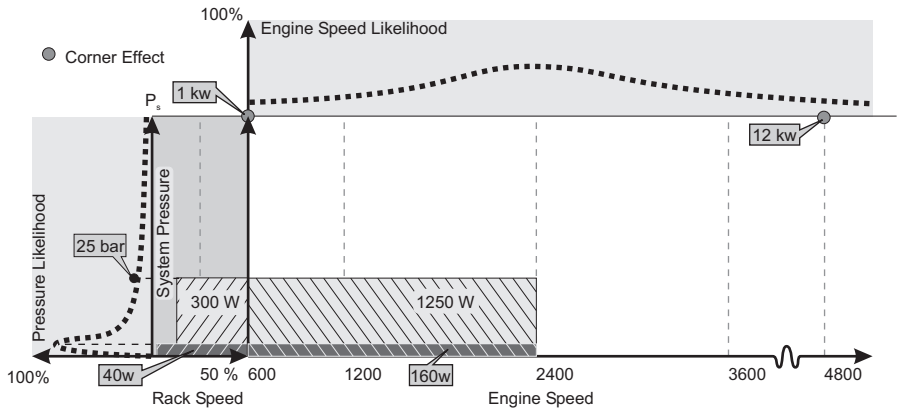

Figure 2.25 *Graph covering energy consumption and losses in a power steering system, where the pump is throttling the surplus flow in order to maintain a constant output flow.*

system. By removing the surplus oil and producing the exact amount of oil required, both efficiency and energy can be improved. There are different solutions to this problem; one solution is to introduce a variable displacement pump instead of a fixed pump with a flow controller. The variable displacement pump will then need an additional actuator to control the displacement. The control actuator can be a pure hydraulic solution. If a more advanced control algorithm is used, the control actuator could be an electro-mechanical or an electro-hydraulic solution. Another solution is to use a directly electrically driven pump. Both the variable displacement pump and the electrically driven pump will minimize surplus oil losses; the reduction with such a solution could reduce energy consumption by 48–64% compared to a conventional fixed displacement pump solution, [35].

If only the pressure is reduced, the efficiency will not change; however, as the amount of assisting torque decreases, energy consumption will also decrease. Due to the decrease in assisting torque, this concept has to be based on a more advanced control algorithm to meet the demands required by the driver, compared to the solutions mentioned above. The algorithm has to take into account vehicle speed, steering angle speed and the steering angle to estimate the assistance required by the driver, [36], [35]. In order to reduce the pressure in the system, the flow delivered from the pump and to the valve unit has to be lowered. By doing this, a reduction of pressure drop over different restrictions in the valve unit will be accomplished, thus reducing energy consumption.

In a traditional, directly driven, fixed displacement pump configuration with a flow control valve, a reduction in pressure is realized by changing the flow metering orifice in the flow controller and by making this orifice variable, [33] [36], see Figure 2.26. By doing this, the flow delivered to the valve unit can be ad-

justed by means of need. This does not reduce the amount of surplus discharge oil fed back to the suction side of the pump, but reduces the pressure in the system. By reducing the pressure, the losses based on the surplus oil are also lowered. At the same time, the losses in the valve unit itself will be reduced. Notice that this change in design will be reflected in the pressure likelihood curve and push the peek pressure down, thereby reducing the overall energy consumption of the system. According to Boots et al. [35], the potential saving with this type of concept is between 28-45%, depending on the strategy of the pump control.

The effects of these two methods of reducing energy consumption have been investigated by R. Herkommer [33]. The best result to reduce energy consumption is to combine the two methods of improvement. However, this combination is impossible to accomplish with a traditional fix displacement pump, which means that a variable displacement pump with an electrical control or a directly electrically driven pump has to be used. With an electrically driven pump, the losses in the generator, power network and the electric motor have to be added. The combination of the two ways of improvement is also possible with an electro-hydraulic or electro-mechanical variable displacement pump.

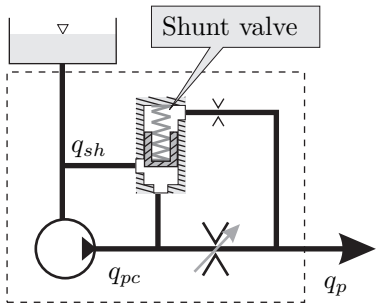

Figure 2.26 *Configuration of a pump with variable flow metering orifice, not included in the picture is the pressure relief valve.*

All solutions mentioned above are based on the assumption of using an open center hydraulic system. Research concerning closed center solutions has been done by several teams in order to reduce the energy consumption of hydraulic power steering system, [37], [38], [39], [40]. By introducing a closed center solution, energy consumption can be reduced drastically; Boots et.al, [35], mention a reduction of 72 % compared to a traditional HPAS system. The problem with a closed center solution is that it has to be produced with high tolerance demands, due to the fact that the pressure sensitivity, $K_p = dp_L/dx_v$, of a closed center valve is high. This means that a small deviation in the valve could lead to drastic changes in the valve characteristic. Due to this, the closed center solution is only used in extreme solutions, such as in Formula 1 cars, [41].

3
Valve Modeling and Area Identification

The geometry of the valve is one of the most important factors when it comes to shape characteristics of a power steering system. It is then quite obvious that this has to be modeled very carefully. Like most component manufacturers, power steering producers are also in need of powerful simulation models to reduce time and cost requirements for the development of new power steering racks. Often when a new power steering rack is developed, the main mechanical structure is basically the same, only the geometry of the valve changes. Generally, new developments start with an initial valve performance and are then changed repetitively until the desired vehicle performance is achieved [42]. To reduce the amount of design iteration, a powerful model of the valve geometry is essential. A large part of the iteration process can then be transferred from hardware to model based optimization.

Depending on the reason for modeling the valve, the approach can be different. If the reason is to design or redesign an existing valve unit, the geometry is of great interest when considering the design variables for the new valve. If the reason is to investigate an existing power steering unit, the area function might be of more interest.

3.1 Geometry Modeling

In general, the geometry that can be adjusted to achieve desired vehicle performance is the area openings of orifices as a function of applied torque. The area openings are dependent on the shape of the orifice. The most common shape is the single-beveled flat valve, displayed in Figure 3.2. Sometimes double-beveled flats are used to achieve a smoother transition in the change of the area opening. In order to model the valve properly, it has to be dissected and studied under

a microscope. In Figure 3.1, the spool is displayed together with a close-up of one of the orifice edges, compare with Figure 3.2.

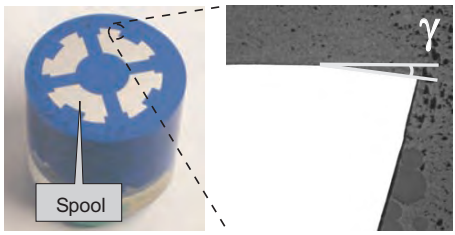

Figure 3.1 *To the left: a cast of the spool is displayed. To the right: a close-up of one edge through a microscope.* Picture scale 50:1.

The validation of the valve configuration is carried out with the help of the previously discussed boost curve. The boost curve describes the characteristics of the valve accurately enough to be used for the validation of the valve unit isolated from the rest of the system; compensation has to be made regarding the friction in the valve unit. The only parameter outside of the valve unit that affects the results of the validation is the flow delivered to the unit. This validation can nearly be achieved with a static simulation, as the pressure or torque relationship can be described by the orifice equation, see Equation 3.1.

$$p_L(T_{sw}) = p_A - p_B = \frac{(q_L - q_P)^2 \rho}{8A_2(T_{sw})c_q^2} - \frac{(q_L + q_P)^2 \rho}{8A_1(T_{sw})c_q^2} \tag{3.1}$$

The equation above also includes the load flow, q_L, which is zero in the boost curve measurement, as the rack is locked during the measurement. The pressure will then vary with the applied torque, T_{sw}, which affects the area openings of the orifices in the Wheatstone bridge. In reality, the flow coefficient, c_q, will vary with the opening geometry and pressure will drop over the orifice. This is not implemented in the model, but rather assumed to take care of small deviations in the geometry after the validation. Experimental investigation concerning the variation in the flow coefficient has been carried out by Birsching [42]. In this investigation, the area openings were first measured, then the valve was assembled and tested concerning pressure build-up. From these measurements, it is possible to establish the flow coefficient as a function of valve displacement. Birsching noticed variation in the value close to center and close to maximal displacement of the valve. These changes were not fully reliable as the resolution in the sensor was not good enough to handle small pressure deviations close to center. The variation close to maximal displacement, the slope of the pressure curve, could result in large errors due to mismatch in the assembly after the geometry measurement. Since the aim of Birsching's work was to design

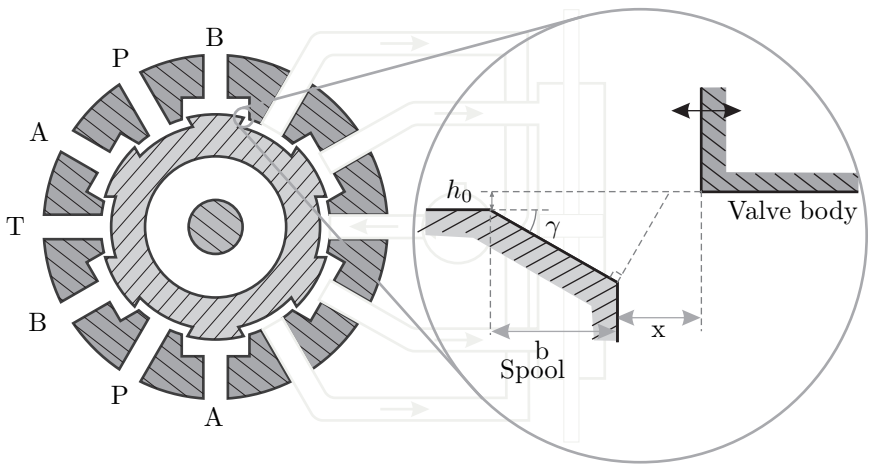

Figure 3.2 *Orifice geometry of valve unit. Figure displaying a single-beveled flat configuration.*

a new valve based on given boost curve requirements, variation in the flow coefficients has been neglected. This being the case, a valve geometry based on this assumption should give the system a characteristic close to the requirement. This assumption is based on the fact that in the manufacturing of these valves, the tolerances will have a greater impact on the characteristic, especially on an individual level.

In order to define the geometry of the valve, some key parameters have to be given such as the angle of grind, γ , the under-lap in zero position, Equation 3.6, the length of land, L, and the clearance between the valve body and the spool, h_0, see Figure 3.2. The area is then calculated by multiplying the gap with the length of the slot. In neutral position, the distance between the slot edges of the valve body and the spool is the gap described in Equation 3.2. After a certain angular displacement, the gap is calculated between the slot edge of the valve body and the normal to beveling surface of the spool, Equation 3.3. Equation 3.4 describes the area transient from the inner slot edge of the spool to the constant clearing, h_0. In neutral position, no torque applied ($T_{sw} = 0Nm$), the opening areas are equal. When torque is applied, half of the orifice opening areas will decrease, referred to as A_2, and the other half will increase, referred to as A_1.

$$A_{1,2} = L\sqrt{x_{A_{1,2}}^2 + (h_0 + b\tan(\gamma))^2} \tag{3.2}$$

$$\text{if} \qquad x_{A_{1,2}} \geq (h_0 + b\tan\gamma)\tan\gamma$$

$$A_{1,2} = L(x_{A_{1,2}}\tan\gamma + b\tan\gamma + h_0)\cos\gamma \tag{3.3}$$

$$\text{if} \qquad h_0\tan\gamma - b \leq x_{A_{1,2}} < (h_0 + b\tan\gamma)\tan\gamma$$

$$A_{1,2} = L\sqrt{h_0^2 + (x_{A_{1,2}}^2 + b)^2} \tag{3.4}$$

$$\text{if} \qquad -b \leq x_{A_{1,2}} < h_0\tan\gamma - b$$

$$A_{1,2} = L \cdot h_0 \tag{3.5}$$

$$\text{if} \qquad x_{A_{1,2}} < -b$$

$$x_{A_1}^2 = \frac{(b_1 - b_2)}{2} + R_{valve}\alpha_v \qquad x_{A_2}^2 = \frac{(b_1 - b_2)}{2} - R_{valve}\alpha_v \tag{3.6}$$

3.2 Area Modeling

Three different ways of determine the valve geometry have been investigated in this work. One destructive method has been used where the valve is cut in half and studied under a microscope, see Figure 3.1. In this case, the measurement was made before the destruction. Another method is to use a coordinate measuring machine; even in this case, the valve has to be disassembled. This does not destroy the valve itself, since the valve can be reassembled. However, the valve is sensitive to mismatch between the spool and the valve body. A small deviation in mounting angle between the valve body and the spool will give an unbalanced pressure curve. The third way is based on pressure measurements, the valve characteristic, and geometry adjustments until a match between the measurement and the simulation appear. This is carried out with the help of an optimization routine. The benefit to this method is eventual variation in the flow coefficient lumped together with the geometry function. When modeling the area instead of the geometry, the physical geometric design is party lost; on the other hand, this connection is only interesting when the power steering valve is designed from the very beginning. If an existing system is to be studied, the geometry of the specific valve is not interesting. When modeling the area, the model can be simplified without losing to much information.

As mentioned previously, the valve consists of multiple sets of orifices. This means that there exists between three and four set metering areas; depending on the valve layout, these can be seen as three or four parallel Wheatstone bridges. In Figure 3.2, there is a multiple of three orifices. In the model, these parallel Wheatstone bridges are seen as one single Wheatstone bridge, see Figure 2.12. When doing this, the deviation that exists between the Wheatstone bridges' areas is neglected. In Figure 3.3, the miss match between the valve body and

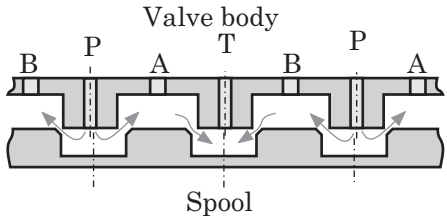

Figure 3.3 *Deviation in the aligning between the groves in the valve body and the spool.*

the spool is illustrated; the centering lines of the lands are not matching. In a production valve, the metering areas are not perfectly aligned, but the valve can be calibrated such that the valve is pressure balanced, $p_A = p_B$ when $T_{sw} = 0$. These variations are measured and the the variation is within $\pm 4\%$ of the maximal displacement*. This variation is illustrated in Figures 3.4 and 3.5, where the area function of a valve with a four multiple orifice configuration is shown. Due to the variation in the alignment of the orifices, a pure geometric area function is not valid when simplifying the valve to a single Wheatstone bridge.

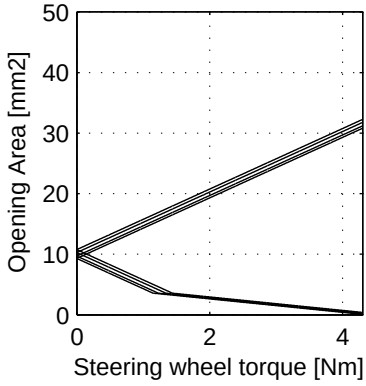

Figure 3.4 *Multiple metering orifices with individual deviation due to tolerances.*

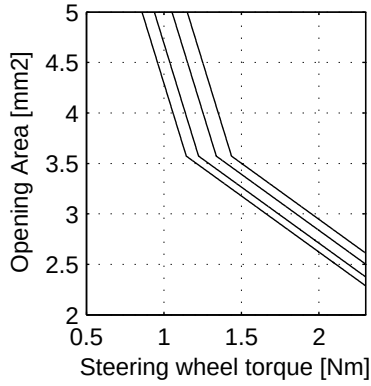

Figure 3.5 *Zoomed area of figure 3.4.*

In Figures 3.6-3.9, the difference between a lumped area function and a single area function is illustrated. The single area function is one ideal area opening based on the geometry of the valve, whereas the lumped area function is an average of, in this case, four individual area openings. As seen in Figures 3.7 and

*This is not statistically verified and is only valid for the studied valve.

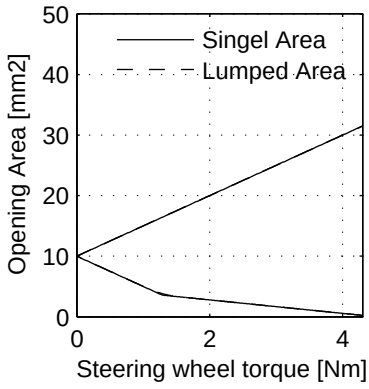

Figure 3.6 *Area openings based on single and lumped area functions.*

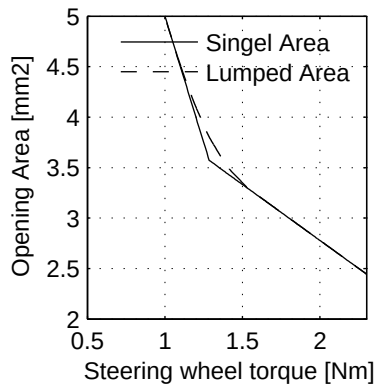

Figure 3.7 *Zoomed area of Figure 3.6.*

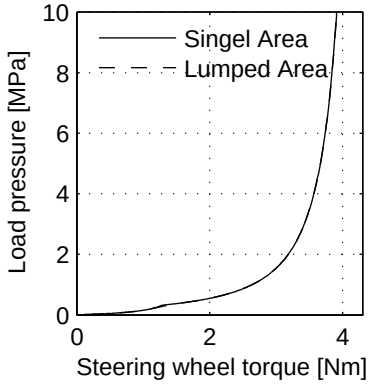

Figure 3.8 *Boost curve with single area and lumped area.*

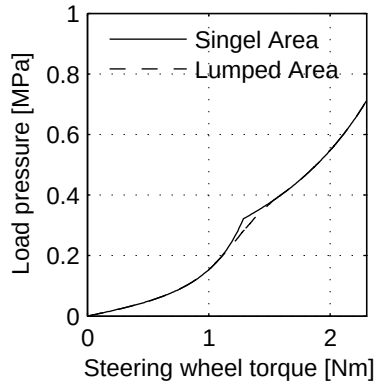

Figure 3.9 *Zoomed area of Figure 3.8.*

3.9, the transition from one area gradient to another is smoother due to the variation in multiple area functions.

In order to model the valve geometry correctly, all Wheatstone bridges, including individual deviations, have to be included in order to cover the real characteristic; however, this would be tedious work. Therefore, another approach has to be used. The modeling approach used in this work has mostly been carried out with the help of the area function instead of the geometric shaping of the valve. On the one hand, it can easily cover deviations in the valve and the function itself can be a simple single expression compared to the geometrical modeling that has to be divided into several regions, see Equations 3.2-3.6. On the other hand, it cannot be directly related to the design of

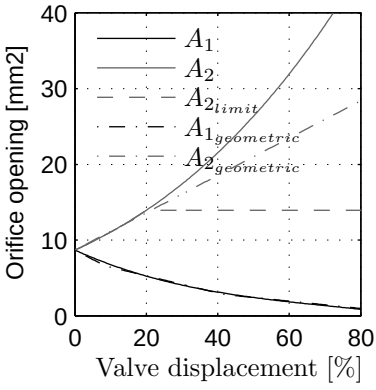

Figure 3.10 *The difference between a polynomial area function and the geometrical approach. Also visible in the figure is the limit in the increasing orifice area due to the valve body area limit.*

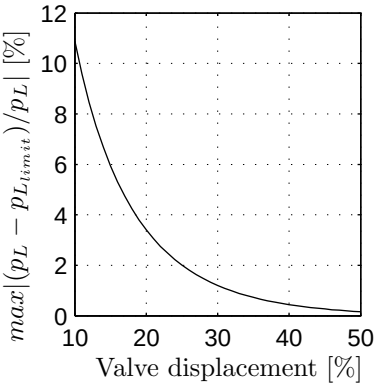

Figure 3.11 *Absolute modeling error due to neglecting the limitation in opening area. The limits start between 20-30% of the maximal valve displacement, which leads to a maximal modeling error of 3%.*

the valve. However, this drawback is not significant, especially when modeling an existing power steering unit.

Polynomial functions that can be used to describe the area are evaluated; it is found that a polynomial function of the third degree is suitable for this purpose, Equation 3.7. The advantage to using a third degree polynomial function is that it continuously covers the whole working envelope. This means that the area function will be continuously derivable.

$$\begin{aligned} A_1 &= K_3 T_{sw}^3 + K_2 T_{sw}^2 + K_1 T_{sw} + K_0 \\ A_2 &= -K_3 T_{sw}^3 + K_2 T_{sw}^2 - K_1 T_{sw} + K_0 \end{aligned} \tag{3.7}$$

In Figure 3.10, a comparison between the two different ways of modeling the valve is displayed, one based on the geometry and one based on the third degree polynomial function, notice the agreement in the closing metering edges during the whole valve displacement. The agreement between the opening edges is also good to a certain point; after this point they start to diverge. However, this is of minor importance, since the closing metering orifices are dominant.

Apart from the metering area discussed so far in this chapter, there are fixed external orifices, which become the dominant restriction, thereby limiting the opening areas when the valve is displaced, see $A_{2_{limit}}$ in Figure 3.10. Primarily, these orifices are between the valve and the cylinder and physically placed on the valve body. The effect of neglecting this limit is displayed in Figure 3.11, where the absolute load pressure error is shown as a function of valve displacement. In a normal valve, the external fixed orifices become dominant between

$20 - 30$ % of the valve displacement. As can be seen, the maximal error in the load pressure curve is approximately 3%, when the opening area function is limited to 20% valve displacement. Error in this region is acceptable. In a non-linear simulation, it is easy to implement this area limit; neglecting the external orifices is primarily beneficial when it comes to linear analysis.

The benefits of using the polynomial function are mentioned prior to the possibility of using one function to represent a lumped model for the valve, thereby also covering tolerances in the valve, which in the geometrical model are tedious and time consuming to cover. The polynomial function is also simpler than the geometric representation of the valve. This method also covers double beveled valve geometry with the same function description. The simple polynomial function is also useful when it comes to identifying the area function with the help of optimization routine, due to fewer parameters that have to be optimized. Below, the required input needed to perform geometric modeling or area function modeling is summarized.

Geometric vs. Area modeling of the valve

Geometric	Area
- Geometry of every metering edge - Individual deviation in matching between the metering edges - Variation in flow coefficient	Boost Curve

3.3 Identification of Area Function with the Help of Optimization

The main input data for the determination of the power steering characteristics is the boost curve. In order to simulate the complete system, the valve geometry must be determined. The geometry can be determined by physical measurements of the valve, but this method is time consuming and not easy to apply during development phases, as discussed earlier. Therefore, the opening area will be determined by optimization. In order to determine the area function related to the boost curve, four parameters need to be determined. Three of these parameters are obtained by optimization; the last can be established by a static calculation based on the pressure drop over the valve, when the valve is not displaced. From Equation 2.12, it is possible to resolve the areas when equal, thereby calculating them based purely on the pressure drop, see Equation 3.8. The results of this gives the coefficient K_0 in Equation 3.7.

$$A|_{T_{sw}=0} = \frac{q_s}{2c_q}\sqrt{\frac{\rho}{p_s}} = K_0 \tag{3.8}$$

When optimization methods are applied, some trivial questions must be set such as:

- What are the optimization parameters?
- Why optimize? What is the function objective?
- How to formulate the optimization problem?

In the present case, the optimization parameter is the opening area from the valve as a function of the valve displacement angle, which is really dependent on the applied steering wheel torque, T_{sw}. The optimization parameters are the three parameters, $K_1 - K_3$, determining the opening area in Equation 3.10. The optimization function is defined by the integrated product of the objective function and weight function, Equation 3.11. The objective function is defined by the absolute value of the difference between the measured load pressure and the determined load pressure based on the opening area, see Equation 3.12. Equation 2.11, described in Chapter 2, determines the calculation of the load pressure used . The optimization problem has been specified to determine the opening area parameters; the objective function is shown in Equation 3.9. In order to improve the precision in the lower part of the boost curve, the objective function has different weighting, see Equation 3.13.

$$Optimization \qquad \begin{cases} \min\limits_{X} F(T_{sw}, X) \\ X_{\min} < X < X_{\max} \end{cases} \tag{3.9}$$

$$X = [K_1, K_2, K_3] \tag{3.10}$$

$$F(T_{sw}, X) = \int_0^{Tsw_{\max}} (F_{Obj}\,(T_{sw}, X) \cdot F_{Weght}\,(T_{sw}))dT_{sw} \tag{3.11}$$

$$F_{Obj}\,(T_{sw}, X) = \underbrace{[|P_{\text{Lcalc}}\,(T_{sw}, X) - P_{\text{Lmeasure}}\,(T_{sw})|]}_{Objective} \tag{3.12}$$

$$F_{Weight}(T_{sw}) = \begin{cases} C_1 & T_{sw} \leq 1 \\ C_2 & 1 < T_{sw} \leq 2 \\ C_3 & T_{sw} > 2 \end{cases} \tag{3.13}$$

The results of one optimization are displayed in Figure 3.12, where both the load pressure, calculated and measured, and representing object function values are displayed. The measured load pressure used for the optimization is in the routine limited to 7 MPa to minimize the effect of the pressure relief valve. Since the curve is strongly non-linear, almost exponential, the object function has to be weighted. In this case, the errors generated below 1 Nm are weighted 400 times higher than values at the end and values under 2Nm are weighted 10 times higher, see Equation 3.13. The results in the form of an area opening function are shown in Figure 3.13. The optimization routine used in this work

is called the Complex Method and was first presented by M.J. Box [43]; a description of this method can also be found in the PhD thesis written by J. Andersson [44].

The obtained parameters for the opening area are used in the following calculations, where the characteristics of the total system are determined. In the present case, the same parameter settings are used for all orifices. In the area function, which is the result of the optimization, not only does it contain the shape of the geometrical area, but also covers eventual variation in the flow coefficient, c_q.

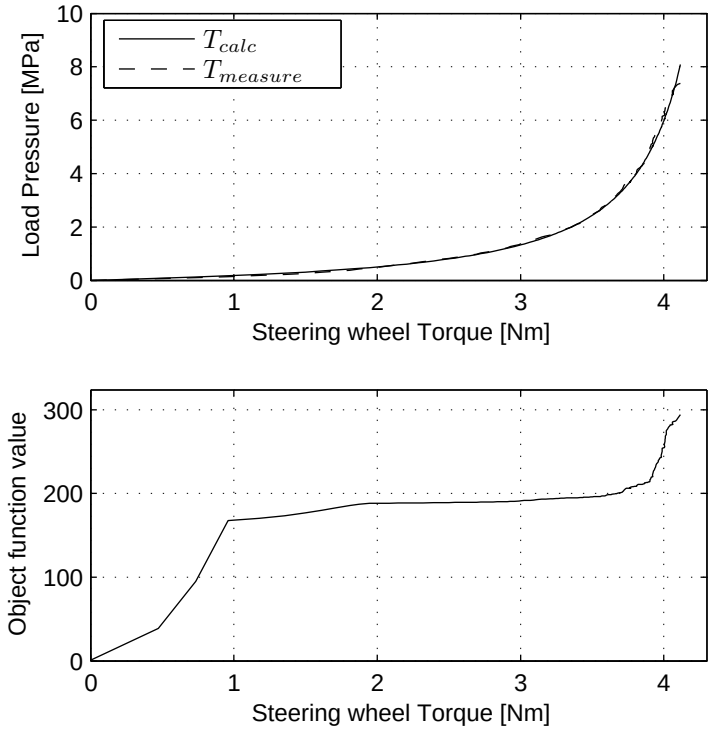

Figure 3.12 *The top graph shows the results of the optimization, measured and simulated load pressure. The lower graph shows the object function value, $F(T_{sw})$, displaying the integrated error between measured and simulated load pressure. Observe that errors below 1 Nm are weighted 400 times harder than errors at high torque.*

It must be noted that the methods presented above are useful when the the valve geometry or area function is not known, *vehicle manufactures*. A valve manufacture that has this knowledge will not benefit from these methods as they are described. However, the optimization routine can be used to generate the geometry from a given boost curve. In the area function described above,

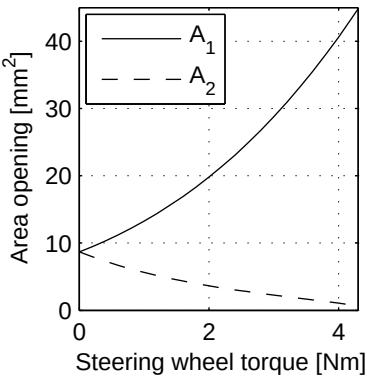

Figure 3.13 *The optimized area function corresponding to Figure 3.12.*

the tolerances and the variation in the flow coefficient are lumped together. If these variations are known, the optimization routine could be used to find a geometry that will fit the boost curve given by the car manufactures. The area function modeling would be interesting for valve manufactures if they would perform stability analysis of the system or carry out analysis of the robustness of the design in the dynamic sense.

In this work, the main reason to model the valve in detail is to be able to build reliable models both linear, for stability analysis, and non-linear models, for functional analysis as well as investigation of non-linear phenomena such as hydraulic lag. These models are described in the following chapter.

4

Modeling of Hydraulic Power Assisted Steering

Modeling and simulation are important parts of improving and developing the design of most systems. The main reasons to utilize modeling and simulation are cost, knowledge and design freedom, [45].

In this thesis, two different approaches to modeling have been used, frequency domain and time. The first approach investigates the power steering system in the frequency domain in order to understand the system's controller and to get information regarding the system's stability and robustness for tolerances. The second approach investigates the system in the time domain. The strength of this approach is that the different components included in the complete system can be modeled in a "close to reality" way, thereby easing the analysis of the components. This way of modeling is also feasible when it comes to introducing and simulating new designs and changes. Both methods have their strengths and weaknesses and they should be seen as compliments to each other. For example, the time domain model is useful when it comes to validating the model parameters used in the linear model. However, stability analysis is hard to perform in a global sense in the time domain.

The system needing to be modeled is displayed in Figure 4.1, where a simplified view of the system is displayed. In the figure, the power steering system is solidly attached to the sub-frame, where the steered wheels are also attached. To reduce the transfer of vibration, the connection between the wheels and the sub-frame is made through rubber bushings, which is also the case between the sub-frame and the body. These bushings can be seen as a spring damper system that connects ingoing parts. Some of the non-connecting parts can also be seen as a spring, for example the tie-rod. A different view of the system is displayed

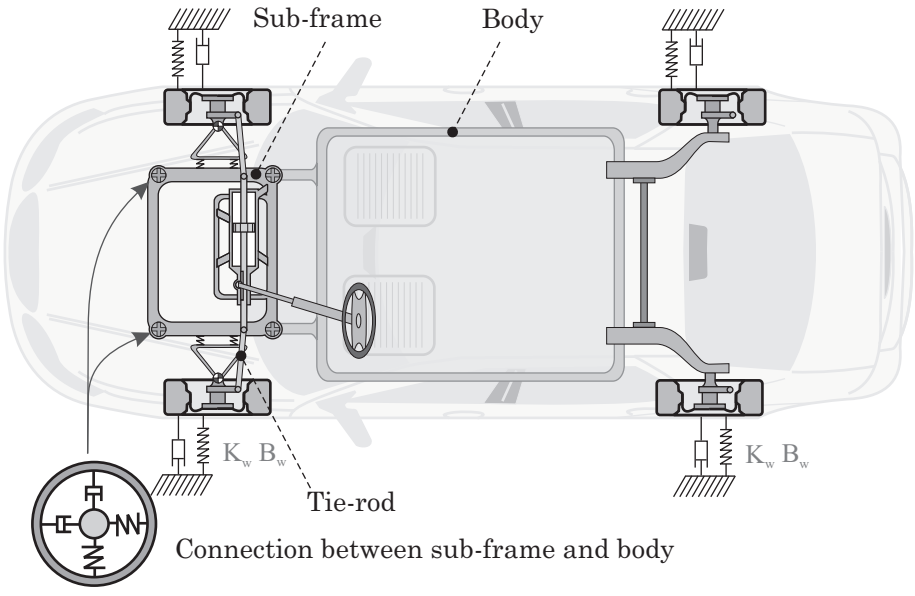

Figure 4.1 *Power steering position connected to the chassis of a vehicle, including the possible connection to the surrounding elements. Connections are illustrated with spring and damper elements. There are other mounting possibilities than the one displayed.*

in Figure 4.2, where the ingoing components are arranged as a multiple spring mass system together with the power steering system. The focus of this work is to study the power steering unit, which also reflects on the model view of the system. It can be seen in Figure 4.2 that the power steering unit is in the center; note also that the mass of the surrounding system is aligned and related to the motion of the HPAS system. The steering wheel and the steered wheels are also transformed from an inertia to a mass. In order to model the system completely, not only the parameters of the power steering system are needed, but the parameters of the surrounding components and the connection between the components also have to be identified.

Depending on the reason for modeling, different complexity levels of the model have to be chosen. In this case, the complexity level can be seen as the level of detail. The complexity and usability of the model is not a linear relationship. As a model grows, the usability of the model increases rapidly. After a certain point, usability does not increase with complexity; it can even decrease, see Figure 4.3. The reason for this halt in increased usability is that the new level of detail is not validated or there exists an amount of uncertainty concerning parameter values. The level of detail could also be unbalanced; part of the model has a high level of detail while a different part has a low level of

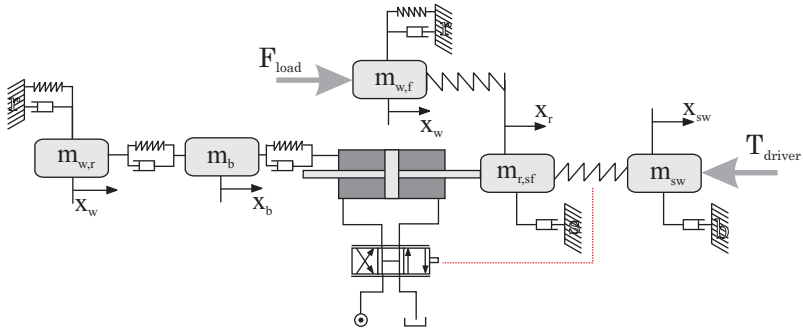

Figure 4.2 *Equivalent system representation of power steering system. Including the wheels ($_{w,f}$, $_{w,r}$), rack ($_r$) including sub-frame ($_sf$), steering wheel ($_{sw}$) and the connection to the chassis. Note the grounding points have different references, s - sub-frame, b - body and r - road.*

detail.

Normally, the level of detail choice comes naturally, especially when the model is used to seek an answer to an already asked question, problem seeking. When a model evolves, it has to be validated with real measurements until a match between the model and reality is acceptable. A subjective judgement based on earlier modeling experiences or system knowledge is acceptable. If no hardware or data exists to be used in the validation of the model, the detail level of the model is naturally low but can still be useful for system understanding and early sizing. In this work, an even simpler view, compared to the

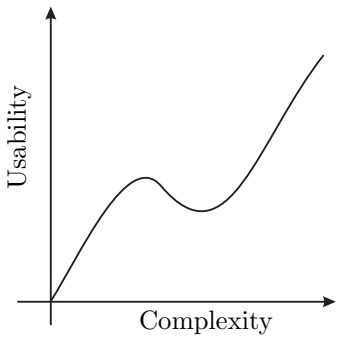

Figure 4.3 *Model usability verses model complexity.*

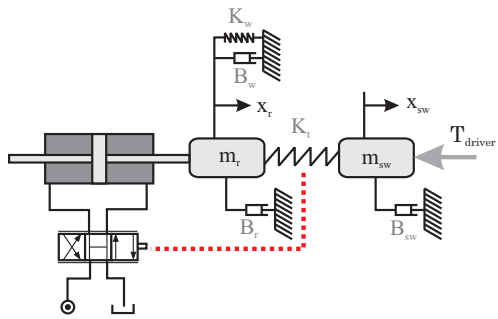

Figure 4.4 *Simplified representation of the system, which is used in this work.*

one displayed in Figure 4.2, has been chosen. In the applied model, the effect of the body is neglected, this is due to the fact that a simpler view of the system, Figure 4.4, has been accurate enough for the studied problems. Involving

the body would lead to an unnecessarily complex model. The motion of the sub-frame in relation to the body is thereby neglected; this information might be interesting from a handling point-of-view, but not when studying the power steering unit. One could argue that the spring damper system, which connects the body and the sub-frame, could affect the dynamic behavior of the steering unit. However, this effect is minor when the body mass is large and could be seen as a ground, equal to the road, in higher frequencies; therefore, it is possible to lump the springs mounted between the body and the sub-frame with the spring effect in the tire. The spring effect in the tie-rods is also neglected. However, this simplification is only valid in the configuration concerning cars; in trucks, the spring coefficient in the linkage system is not negligible.

4.1 Linear Model

When it comes to stability analysis and system understanding, the linear view of the system is suitable. Dynamic connection and interaction between the ingoing components can be studied. In this section, the linear model used in this work is presented along with analysis regarding stability and dynamic robustness of the system. Below are the equations describing the system as Figure 4.4 stated. Note that all motions are linear and related to the motion of the steering rack.

The force of the steering wheel is described in Equation 4.1 below. In this equation, the torque applied by the driver, T_{driver}, is transferred to a linear force by the radius of the pinion gear, r_r.

$$\Sigma F_{sw}: \quad \ddot{x}_{sw} m_{sw} + B_{sw}\dot{x}_{sw} + K_t(x_{sw} - x_r) - \frac{T_{driver}}{r_r} = 0 \tag{4.1}$$

Equation 4.2 describes the rack, also including the tires.

$$\Sigma F_{sw}: \quad \ddot{x}_r m_r + (B_r + B_w)\dot{x}_r + K_t(x_r - x_{sw}) + K_w x_r + F_L = 0 \tag{4.2}$$

The hydraulic system is described according to Equation 4.3.

$$\dot{p}_L = -\frac{K_c}{C} p_L + \frac{K_q}{C} x_v - \frac{A_p}{C}\dot{x}_p \tag{4.3}$$

The actuation of the valve is created by the difference between steering wheel position and the rack position, Equation 4.4.

$$x_v = x_{sw} - x_r \tag{4.4}$$

As previously mentioned, the power steering system is a closed loop system where the controlled variable is the position of the rack. The input and reference signal is the steering wheel angle. This can be seen as a classic follower servo solution with a weak controller and manual feed forward. Using the linear system to understand the fundamental principle of the system is useful. In

Figure 4.5, the system is illustrated as a block diagram, which is based on the equations presented above, Equations 4.1-4.4. In the block diagram, the input signal is the driver's torque, T_{driver}, and the output is the position of the steering rack, which represents wheel angle on the steered wheels. All of the motion in the system is transferred to linear motion related to the motion of the steering rack. In the block diagram, the control loop is also visible; the reference value is given by the position of the steering wheel. Since the system contains a closed loop, the question regarding stability is interesting. In order to study the stability margins, the open loop system is of interest. The open loop system in Figure 4.5 is marked with a dashed line. As mentioned earlier, activation of the hydraulic system is accomplished by a difference in the steering wheel angle and the angle of the pinion. When the system motion is transferred to pure linear motion, the difference between the steering wheel position and the position of the steering rack is shown. The difference between them creates a valve displacement, x_v, which modulates the pressure within the hydraulic cylinder.

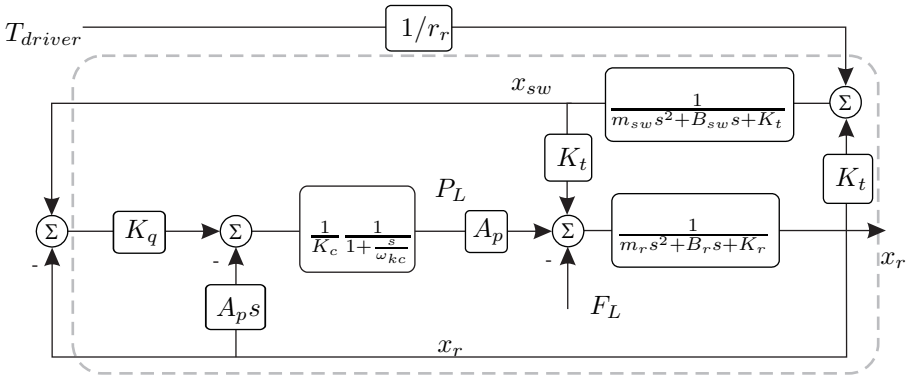

Figure 4.5 *Block diagram of the power steering system, open loop system is outlined by the dashed line*

A state space model of the open loop system is used in linear analysis of the system concerning stability margins, Equations 4.1 and 4.1. In the model, most of the parameters are related to the mechanical structure, such as masses, spring coefficients and the viscous friction, also included are the hydraulic coefficients that vary depending on the working points. The working point dependency of hydraulic coefficients has to be established in order to be able to perform system stability margin analysis.

$$\dot{x} = Ax + Bx_v \tag{4.5}$$

$$
\begin{aligned}
x &= \begin{bmatrix} x_r & \dot{x}_r & x_{sw} & \dot{x}_{sw} & p_L \end{bmatrix} \\
A &= \begin{bmatrix} 0 & 1 & 0 & 0 & 0 \\ \frac{-K_w - K_t}{mr} & \frac{-B_r}{m_r} & \frac{K_{tor}}{m_r} & \frac{B_{sw}}{m_r} & \frac{A_p}{m_r} \\ 0 & 0 & 0 & 1 & 0 \\ \frac{K_t}{m_{sw}} & \frac{B_{sw}}{m_{sw}} & \frac{-K_t}{m_{sw}} & \frac{-B_{sw}}{m_{sw}} & 0 \\ 0 & \frac{-A_p}{C} & 0 & 0 & \frac{-K_c}{C} \end{bmatrix} \\
B^T &= \begin{bmatrix} 0 & 0 & 0 & 0 & \frac{Kq}{C} \end{bmatrix}
\end{aligned} \tag{4.6}
$$

4.1.1 Calculation of the hydraulic coefficients

In order to make the state space model complete, the hydraulic coefficients, K_q, K_c and C have to be established. Equation 4.3 is a linearization of the equations describing the hydraulic system and the coefficients mentioned above are linear coefficients valid only in the working point used for the calculation.

The calculation of these coefficients is essential for the stability analysis of the power steering system and is used for calculating the stability margins of the system in different working points, as will be shown later. In order to design controllers for future enhanced functionality, a knowledge of the system dynamic and stability is essential.

The first two equations to be linearized are first presented as Equations 2.3 and 2.4 in section 2.3. These equations concern the load flow, q_l, and the system flow, q_s, dependency of the system pressure, load pressure and valve displacement, p_s, p_L and x_v, and are the orifice equations. The results of this linearization are displayed in Equations 4.7 and 4.8.

$$Q_L = K_{q1}X_v + K_{c2}P_S - K_{c1}P_L \tag{4.7}$$

$$Q_S = -K_{q2}X_v + K_{c1}P_S - K_{c2}P_L \tag{4.8}$$

The load flow can also be described by the motion of the hydraulic cylinder and the compressibility in the cylinder. This equation is considered the continuous flow equation and the linearized result is displayed in Equation 4.9. Also, system flow, q_s, will variate due to compressibility and possible variation in the delivered flow from the pump. Later in this analysis, the variation due to the pump will be neglected but is kept here for completeness, Equation 4.10.

$$Q_L = A_p s X_r + \frac{V_0}{2\beta_e} s P_L \tag{4.9}$$

$$Q_p - Q_s = \frac{V_v}{\beta_e} s P_S \tag{4.10}$$

With the help of Equations 4.8-4.10, the load pressure can be resolved as a function of the valve displacement, x_v, rack position, x_r and the flow delivered

by the pump, q_p. In Equation 4.11, the hydraulic coefficients, K_c and K_q, are identified.

$$\begin{aligned} P_L = & \underbrace{\frac{K_{c1}}{K_{c1}^2 - K_{c2}^2}}_{=1/K_c} \overbrace{\frac{\left(1 + \frac{V_V}{K_{c1}\beta_e}s\right)}{\left\{1 + 2\frac{\delta_0}{\omega_0}s + \frac{s^2}{\omega_0^2}\right\}}}^{\approx \frac{1}{1+\frac{s}{\omega_n}}} \cdot \\ & \left\{ \underbrace{\frac{\left(1 + \frac{V_V s}{\left(K_{c1} + \frac{K_{q2}}{K_{q1}}K_{c2}\right)\beta_e}\right)}{1 + \frac{V_V}{K_{c1}\beta_e}s}}_{\approx 1} \underbrace{K_{q1}\left(1 + \frac{K_{c2}K_{q2}}{K_{c1}K_{q2}}\right)}_{=K_q} X_v \right. \\ & \left. - \frac{K_{c2}}{K_{c1}} \frac{1}{1 + \frac{V_V}{K_{c1}\beta_e}s} Q_p - A_p s X_r \right\} \end{aligned} \tag{4.11}$$

Some of the dynamic in the equation can be neglected. The second order dynamic formed by δ_0 and ω_0 is over damped and can, therefore, be separated into two first order filters, where the break frequencies can be described according to Equations 4.12 and 4.13. Notice that one of the resulting frequencies from the separation fits the break frequency in the nominator, making it possible to reduce the dynamic to a low-pass filter of the first order. The dynamic concerning the valve displacement is neglected, due to the fact that the break frequencies are close to each other and, therefore, cancel each other out.

$$\begin{aligned} \omega_0 = & \sqrt{\frac{2\left(K_{c1}^2 - K_{c2}^2\right)}{V_0 V_V}}\beta_e \\ \delta_0 = & \frac{1}{\sqrt{2}} \frac{K_{c1}}{\sqrt{K_{c1}^2 - K_{c2}^2}} \frac{\frac{V_0}{2} + V_V}{\sqrt{V_0 V_V}} \end{aligned} \tag{4.12}$$

$$\begin{aligned} 2\delta_0\omega_0 = & \frac{2K_{c1}\left(\frac{V_0}{2} + V_v\right)\beta_e}{V_0 V_V} \approx \frac{K_{c1}\beta_e}{V_V} = \omega_t \\ \frac{\omega_0}{2\delta_0} = & \frac{K_{c1}^2 - K_{c2}^2}{K_{c1}} \frac{\beta_e}{\frac{V_0}{2} + V_v} = K_c \frac{\beta_e}{\frac{V_0}{2} + V_v} = \omega_n \end{aligned} \tag{4.13}$$

The load pressure can then be reduced and described as Equation 4.14.

$$P_L = \frac{1}{K_c\left(1 + \frac{s}{\omega_n}\right)} \left(K_q X_v - \frac{K_{c2}}{K_{c1}\left(1 + \frac{s}{\omega_n}\right)} \underbrace{Q_p}_{\approx 0} - A_p s X_r \right) \tag{4.14}$$

The hydraulic coefficients can be described as in Equations 4.15 and 4.16.

$$K_c = \frac{K_{c1}^2 - K_{c2}^2}{K_{c1}} \tag{4.15}$$

$$K_q = K_{q1}\left(1 + \frac{K_{c2}K_{q2}}{K_{c1}K_{q1}}\right) \tag{4.16}$$

The coefficients consist of partially linearized coefficients relating to the linearization of the orifice equation describing the load flow and the system flow, Equations 2.3 and 2.4 in section 2.3. As seen in these equations, they depend on a specific working point referring to a certain level of system pressure, load pressure and valve displacement. The valve displacement gives the area, A, and the area gradient, w, Equations 4.17-4.20.

$$K_{q1} = -c_q\sqrt{\frac{p_S - p_L}{\rho}}w\left[-x_v\right] - c_q\sqrt{\frac{p_S + p_L}{\rho}}w\left[x_v\right] \tag{4.17}$$

$$K_{q2} = c_q\sqrt{\frac{p_S - p_L}{\rho}}w\left[-x_v\right] - c_q\sqrt{\frac{p_S + p_L}{\rho}}w\left[x_v\right] \tag{4.18}$$

$$K_{c1} = \frac{c_q A\left[-x_v\right]}{2\sqrt{(p_S - p_L)\rho}} + \frac{c_q A\left[x_v\right]}{2\sqrt{(p_S + p_L)\rho}} \tag{4.19}$$

$$K_{c2} = \frac{c_q A\left[-x_v\right]}{2\sqrt{(p_S - p_L)\rho}} - \frac{c_q A\left[x_v\right]}{2\sqrt{(p_S + p_L)\rho}} \tag{4.20}$$

By using the expressions derived in section 2.3, Equations 4.17-4.20 can be simplified by using Equation 4.21.

$$\begin{aligned} p_S - p_L &= \frac{\rho}{4}\left(\frac{q_s}{c_q A\left[-x_v\right]}\right)^2\left(1 + \frac{q_L}{q_s}\right)^2 \\ p_S + p_L &= \frac{\rho}{4}\left(\frac{q_s}{c_q A\left[x_v\right]}\right)^2\left(1 - \frac{q_L}{q_s}\right)^2 \\ q &= \frac{q_L}{q_S} \end{aligned} \tag{4.21}$$

Instead of depending on the pressure as a working point, the coefficients depend on the actual valve displacement and current load flow, q_L. Notice that the load flow is normalized with the system flow and noted as q. By doing so, these equations are reformed into Equations 4.22–4.25.

$$K_{q1} = -\frac{q_s}{2}\left((1+q)\frac{w\left[-x_v\right]}{A\left[-x_v\right]} + (1-q)\frac{w\left[x\right]}{A\left[x\right]}\right) \tag{4.22}$$

$$K_{q2} = \frac{q_s}{2}\left((1+q)\frac{w\left[-x_v\right]}{A\left[-x_v\right]} - (1-q)\frac{w\left[x\right]}{A\left[x\right]}\right) \tag{4.23}$$

$$K_{c1} = \frac{c_q^2}{q_s\rho}\left(\frac{A\left[-x_v\right]^2}{(1+q)} + \frac{A\left[x_v\right]^2}{(1-q)}\right) \tag{4.24}$$

$$K_{c2} = \frac{c_q^2}{q_s\rho}\left(\frac{A\left[-x_v\right]^2}{(1+q)} - \frac{A\left[x_v\right]^2}{(1-q)}\right) \tag{4.25}$$

By reformulating Equation 4.14, the hydraulic system can be described as in Equation 4.26, with the capacitance given in Equation 4.27.

$$\dot{P}_L = -\frac{K_c}{C}P_L + \frac{K_q}{C}X_v - \frac{A_p}{C}\dot{X}_p \tag{4.26}$$

$$C = \frac{\frac{V_0}{2} + V_v}{\beta_e} \tag{4.27}$$

In Figures 4.6-4.8 below, the hydraulic coefficients are plotted for different values of valve displacement and normalized load flow. The value of the coefficients is normalized based on the value at zero valve displacement. As seen in the graph, the coefficients strongly depend on the working point, both valve displacement and load flow. An additional coefficient is calculated from the pressure dependent flow gain, K_c and the flow gain, K_q; the result is pressure gain, $K_p = \delta P_L/\delta x_v$, see Equation 4.28. This coefficient reflects the derivative of the boost curve due to the linear relationship between the applied steering wheel torque, T_{sw}, and the valve displacement, x_v. Since the boost curve is, by its design, highly non-linear, the hydraulic coefficients inherit this non-linearity. Based on the knowledge of the hydraulic system and the mechanical connections, it is now possible to perform stability analysis.

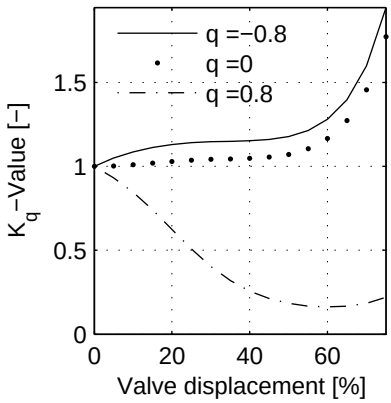

Figure 4.6 *Variation in the flow gain, K_q, as a function of valve displacement and for different values of normalized load flow, q.*

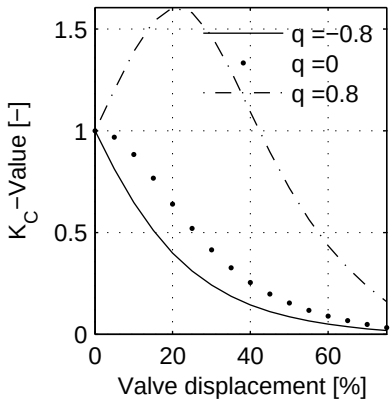

Figure 4.7 *Variation in the pressure depending flow gain, K_c, as a function of valve displacement and for different values of normalized load flow, q.*

The K_q, K_c and K_p values displayed in Figures 4.6-4.8 are normalized with respective value at q=0 and x=0.

$$K_p = \frac{K_q}{K_c} \qquad (4.28)$$

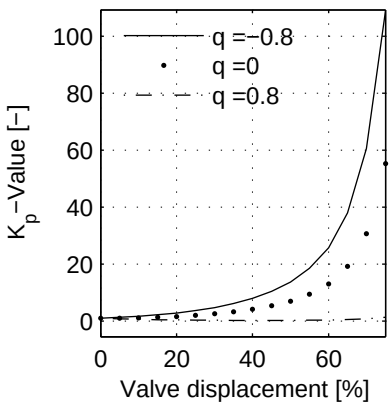

Figure 4.8 *Variation in the pressure gain, K_p, as a function of valve displacement and for different values of normalized load flow, q.*

4.1.2 Stability analysis

Power steering systems are closed loop systems; therefore, there is a possibility to design a system that is instable. Stability problems in the power steering unit normally result in limited cycling in the position feedback, which in turn results in vibration and noise. The phenomena with limit cycling is a common problem and is called chattering, also mentioned as shuttering, shuddering or hydraulic grunt. The analysis carried out in this section is based on a power steering unit for a truck, see Figure 4.9. The linear model is used to explain the chattering phenomena. The design of the system is similar to the hydraulic power steering units found in a car. The linkage between the HPAS unit and the wheel has a different design. The HPAS unit is solidly attached to the frame and spring coefficients and dampening between the rack and the frame is, therefore, neglected. In the case studied, the linkage between the HPAS unit and the wheel is more complex; the stiffness in the linkage is not negligible.

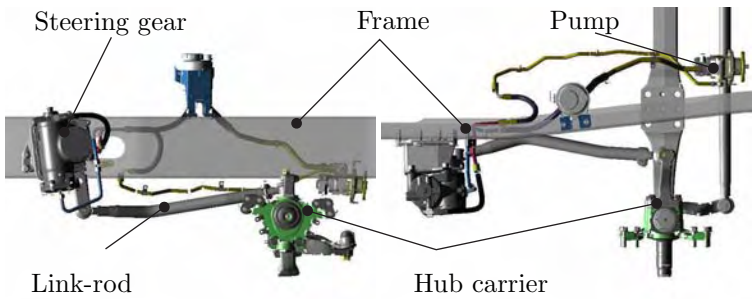

Figure 4.9 *Steering linkage for a truck including power steering unit with pump hoses and oil reservoir.*

The stability analysis of the system is done in the open loop system. The system used is described in the state space mode, see Equation 4.29. The corresponding equivalent system is displayed in Figure 4.10. The open loop system is defined by the transfer function, $G_o(s) = x_r/x_v$, which is formed with the help of the state space model.

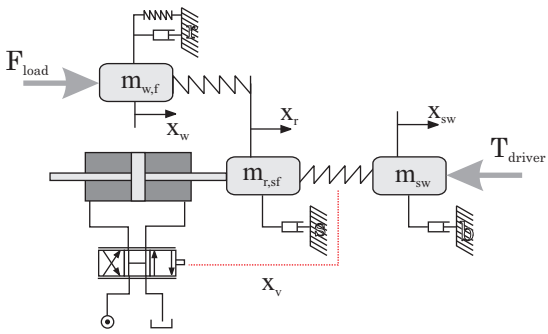

Figure 4.10 *Equivalent system representation of the power steering systems in a truck.*

$$
\begin{aligned}
\dot{x} &= Ax + Bu \\
y &= Cx + Du \\
x &= \begin{bmatrix} x_w & \dot{x}_w & x_r & \dot{x}_r & x_{sw} & \dot{x}_{sw} & p_L \end{bmatrix} \\
A &= \begin{bmatrix}
0 & 1 & 0 & 0 & 0 & 0 & 0 \\
\frac{-K_t - K_{lr}}{m_w} & \frac{-B_w}{m_w} & \frac{K_{lr}}{m_w} & 0 & 0 & 0 & 0 \\
0 & 0 & 0 & 1 & 0 & 0 & 0 \\
\frac{K_{lr}}{m_r} & 0 & \frac{-K_{lr} - K_{tor}}{mr} & \frac{-B_r}{m_r} & \frac{K_{tor}}{m_r} & \frac{B_{sw}}{m_r} & \frac{A_p}{m_r} \\
0 & 0 & 0 & 0 & 0 & 1 & 0 \\
0 & 0 & \frac{K_{tor}}{m_{sw}} & \frac{B_{sw}}{m_{sw}} & \frac{-K_{tor}}{m_{sw}} & \frac{-B_{sw}}{m_{sw}} & 0 \\
0 & 0 & 0 & \frac{-A_p}{C} & 0 & 0 & \frac{-K_c}{C}
\end{bmatrix} \\
B^T &= \begin{bmatrix} 0 & 0 & 0 & 0 & 0 & 0 & \frac{Kq}{C} \end{bmatrix} \\
C &= \begin{bmatrix} 0 & 0 & 1 & 0 & 0 & 0 & 0 \end{bmatrix}
\end{aligned}
\tag{4.29}
$$

In Figure 4.11, the bode plot of the open loop system is shown. The working point is zero valve displacement and no load flow, $x_v = 0$ and $q = 0$. In the graph, the resonance frequency of the system is $\approx$ 200 Hz. The dip in the amplitude curve at 5 Hz is due to the steering wheel, which at its resonance frequency annuls any incoming signals. In this case, the system is stable and the system should have no problems with chattering. However, the system gain is strongly dependent on the working point as discussed in section 4.1.1. In Figure 4.12, two other working points are evaluated, one which is stable and one where the amplitude margin is negative, which will result in an unstable system behavior. In order to verify the stability margin for the system, every possible working point has to be evaluated or at the least, identify the area in the working envelope that could cause stability problem.

The rest of this section focuses on using the linear model to explain the shuttering problem; the case is also described in paper [I]. Measurements of the studied scenario are displayed in Figure 4.13, where different variables are plotted on the same graph. The graph shows measurements where the steering unit is driven by the load rather than the torque applied by the driver. This is representative of a vehicle exiting a curve; the aligning torque acting on the wheel drives the power steering system, at the same time the driver applies torque to the steering wheel to control the returning motion. This in turn means that the motion on the steering gear and the applied steering wheel torque are working in opposite directions, resulting in negative load flow, $q < 0$.

In the beginning of the sequence, Figure 4.13, the system is at rest and the force balance between the external load and the force generated by the hydraulic system, $p_s \approx 63\ bar$, plus manual torque, $T_{sw} \approx 3.7\ Nm$, are equal. The driver lets go of the steering wheel, t=7.9 s, and the returning motion is started. At t=8.25 s, oscillation in the system starts, which causes vibration and noise. Even though the system has unstable behavior, the main task, assisting

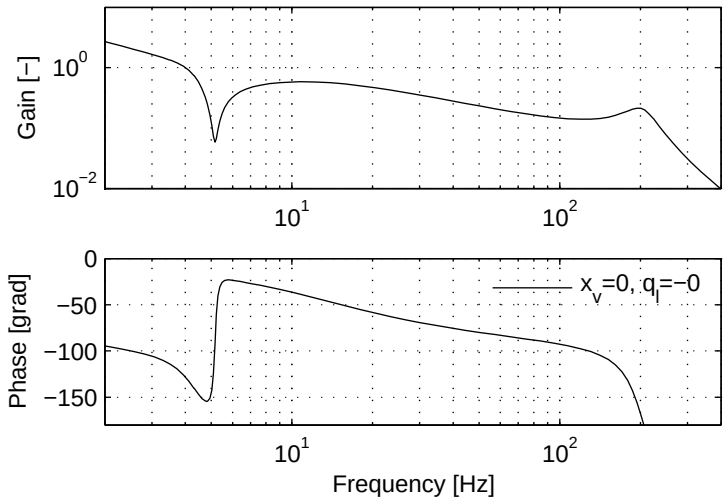

Figure 4.11 *Bode plot of the open loop system, G_o. Working point: $x_v = 0$, $q_L = 0$. The dip in the gain and phase plot at approximately 5 Hz is due to the resonance frequency of the steering wheel.*

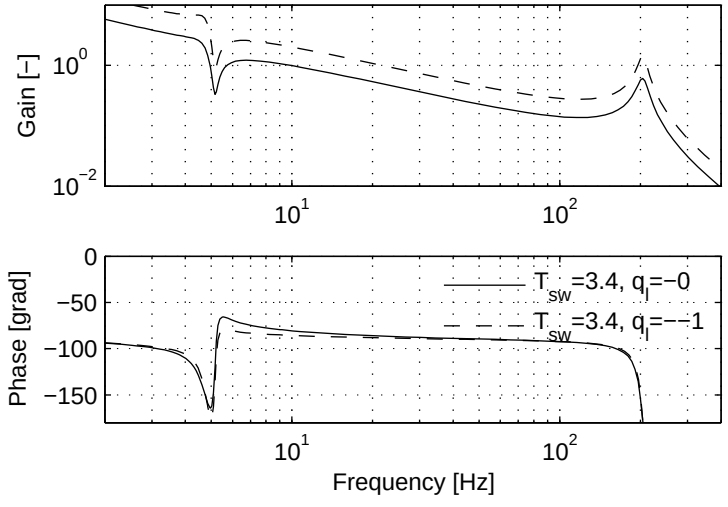

Figure 4.12 *Bode plot of the open loop system, G_o. Two different working points. The working point defined by the solid line will result in a stable system; whereas the working point defined by the dashed line has a negative amplitude margin and will result in an unstable system.*

the driver, is not noticeably reduced. Therefore, the problem with chattering is seen as a quality problem. At t=9.05 s, the vibration disappears. In order to explain the behavior of the system, the amplitude margin of the system is investigated and plotted as a function of the load flow and applied steering wheel torque, which are the two variables that define the working point, see Figure 4.14. In the figure, the contour lines represent the amplitude margin for the actual working point.

The working point trajectory of the case displayed in Figure 4.13 is inserted and also defined with time stamps, notice that the trajectory starts in an area defined by the working points which are stable. Between T=8.1 and T=8.3, the working point trajectory enters the unstable area of the system and will stay there until T=8.9, which defines the system in an unstable area, working envelope between 8.2 s to 8.9 s. This linear analysis can be used to explain the chattering phenomena; it could also be used to avoid chattering. The chattering phenomena often appears after the vehicle is put into production, due to the fact that the characteristic of the steering system is somewhat individual from system to system, as all components are produced with tolerances. The deviation in the geometrical shape and matching will give every system and especially the valve an individual characteristic. This variation could result in instability in the closed loop system and chattering. In the design of the valve or the system, vehicle manufactures specify the characteristic of the valve to the power steering manufactures, which respond to the demand by delivering a specification of tolerances that may be produced. Such an example is seen in Figure 4.15, where the valve producer has specified the tolerances regarding the outcome of production. The curves in the graph specify the inner and outer limits of the produced valves. The analyzes preformed above were preformed on a characteristic close to the inner curve. Based on this graph, the spread in characteristics could be analyzed in order to secure the stability of the system. In order to prevent the shuttering problem, the valve design could, with the help of the model presented above, be evaluated for stability before the vehicle is put in production and there by reduce the risk of chattering later in the production. Further discussion concerning the subject can be found in paper [I], where a plot similar to figure 4.14 is shown with a nominal valve characteristic.

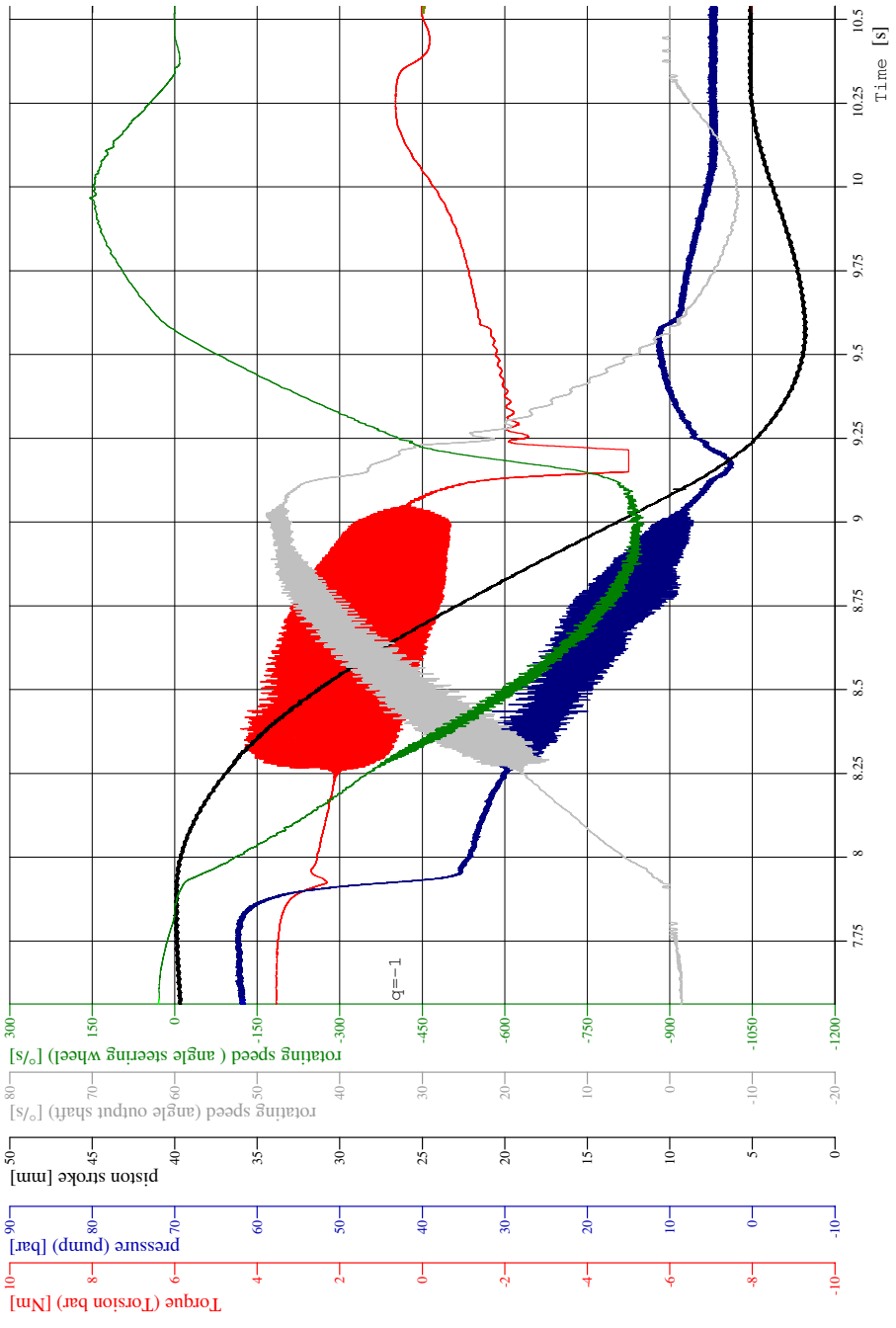

Figure 4.13 *Measurements of a chattering problem. The scenario is a returning motion where the steering wheel speed and applied steering wheel torque work in opposite directions.*

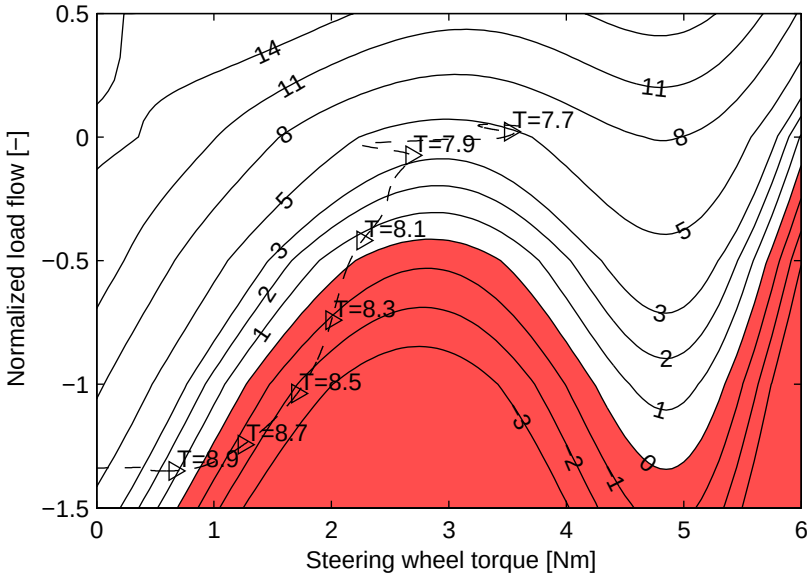

Figure 4.14 *The stability margin in the working envelope characterized with the amplitude margin as contour lines. Red area represents negative amplitude margin and instability in the steering system. In the plot, the trajectory from Figure 4.13 is visualized with time stamps.*

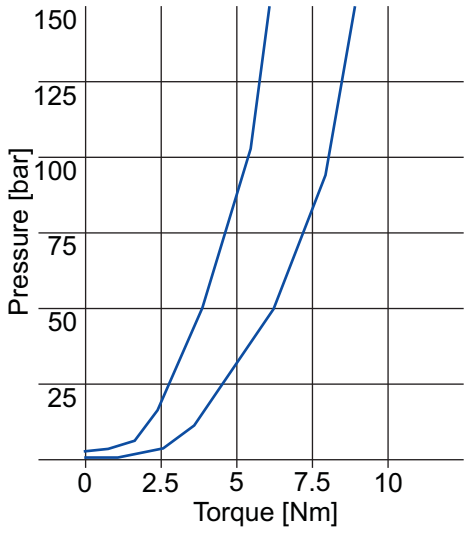

Figure 4.15 *Tolerance specification from the valve manufacture.*

4.2 Non-linear Model

The non-linear modeling approach investigates the system in the time domain. The strength of this approach is that the different components included in the complete system can be modeled in a "close to reality" way, thereby easing the analysis of the components and test if the system meets specifications. This way of modeling is also feasible when it comes to introducing and simulating new designs and changes. When it comes to model validation, the non-linear model is suitable as the available measurements are normally in the time domain. Validating the model is essential in order to gain confidence in the model and ensure that the level of modeling is enough to cover the interesting system dynamics or phenomena. It is also necessary to establish values for unknown parameters such as friction.

Every modelling effort starts with a problem related to either a dysfunction in a component or machine, or too small of a knowledge base [46]. Different problems have been evaluated in the project such as chattering, dynamic catch-up and the early validation of the active pinion concept. Even if the nature of the problem is that a linear model has to be used to solve or explain a problem, or generate a controller, the non-linear model has to be used. This makes it possible to validate the model with real facts, measurements in the time domain. When a linear model has to be used, which is the case with the chattering problem, the validated model coefficients and the modeling level are transferred from the non-linear model to the linear model.

The non-linear simulation has been useful in the three different cases below. Both friction in the power steering unit and the dynamic catch-up are strongly non-linear, which makes the non-linear simulation suitable. In this project, the program used for non-linear simulation is the HOPSAN simulation package, [47], which also incorporates optimization used for validation of the models and finding the coefficients such as friction coefficients.

4.2.1 Friction in the HPAS unit

In the non-linear approach, the components' properties can be changed with the states of the system such as friction, which is a non-linear behavior, for example stick slip friction. Friction is one of the hardest things to estimate in the modeling process and often has to be validated with measurements in order to be implemented in the model. In paper [III], the friction in the steering unit is investigated and validated with measurements; it was found that the friction in the HPAS system apart from velocity is also strongly dependent on the system pressure. This can be understood if the design of the cylinder seals is studied. In Figure 4.16, one of the seals is visible and the shape of the seal is such that the contact force between the sealing element and the cylinder rod increases with increasing pressure, which in turn increases the friction level. Also visible in the figure is the so-called yoke, whose purpose is to generate friction in the steering rack to suppress some of the disturbances entering from

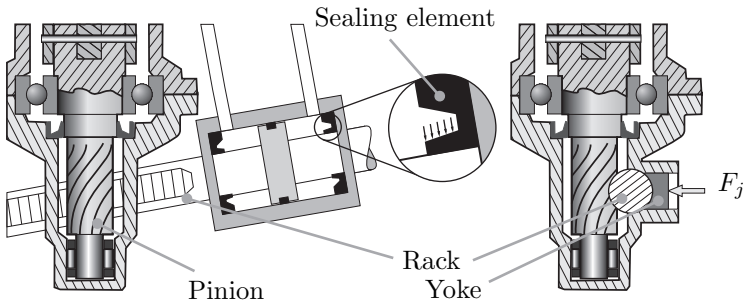

Figure 4.16 *Friction in the steering rack depends on the pressure due to the shape of the seals. Also visible in the figure is the so-called yoke, which creates a coulomb friction to suppress disturbance entering the steering gear.*

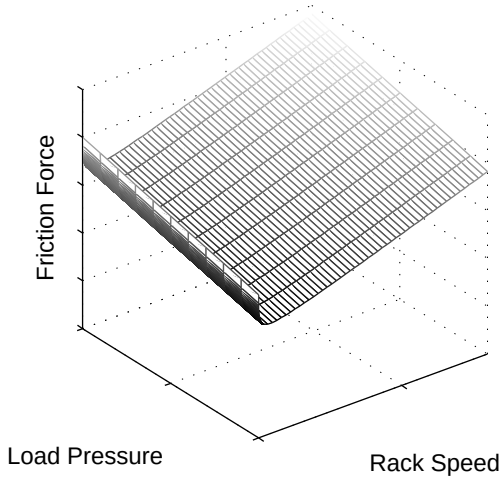

Figure 4.17 *Stribeck friction model with correction for pressure variation.*

the wheels, [48] [49]. The friction model used is based on the Stribeck model with modification for variation in pressure, Equation 4.30. A 3D-plot of the friction is visible in Figure 4.17.

$$F_{friction} = \frac{F_s}{1 + \left(\frac{\dot{x}_p}{\dot{x}_{p0}}\right)^{\tau}} + B_p \dot{x}_p + K_{p_l} p_L \tag{4.30}$$

4.2.2 Dynamic catch-up

The non-linear models of the power steering unit have been used in most of the work presented in the papers appended to this thesis. In paper [II], the

non-linear model is used together with measurements to investigate the static catch-up and hydraulic lag. The model included apart from a detailed model of the steering gear and valve also a detailed pump an line model this to be able to cover the effects introduced by the Expansion Chamber Attenuator, ECA. It is shown that the ECA is the main cause of hydraulic lag, due to the volumetric expansion of the ECA in the pressurization phase. The ECA is adapted late in the design proses of the power steering unit and main task is to reduce the noise level of the power steering unit. In order to avoid dynamic catch-up/hydraulic lag, the effect of the ECA has to be considered early in the design process. In this early phase of the design, non-linear simulation of the system can be used to take the effect of the ECA into account.

4.2.3 Co-simulation with vehicle model

This thesis covers the hydraulic power steering unit in a vehicle, which is to be seen as a system in a system. In order to optimize the characteristic of the whole vehicle, complex multi-domain systems are necessary. In these cases, co-simulation techniques can be useful to make use of expert knowledge in each domain, [50]. In these co-simulations the non-linear model is useful as it gives a close to reality result in the time domain. In paper [III], a co-simulation between a power steering system and a bicycle model was performed. The idea with the vehicle model was to generate realistic load force on to the steering rack model depending on the given driving scenario, vehicle speed and steering wheel angle, [51] [52] .

By connecting the vehicle model to the power steering model, the possibility to simulate the HPAS system with more realistic reaction forces is created. The connection between the vehicle model and the HPAS model is in the tie-rods and the steering wheel. The forces are calculated in the vehicle model with the steering angle from the HPAS model. Engine speed, vehicle speed and the steering wheel angle are variable in the two models. The steering wheel angle is the input reference for the driver model implemented in the HPAS model; the output from the driver model is the torque applied to the steering wheel. Engine speed is used in deciding pump speed. Vehicle speed is sent to the model due to the fact that it is necessary for the calculation of the tie-rod forces. These variables can be changed freely during the simulation, see Figure 4.18. The results of the co-simulation will not have the same accuracy as the HPAS simulation based on driving scenario measurements, due to the errors in both models combined. Nevertheless, the results of the co-simulation are accurate enough to draw conclusions about the characteristics of the HPAS design, when changes are introduced.

Co-simulation is also used frequently in the design of the active pinion concept, which is presented in Chapter 5. In this case, the non-linear model has been co-simulated with the control strategies. This eases the transitions between the desktop design and the test rig. In Figure 4.19, the possibility to

switch between the HPAS simulation model and the hardware in the test rig, or test vehicle, is displayed; this enables the controller to be used for all of the solutions.

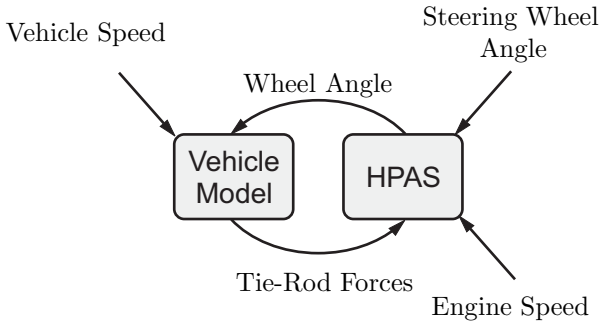

Figure 4.18 *Schematic sketch of the co-simulation. Displayed are the variable exchanges between the models and the external input variables.*

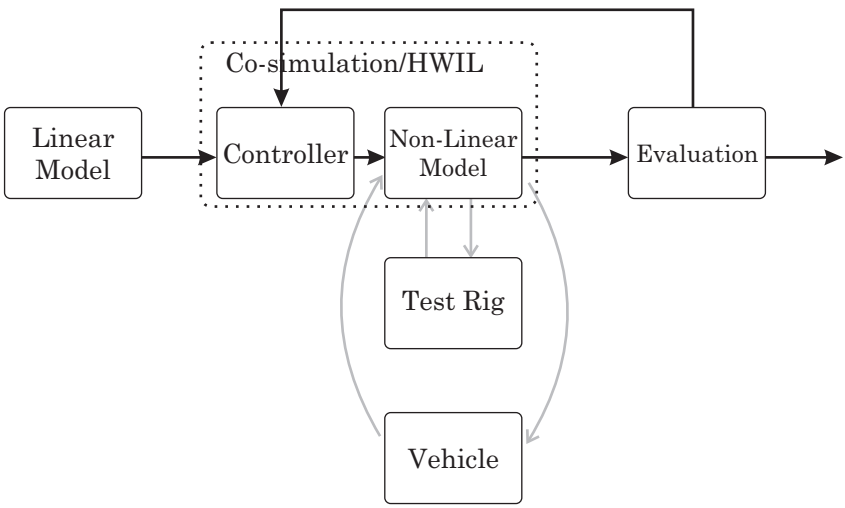

Figure 4.19 *Co-simulation of the controller design. The figure illustrates the change of test objects from model to test rig and finally to full vehicle test.*

5
The Active Pinion Concept

In order to drive a car there are three fundamental inputs required from the driver, acceleration, retardation and steering. The interfaces with the driver are the throttle pedal, brake pedal and steering wheel, which basically activate the engine/drive train, brakes and the steering gear. During the last two decades, different functions have been added to assist the driver, for example cruse control, which takes over the control of the engine in order to assist the driver in maintaining a preset vehicle speed, and anti-lock brakes, ABS, which prevent lock-up of the wheels during braking, thereby making it possible to steer the car out of a critical situation. These two examples are two among many more functions that have been introduced to assist the driver. Note that all of these functions have been added to manipulate either the engine/drive train, the brake system or a combination of the two. There are few examples of functions that enable the steering system. This is partly due to low flexibility controlling today's hydraulic power steering systems, but is also due to legislation and fail safe issues.

The need for new functions in HPAS systems is essential if these systems are to be used in comfort or active safety functions in the near future. Even if the EPAS system might be dominant in the long-term future, the HPAS system is needed in the near future for passenger cars of the larger and luxury model segments. The reason for this is the limitation in power supply by 12V and 14V systems, which leads to limitations in peak power out-take by the electrical power steering system. EPAS systems will not pe powerful enough until 42V systems are installed in passenger cars. Breitfeld argues that even 42V systems might not be powerful enough, as other systems are also converting from hydro-mechanical to electro-mechanical systems [18]. Based on this, the active pinion concept was developed to enable comfort and active safety functions dealing

with the steering gear.

In this chapter, the active pinion concept will be described in detail, both when it comes to the design of the highly functional power steering system and how this concept can be used in different applications, both comfort and active safety applications. Note that the aim of this research is not to develop comfort or active safety functions; but rather to provide an actuator that can be utilized by comfort and active safety functions. In order to understand the functionality of the system and how it can be utilized, some of the applications will be described briefly.

5.1 Application for the Active Pinion

The idea to introduce more functionality into the steering system is to support the driver. In Figure 2.2, Chapter 2, a complete steering system is presented in a schematic sketch. In the figure, the steering system is divided into three main parts, the controller, the power steering system and its interaction with the vehicle. In the system, the driver is the main controller and the power steering system is a pure actuator. As seen in Figure 2.2, external disturbance can affect all of these parts. Adding more functionality to the steering system could be used to unload the driver or support the driver in critical situations, and some external disturbances could be compensated for.

J. Ackermann shows how an active steering system can be used for compensating crosswind and μ-split braking, [13] [14]. The actuator used in Ackermann's study could add a small corrective steering angle to the steering angle commanded by the driver, thereby compensating for the crosswind and μ-split situation. Switkes et al. propose a system that would guide the driver with haptic feedback in order to avoid lane departure accidents, [53] [54]. Von Groll et al. have investigated and tested the possibility to suppress unwanted road disturbances transmitted to the driver, [55]. All of these features focus on performing a control task without retracting the driver from the control loop [56]. There are also attempts to more or less remove the driver from the control loop, which aim towards an Automated Highway System, AHS, [57], [58]. This system could be considered auto pilot for cars.

The research projects presented above utilize steer by wire systems or systems with an additional actuator in series with an existing hydraulic power steering system and show that additional functionality can be used for both comfort and active safety features. The potential for saving lives with active safety features has been realized with the introduction of the dynamic yaw control systems like the ESP. According to the U.S National Highway Traffic Safety Administration, NHTSA, up to 2211 lives per year in the USA could be saved by making dynamic yaw control systems standard, which is why the NHTSA proposed a law requiring ESP as a standard in all newly produced cars effective from 2008, [7].

The states available in the steering wheel are the torque and the angle; these

are the states that can be modified and manipulated to assist the driver, either separately or combined. In order to manipulate or modify these states freely, they have to be decoupled between the steering wheel and the steered wheels. A full decoupling in both states is representative for steer by wire systems. The concept presented here called active pinion can only realize a decoupling of the torque. In the subsections below, the application/functions that can be realized with the help of the active pinion are presented. The application/functions are divided into comfort functions and active safety functions.

The concept presents only the torque that can be affected during normal driving. Changing the torque freely opens the possibility to change the haptic feedback depending on the driving situation and communication with the driver. There is one special case of angle control, which is when the driver lets go of the steering wheel.

5.1.1 Active safety functions

Generally, vehicle safety issues can be classified into two different categories: Passive Safety and Active Safety. Active safety refers to the assistance given to the driver in more and less critical situations to avoid an accident. Passive safety features concern the protection of the driver when the car is involved in an accident (Seat Belts, Deformation Zone etc.). A list of active safety features is presented below, some of which are in use today, while others might be introduced in future production cars.

- ABS, Anti-lock Brake System, [59]
- TCS, Traction Control System, [59], [1]
- ESP, Electronic Stability Program, [59]
- ACC, Adaptive Cruise Control, [60], [9]
- Active Steering System
- LKAS, Lane Keeping Assist System

The use of active safety features has exploded during the last decade. One of the first add-ons to vehicles was the Anti-lock Brake System, ABS, which is standard in most cars produced today. More recently introduced is the Electronic Stability Program, ESP [59]. The ESP system is a closed loop system designed to improve vehicle handling. This is carried out by an intervention in the brake system or with the help of the power train. This system has been proven to be effective with regard to technical performance, [5]; however, the results of the system, with regard to actual safety, are hard to prove. A recent investigation based on accident statistics was conducted by the Swedish

National Road Administration, [4]. In this report, the effectiveness of ESP systems was proven to increase safety up to 38%, especially concerning winter road conditions.

Adaptive Cruise Control, ACC, is a more advanced cruise control system, where speed is a lower priority unlike the conventional cruise controller. In ACC, the distance or time gap to surrounding vehicles is measured and vehicle speed is adjusted to the current traffic situation. This system can also be used for collision warning or avoidance. Active Steering Systems assist the driver by controlling the yaw and roll dynamic similar to ESP. Instead of using the brakes as an actuator, the steering is used to control the vehicle dynamics. An additional steering angle of maximum three degrees is produced without interfering with the driver. Active Steering System performance is better than ESP system performance [14]; however, the requirement of an additional actuator increases the cost of the system making it less desirable.

Samples of applications that can utilize the increased functionality in the active pinion are listed below:

Lane Keep Assist, LKA Function that helps the driver avoid lane departure accidents by adding a guiding torque to the steering wheel.

Emergency Lane Assist Using both camera and radar, Emergency Lane Assist can also monitor oncoming vehicles. If the driver crosses the lane markers and does not respond to the buzzer, the system reacts by applying additional steering force to help steer back into the intended lane, [61, 62].

Active Yaw Control with Torque Feedback Active safety function that superimposes a guiding torque during large body sideslip angle conditions in order to guide the driver into a stable state of driving.

The focus of this thesis regarding active safety features in passenger cars is limited to LKA systems, where the focus is to develop a HPAS system that has the ability to produce an offset torque on the steering wheel. Many road or lane departure accidents are caused by the driver's lack of attention. In many cases, this is due to distractions, drowsiness or intoxication. The LKA system briefly described here intends to be used as an active safety feature aimed at decreasing the amount of unwanted lane departures, [16].

In order to assist the driver to avoid potential lane departure accidents, the road path has to be monitored and the car's position on the road estimated. This is done with the help of a camera, which calculates the distance to the left and right lane markings. With these measurements, the position of the vehicle can be estimated. However, this is not enough to calculate an offset torque to guide the driver; the direction of the vehicle in reference to the road has to also be known. From this, an optimal steering angle is calculated and compared to the actual steering angle. If the difference between calculated and actual steering angle or the lateral deviation is greater than the threshold value, an offset torque is calculated and applied. A sketch of the technical solution

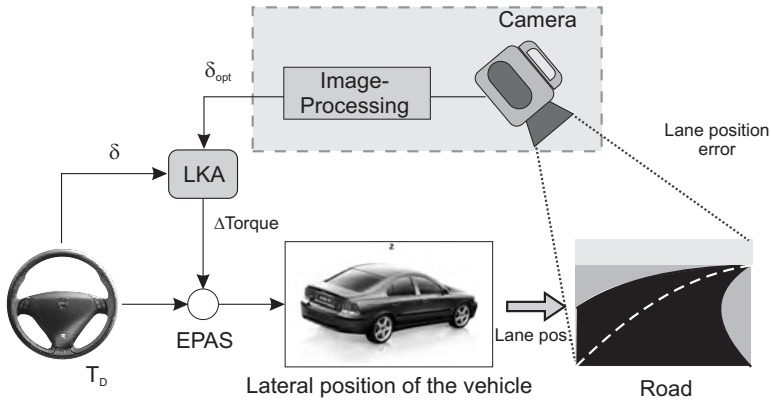

Figure 5.1 *Technical principle of the Lane Keeping Assist System, LKAS.*

regarding the LKA system is displayed in Figure 5.1. More information about LKA control can be found in [63].

The challenge in developing such kinds of functions lies in the determination of dangerous situations and the design of appropriate warning/intervention strategies. This system is intended to go unnoticed by the driver and intervene only when the driver mismanages steering control. Unlike systems that issue an audible sound, the system presented in this thesis uses a tactile feedback via the steering wheel as a warning device. The torque is designed to communicate to the driver the appropriate steering wheel angle required to return to the lane, Figure 5.2. There are other solutions to achieve lane keeping assist than applying torque to the steering wheel. One solution that Daimler-Benz has developed adds a correction to the driver's applied steering angle [15]. This solution aims more towards autonomous driving. Active safety features are going to play a more important roll in future safety strategies; therefore, it is essential that vehicle sub systems are adjusted to meet new demands.

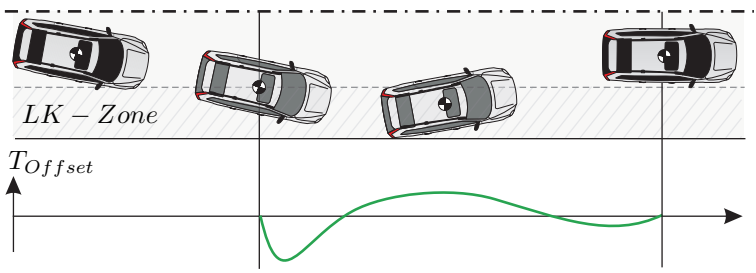

Figure 5.2 *Schematic sketch of a maneuver where the LKA system is used.*

5.1.2 Comfort functions

As mentioned earlier the active pinion concept could also be used for comfort functions. Note that the aim of this research is not to develop comfort functions, but to provide an actuator that can be utilized by comfort and active safety functions. Briefly described below are some of the proposed comfort functions that could utilize increased functionality. A more detailed description of the functions can be found later in this section. All of the functions below have not been fully evaluated, due to the fact that the functions utilize the power steering unit in the same way.

Proposed comfort function

- Variable Assist
- Virtual Boost Curve
- Parking Pilot
- Lane Keeping Assist, LKA
- Torque Reference Generator

Variable Assist

Different assistance curves depending on vehicle velocity are not new. They are available as options on new cars. This function has been described earlier in Chapter 2.

Virtual Boost Curve

This function is similar to speed dependent assist. In speed dependent assist, the curve is predetermined by the geometric design of the valve. In the active pinion or the assistance curve, the boost curve can be designed more freely to meet system requirements. This means that the desired characteristic could be implemented in the controller as a look-up table.

Parking Pilot

The task in an automatic parking scenario is pure position control, where the car is to follow a trajectory specified by the automatic parking system, see Figure 5.3, [64]. Automatic parking systems utilize the functionality of the positioning control of the steering rack and can take control of the steering wheel. In this case, parking performance regarding speed and accuracy is dependent on the dynamic performance of the steering actuator. The more accurate the control of the steering actuator, the smaller the deviation in the parking maneuver.

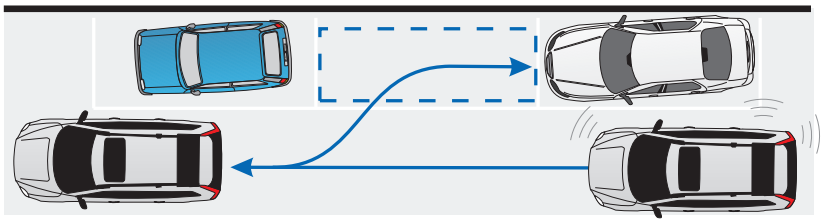

Figure 5.3 *Auto Park maneuver where the active pinion concept could be used to position the steering wheel.*

Lane Keeping Assist, LKA

The LKA system, also mentioned under the active safety feature, can be used as a comfort feature to help the driver keep his/her car in the right lane. Switkes et al describe the system as a spring between the car and the road center line, which attracts the vehicle to the lane center, [53]. This spring force is built into the torque control of the steering wheel and the feeling is similar to riding on tracks built into the road, see Figure 5.4. The driver still has control of the vehicle and can easily overcome the syntectic forces generated by the system. This system could be compared with the Adaptive Cruise Control, ACC, see section 5.1.1, which controls the position of the vehicle in the longitudinal direction in relation to the vehicle in front; whereas, the LKA controls the vehicle's lateral position.

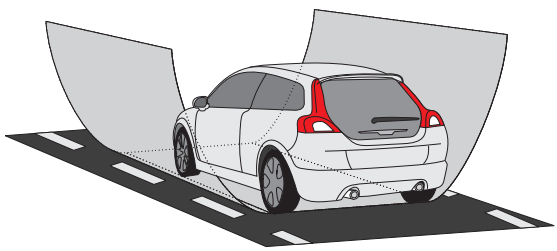

Figure 5.4 *Lane Keeping Assist as a comfort function, where an additional steering wheel torque is applied in order to keep the car in the center of the lane.*

Torque Reference Generator

The idea behind the torque reference generator is to decouple the steering wheel torque and the forces acting on the steering rack and to add a syntectic steering feel. The reason for this is to introduce the possibility to design the steering feel based on the attitude of the car and steering wheel. It would be possible to move some of the steering feel characteristics from a mechanical design to software implementation, which would ease the possibility to also

apply a distinctive brand genetic steering feel. It is also possible to suppress unwanted disturbance, such as steer torque.

5.2 Working Principle

In order to increase the functionality of a traditional HPAS system, an extra degree of freedom is added to the valve. In an unmodified valve, the activation of the valve unit is in direct relation to the torque applied to the steering wheel. To obtain an extra degree of freedom, the actuation of the valve has to be split-up and an extra possibility to actuate the valve has to be introduced. The most logical place to introduce a second point of actuation is in between the pinion and the valve body, which are normally connected rigidly, see Figures 5.5 and 5.6.

The rotation angle of the pilot motor is transferred into a linear axial motion with the help of the excenter. The linear motion is transferred into a rotational motion by the inclined grow in the valve body and the pin stuck to the pinion. The valve body will still be connected to the pinion, but the actuator will enable the function to add or subtract an offset angle on the valve body relative to the pinion. By actively changing this angle, it is possible to increase or decrease the amount of assistance created by the hydraulic system. It's also possible to create negative assistance. By adding this extra angle, the pressure modulated

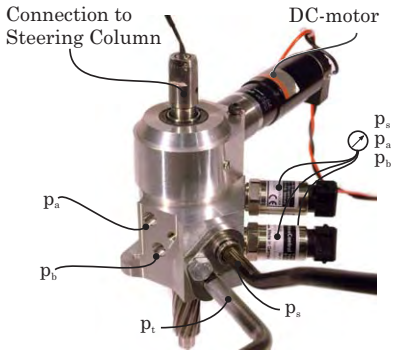

Figure 5.5 *Overview of the valve including the DC-motor.*

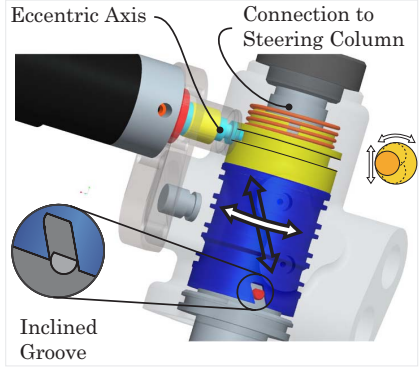

Figure 5.6 *Close-up view of the valve.* ***Click on the figure to se a 3D-model of the concept, (U3D).***

by the valve can be changed to add or retract an offset torque to or from the steering wheel. This can be more easily understood if the static boost curve is studied, see Figure 5.7. In the figure, the absolute value of the assistance torque is plotted as a function of applied torque on the steering wheel. The black curve is the traditional curve, without an offset angle and the gray line symbolizes a

curve with a slight offset angle. The effect of the offset angle is the change in the effective angle difference between the valve body and the spool, as well as the assistance curve.

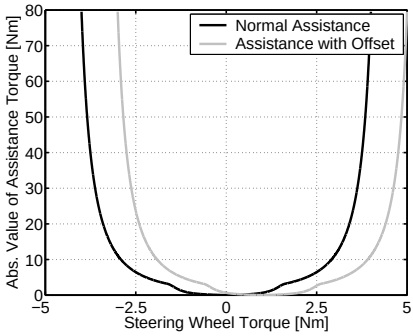

Figure 5.7 *Static boost curve, traditional (black) and with an angular offset (gray). Observe absolute value of the assistance torque is plotted.*

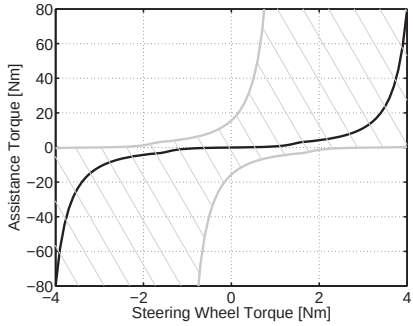

Figure 5.8 *Limit for working boundary when max offset angle is* $\pm 2^\circ$.

By freely changing the offset angle, the amount of assisting torque can be changed. The working boundary for a valve with maximal angular displacement of $\pm 2^\circ$ is shown in Figure 5.8. The gray line in the figure is the outer limit of the variation of the static boost curve. Notice that this graph deals with the static characteristics; the effect of the differential angle will be different under the influence of the dynamic and the pumping motion of the steering rack. The graph is still useful in understanding the concept of the active pinion.

5.2.1 Hardware design

All of the prototypes built in this project are based on already existing power steering units and valves. There are two reasons for this choice; one is the limitation in the prototype workshop at the university and the other is due to the fact that concept is to be seen as a modular added to an existing power steering solution. Since the prototype and the chosen concept are based on a production valve, the mechanical interfaces are identical to the normal valve, which makes it easier to change between a normal valve and a valve based on the active pinion concept. The modifications performed on these valves focus on the valve unit, where the housing of the valve has been modified in order to hold the pilot motor and in the latest design, the pressure sensors used in testing.

In Figure 5.9, the components included in the active pinion are shown. The picture shows the pilot motor including the gearbox and holder of the excenter, the valve body, spool, pinion including the torsion bar and the housing of the

valve. The prototype in the figure is prototype number V*. In the figure, a close-up on the inclined grove is shown as well as the configuration of the excenter. The valve body has been adapted to be controlled by the pilot motor by adding

Figure 5.9 *Photo of the mechanical design of the Active Pinion. Seen in the picture from the left are the DC-motor including the excenter, the valve body with the inclined grove, the spool, the pinion including the torsion bar and the pin guiding the valve body and finally the housing of the valve. This is prototype IV.*

a track for the excenter. An inclined grove has been created in the lower part of the valve body to be used as a transformation from the linear axial motion to a rotational motion. The track is built into a separate part called the crown, see Figure 5.10. The crown is glued to the original valve body and secured with the help of three pins, it also includes channels to drain the upper part of the housing to tank to avoid pressure build-up during valve body displacement. The inclined grove was initially ground directly into the valve body; however, the valve body material was too soft to cope with the forces. This resulted in deformation of the inclined grove and play between the grove and the pin secured to the pinion. In the latest prototypes, the grove is defined by two hard metal plates, which are held in place with the help of two rivets each, see Figure 5.10 .

The spool is left untouched. A pin has been mounted on the pinion in order to guide the valve body. On the torsion bar, a full bridge contains four strain gages that have been mounted to be able to measure the torque applied to the valve. The wires exit in a hole drilled in the top of the torsion bar; the holes are sealed to avoid leakage, see Figure 5.11. By measuring the torque inside the valve, the torque also allows valve displacement due to torque applied to the steering wheel.

The housing is modified to hold the pilot motor making it possible to access the crown on the valve body. In the latest prototype, the mounting of the pilot motor was made flexible to handle different packing scenarios in a car. This setup allowed six discrete directions of the pilot motor, see 1 in Figure 5.12. In

*The difference between prototype number V and IV is the housing.

Figure 5.10 *Design of the valve body including the crown, 1, and the inclined grove, 2. The crown is glued to the original valve body and secured with the help of pins.*

Figure 5.11 *Full bridge contains four strain gages, which have been mounted on the torsion bar. The wires exit in two drilled holes in the top of the torsion bar.*

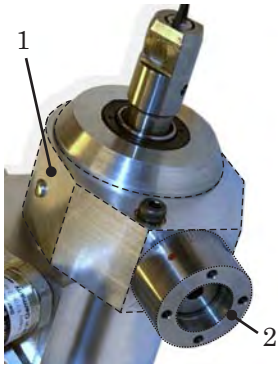

Figure 5.12 *Holder of the pilot motor, 1, including the mechanical calibration device of the excenter, 2. The pilot motor holder can be rotated around the main housing in order to minimize packing problems in a prototype car.*

the production of the prototype, the load pressure calibration, $p_L(T_{sw}, \alpha_{AP}) = 0$, of the main valve lay-out was lost. This could be compensated electrically with the help of an offset angle on the active pinion angle, α_{AP}, but would result in an unsymmetrical actuation of the active pinion and reduction in the working envelope. To compensate for this problem, the possibility for external calibration was added to the housing, see 2 in Figure 5.12.

Limitation

In order to have full functionality and flexibility in the control of the steering system, both the angle and the torque have to be controllable. In this concept, only the torque can be changed independently of the forces acting on the steering rack. Angel freedom can be added by combining the active pinion system with an active steering system, [10], [65], [66]. A combination of the active steering system and the active pinion concept would lead to freedom in both angle and torque, giving it similar functionality to steer-by-wire systems.

The torque generated by the steering wheel is also limited in the active pinion concept. The limitation is mainly due to the limitation in actuation and generated differential angle. This will also be discussed below when it comes to fail safe.

Fail safe

The active pinion concept is built on a pure hydraulic solution, which in the basic design is a robust solution. The active pinion adds a few moving parts, which could fail and different types of failure modes related to the active pinion concept can be identified.

- Sensor failure
  - Torque sensor
  - Pilot motor sensor
  - Pressure sensor
- Actuator failure
  - Position of the excenter is *in neutral* position.
  - Position is ***not*** *in neutral* position.

The main failure is if the pilot motor can not be activated. In this case, there are two scenarios; the excenter is in a *neutral* position or ***not*** *in a neutral* position. If the *excenter is in a neutral* position, the effect of the failure is minimal. The additional functions acquired by the active pinion are not available. This is not critical when the power steering system is based on a traditional HPAS solution. The basic function of assisting the driver is still available and the functionality is the same as in a car without the active pinion concept.

If the *excenter is* ***not*** *in a neutral* position, an offset torque on the steering wheel will result. The maximal torque that the driver has to apply to the steering wheel is limited to the maximal displacement on the valve body. This scenario can be solved by adding a mechanism that relocates the excenter into neural position, which reduces the severity of the failure to a loss of additional power steering functionality. Another solution is to shut down or reduce the flow through the valve, thereby removing the assisting function in the power

steering system. In the case of sensor failure, the functionality associated with the active pinion can be disabled, and the system functionality reduced to a level equal to a traditional HPAS system. In order to detect sensor failure, the system has to have some redundancy concerning the sensors, a model based sensor failure detection or a combination of the two. The need for different sensors will be discussed later in this chapter.

The fail safe issue has not been a focus in this work; but from the discussion above, the worst case scenario of failure could result in the driver's torque being subjected to an offset, which is limited regarding size. The size of the offset torque depends on the limitation of the maximal valve displacement that the active pinion can perform. This torque is approximately 3 Nm in the current prototype.

5.3 Design Aspects of the Concept

Different design aspects have to be considered, both concerning the mechanical design of the actuation and the valve layout or hydraulic characteristics. The prototypes built in this project have all been based on existing valve and rack and pinion solutions on the market, thereby containing a predefined valve characteristic and geometric boundaries. The reason for using existing valves is due to the fact that the valve unit is extremely sensitive to variation in tolerances, as discussed earlier, and needs highly specialized production equipment, which is not available in the university workshop.

In further development, the valve characteristic is also a variable that has to be considered. The characteristic in the valves used in the prototypes is highly non-linear and shaped for optimal functionality to assist the driver with no consideration to additional applications, such as the active pinion. In order to take these characteristics into account when designing the main characteristic of the valve, different aspects have to be considered:

- Fail safe
- Robustness of the control algorithm
- Implemented functions continuous/intermentent use

The *fail safe* issue discussed earlier would benefit from a characteristic similar to the one used in the prototype today. This would give the power steering system the same functionality and characteristic of today's power steering systems in fail safe mode. Only the additional functionality would be disabled.

Today the *control algorithm* is highly dependent on the characteristic of the valve and working point. From a control point-of-view, the valve characteristic is not optimal as it gives a highly non-linear behavior in order to be able to handle the non-linear characteristic of the valve, see Figures 4.6-4.8 in Chapter 4. This type of controller is also sensitive to variation in the characteristic and has to

be tuned individually for every valve. A more linear characteristic would lead to a more robust controller, which would be less sensitive to individual variation. This type of characteristic would require the active pinion, pilot motor, to be constantly active to give the right steering feel.

The implemented functions also have different requirements regarding controllability, both control precision and dynamic response. Also, the use of the active pinion concept is different between functions; some functions use the active pinion continuously, while others use the concept more intermittent. The high demands on controllability are set by the Torque Reference Generator, TGR, which is continuously applied to a syntectic steering wheel feel. The control of this function benefits from a more linear characteristic. On the other hand, if all of the functions except the TRG are to be used, a classic valve characteristic is preferred, due to the fact that the active pinion would only be active and controlling the system intermittently. In this case, most of the time the power steering relies on the characteristic given by the geometric shaping of the valve as a normal power steering unit; and the active pinion would only be needed when requested by an external application like the parking pilot system or lane keeping assist system. These systems also have a lower demand on dynamic response and control precision.

The mechanical design can be optimized, especially concerning the actuation of the active pinion. In the prototype, the mechanical design is a compromise due to the hereditary of the chosen base valve unit; a pin and an inclined grow are used, see Figure 5.6. The durability and functionality can be improved by shaping and increasing the amount of guiding element.

5.3.1 Potential problems with the current solution

During the developmental process, different problems have occurred with the prototypes. The main problems have been associated with backlash and friction. There are different places in the design where backlash problems can occur. In Figure 5.13, the main problems areas are pointed out.

Inclined grow This is the most critical place when the play is close to the actual actuation, depending on the angle of the inclined grow. In the prototype, the angle of the grow is 30 degree and is dominant. In the early prototypes, the grow was machined out from the valve body; due to the soft material in the valve body, the grow was deformed resulting in a backlash problem.

Excenter Backlash can occur between the excenter and the track. The effect of the play is reduced in the prototype depending on the inclination of the grow.

Gearbox Backlash can occur in the pilot motor gearbox. The play in the gearbox is also reduced equal to the effect in the excenter. It is also

reduced depending on the position of the excenter. Neutral position of the excenter is the worst case scenario.

Housing of the excenter This has to be rigid so no deformation can occur during actuation of the excenter. This has been a problem in the prototype due to friction between the housing and the valve body resulting in high actuation forces. In a solution where the axial motion is avoided, the friction forces would also be significantly reduced, also causing a significant reduction in the actuation forces.

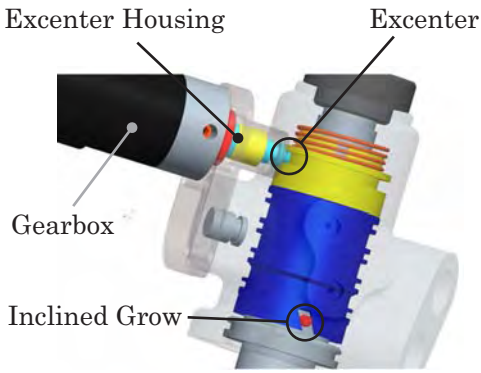

Figure 5.13 *Places with potential backlash problems.*

The problem of friction is mainly related to the axial motion of the valve body. The sealing rings on the valve body are optimized for a rotational motion, not axial motion, which is the case in the prototypes. Friction results in higher actuation forces generated by the pilot motor and the problem increases with increasing pressure, see Figure 5.14. There are solutions that can solve or reduce this problem. One solution is to modify the sealing rings to reduce the influence of the pressure; this can be achieved by reducing the areas in contact with the valve housing. There are also methods to avoid the axial movement of the valve body, which would drastically reduce friction due to the sealing rings. However, this was not possible within the prototype, due to the configuration of the donator valve.

5.4 Control Concepts

The application discussed earlier requires three different controlling modes, position control, offset torque control and free torque control. In this research, two of the control methods have been designed and investigated, position control and offset torque control. In this section, the controller will be discussed and the results from the test rig will be presented. The controller will also be

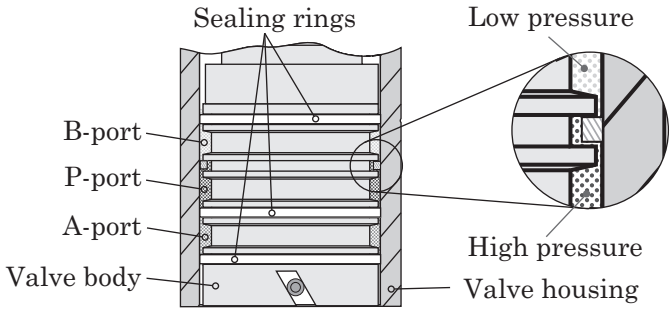

Figure 5.14 *Friction problems due to the sealing rings. The friction problem will increase with increasing load pressure. High load pressure increases the normal force acting on the sealing ring as well as friction.*

related to different applications, which also have different requirements on the sensor equipment.

5.4.1 Position control

In Figure 5.15, a block diagram of the complete steering servo is shown. x_v is the output signal from the electric servo motor, and x_r is the position of the rack. The corresponding bode plot is shown in Figures 5.16 and 5.17. Lower frequencies indicate the expected pure integration, followed by a lag, point 1. An anti-resonance associated with the spring mass system due to the steering wheel and the torsion bar, is marked point 2, while point 3 represents the hydraulic resonance associated with the hydraulic spring and the rack mass.

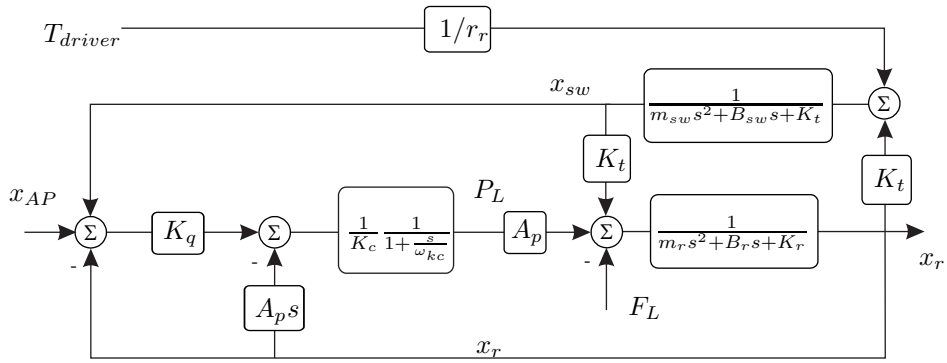

$$x_{AP} = \alpha_{AP} r_v$$

Figure 5.15 *Block diagram over the power steering unit including the external actuation of the valve unit.* $G_{sys} = x_r/x_{AP}$, $F_L = 0$, $T_{Driver} = 0$

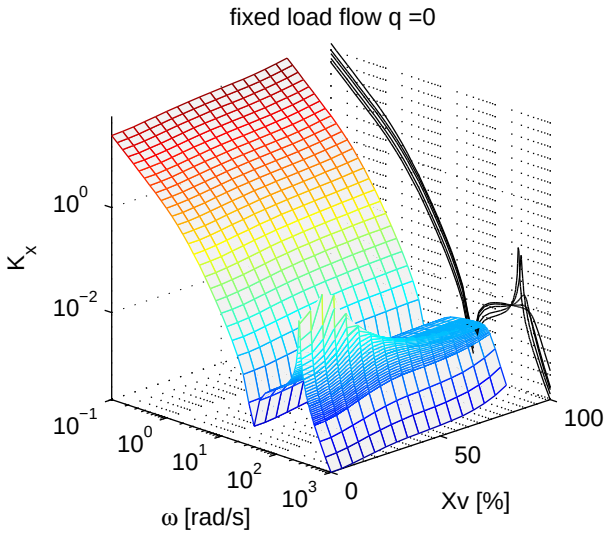

Figure 5.16 *3D-bode plot of the system. G_{sys} defined by a block diagram.*

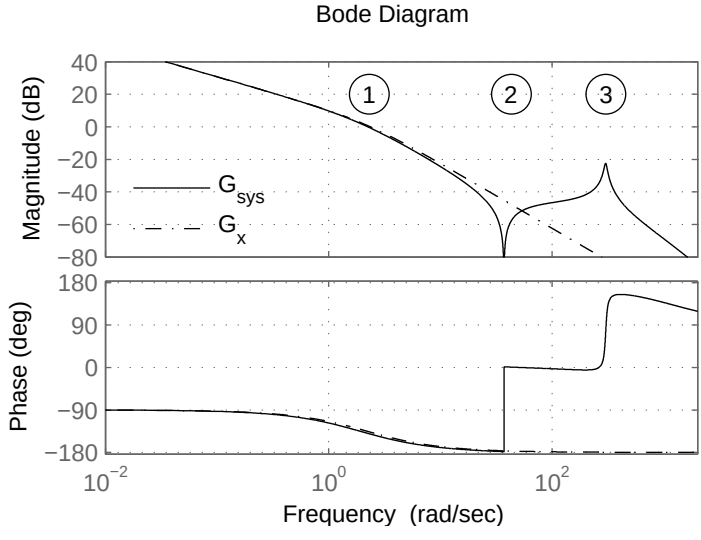

Figure 5.17 *A section of Figure 5.16 with fixed valve displacement. Also included is the system approximation, G_x.*

The basic structure of the controller is a PI-controller with a pre-filter design to shape the closed system to pre-defined characteristics, Figure 5.18. Similar architecture of the controller has been used by Krus & Gunnarsson [67]. The assumption is that the characteristics of the open loop system are simplified into G_x, see Equation 5.1 and Figure 5.17.

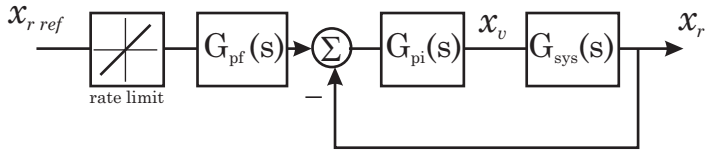

Figure 5.18 *Regulator structure in the position controller.*

$$G_x(s) = \frac{K_x}{s\left(\frac{s}{\omega_x} + 1\right)} \tag{5.1}$$

In G_{pi} in Equation 5.2, apart from the traditional PI-controller, there is a correction in order to compensate for the dynamics in G_x. This makes the controller regulate not only on the position but also the velocity. In order to secure a continuously derivable position reference, a rate limiter is added to the controller.

$$G_{pi}(s) = K_{pi}\left(\frac{\frac{s}{\omega_i} + 1}{\frac{s}{\omega_i}}\right)\left(\frac{s}{\omega_x} + 1\right) \tag{5.2}$$

When the close loop is derived according to Equation 5.3, it can be rewritten by introducing the coefficients shown in Equation 5.4.

$$G_c(s) = \frac{G_x(s)\,G_{pi}(s)}{G_x(s)\,G_{pi}(s) + 1} = \frac{\frac{s}{\omega_i} + 1}{\frac{s^2}{\omega_a^2} + \frac{2\delta_a}{\omega_a} + 1} \tag{5.3}$$

$$\omega_c = K_{pi}K_x \qquad \omega_a = \sqrt{\omega_c\omega_i} \qquad \delta_a = \frac{\omega_a}{2\omega_i} \tag{5.4}$$

To further form the controller, a pre-filter is assigned to take care of the numerator in the closed loop system and further increase the phase margin at the resonance frequency for the closed system, Equation 5.5.

$$G_{pf}(s) = \frac{\left(\frac{s}{\omega_a} + 1\right)}{\left(\frac{s}{\omega_i} + 1\right)} \tag{5.5}$$

In the controller tuning process, the cross over frequencies, ω_c and δ_a, are the characteristics that can be changed to meet the performance requirements of the position controller. In order to compensate for non-linear characteristics, the

static gain, K_x, and the system dependent frequency, ω_x, are calculated and fed to the controller. These characteristics will vary with the valve position and the speed of the rack. The working point dependent parameters in the linearization are mainly the flow gain, flow-pressure coefficient and the dynamics in the pressure build-up, K_q, K_c, as seen in Figures 4.6 and 4.7. The variation affects

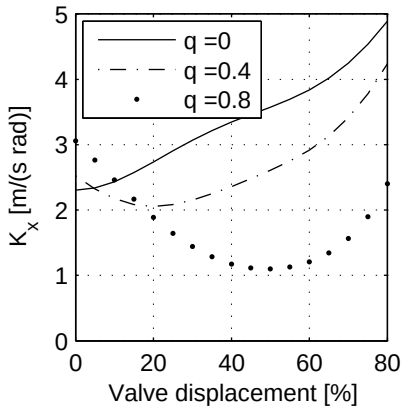

Figure 5.19 *Variation in the gain of the open loop system refereed into Equation 5.1 along with variation regrading valve displacement and load flow.*

the static gain of the system and the system dependent break frequency, see Figure 5.19. In order to calculate the system dependent characteristics, valve displacement has to be established. As described earlier, valve actuation is a combination of electrical actuation by the pilot motor and mechanical deflection of the torsion bar. The most suitable way to establish the mechanical deflection is to measure the applied torque on the torsion bar, which together with the pilot motor angle gives the total displacement of the valve, α_v. It is also possible to use the pressure and via the static characteristics of the valve calculate the valve angle. The valve angle estimated from the pressure is slightly filtered due to the dynamics of the pressure build-up. However, the dynamics in the mechanical deflection of the valve will be in the lower dynamics and are limited by the frequency of the spring mass system.

Results from measurements

Position control is used during automatic parking maneuvers; the forces acting on the steering rack depend on the friction between the surface and the tires. A test rig has been designed and used for prototype testing in this project; a description of the test rig can be found in [68]. In the test rig, a simple hysteresis model of the tires is applied, which assumes that the tie-rod force will increase with the deflection of the tires until full slip occurs. In Figure 5.20, a position step response is shown. The dynamics of the step response are slower

than the requested dynamics of the controller due to saturation; the dynamic without saturation is 2.5 Hz. The effect of saturation is further investigated and described in paper [VI]. Figure 5.21 shows the actuation of the valve; notice that the valve has to work hard during the motion of the rack, which is a phenomenon related to the configuration of the valve. As the rack moves, it initiates movement in the steering wheel. Since the connection between the steering wheel and the rack is via the torsion bar, the movement also initiates torque, see Figure 5.22, and actuation of the valve. These disturbances introduced by the mechanical actuation of the valve have to be compensated for with the electric pilot motor. The load pressure together with the applied load during the cycle are shown in Figure 5.23. Further results are displayed in Figures 5.24 and 5.25, where sinus and ramp signals are used as references.

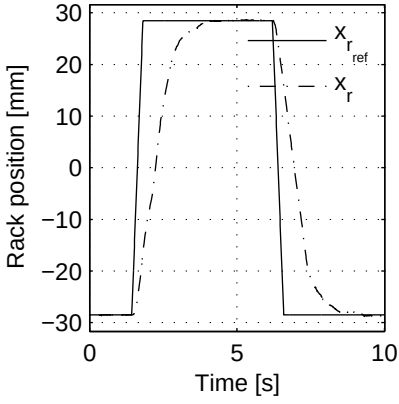

Figure 5.20 *Step in steering rack position.* $57mm = 440,6^o$ *on the steering wheel.*

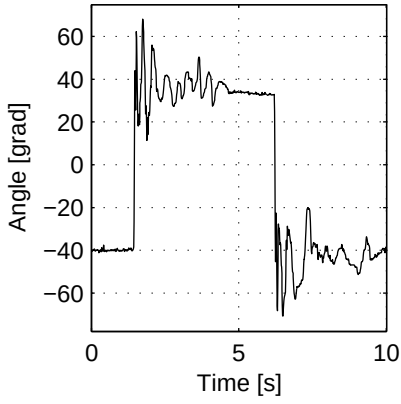

Figure 5.21 *Displacement of pilot motor. Notice that the pilot motor maintains the force balance in between the steps.*

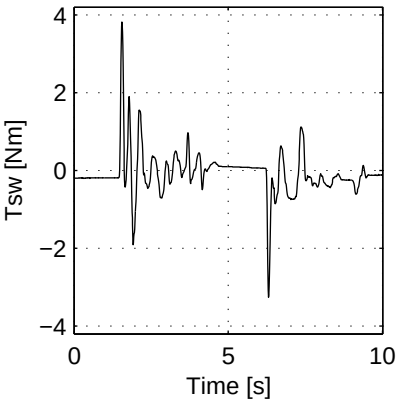

Figure 5.22 *Steering wheel torque.*

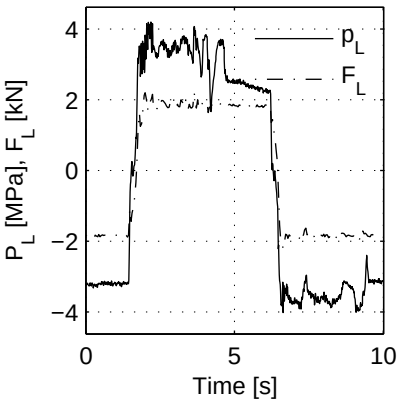

Figure 5.23 *Load pressure in the cylinder.*

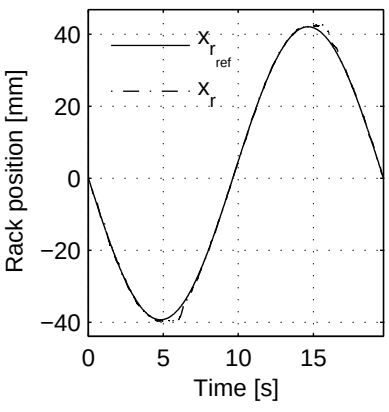

Figure 5.24 *Sinusoidal reference to the steering rack position.*

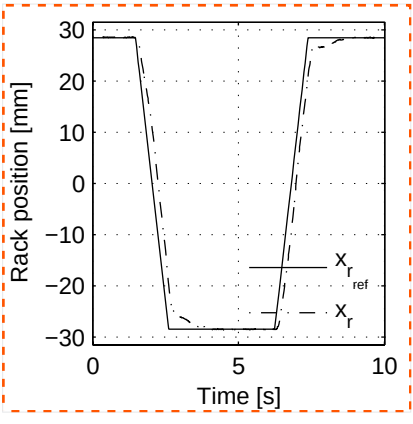

Figure 5.25 *Ramp response in steering rack position. (Click to see a film clip)*

5.4.2 Offset torque control

The offset torque mode is meant to modify the pressure torque relationship established by the valve. Statically, a relationship between the applied steering wheel torque, T_{sw}, and the generated assisting pressure exists. This is also mentioned as assisting torque, $T_{assistance}$, and has been discussed earlier and often visualized with the boost curve. Based on this relationship, a relationship between the applied steering wheel torque and the total force acting on the steering rack exists, later related to the total torque, T_{tot}. In order to generate offset torque, the relationship between T_{sw} and $T_{assistance}$ has to be changed. To generate additional offset torque, the assisting torque has to be reduced and steering wheel torque has to increase. This change is carried out by the active pinion, which changes the relationship between steering wheel torque and assisting torque. When changing this relationship, it is essential to keep track of the total torque generated by the rack, or the sum of manually and hydraulically generated torque. Total torque, T_{tot}, does not change with the modulation of the valve and is dependent only on the external load, see Figure 5.26. This relationship is based on the valve characteristic and depends on the shaping of the valve as discussed earlier.

In Figure 5.27, the relationship is visualized where the assisting torque, $T_{assistance}$, is reduced to add an offset torque, T_{offset}, to the steering wheel. The torque the driver would sense with no intervention is named T^*_{sw} in the figure. To establish the reduction in assisting torque, the normal relationship between assisting pressure and steering wheel torque has to be known. This relationship is based on the characteristics of the valve and can be established for each total torque value either by solving the non-linear equation system, Equations 5.6-5.8, or by creating a look-up table with steering rack speed, total torque as input and the related normal assisting torque, $T_{assistance}$, as output.

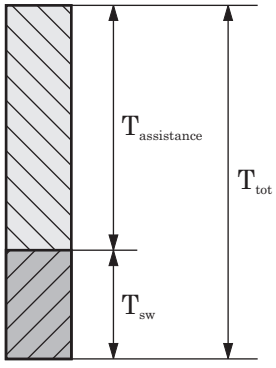

Figure 5.26 *Torque ratio between assistance and manually applied torque, when the active pinion is passive.*

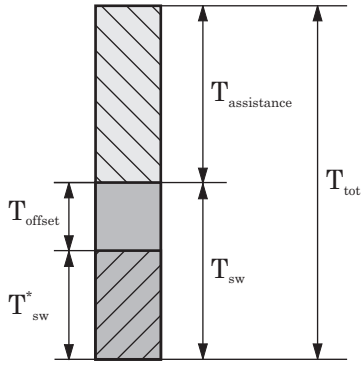

Figure 5.27 *Torque ratio between assistance and manual applied torque when the active pinion is activated.*

$$T_{tot} = T_{sw} + p_L A_p r_r \tag{5.6}$$

$$p_L\left(T_{sw}, q\right) = \frac{\rho q_p}{8 c_q^2}\left(\left(\frac{q-1}{A_2\left(T_{sw}, \alpha_{AP}\right)}\right)^2 + \left(\frac{q+1}{A_1\left(T_{sw}, \alpha_{AP}\right)}\right)^2\right) \tag{5.7}$$

$$q = \frac{\dot{x}_r A_p}{q_p} \tag{5.8}$$

Figure 5.28 represents the structure of the offset torque controller, where the first part, marked 1, calculates the new load pressure that has to be generated in order to create the offset torque. The characteristic of the valve is used to calculate the pressure that would be present with no intervention,P_{LN}. This pressure, P_{LN}, is reduced with an amount representing the offset torque, $P_{Loffset}$, thereby creating a load pressure reference, P_{Lref}.

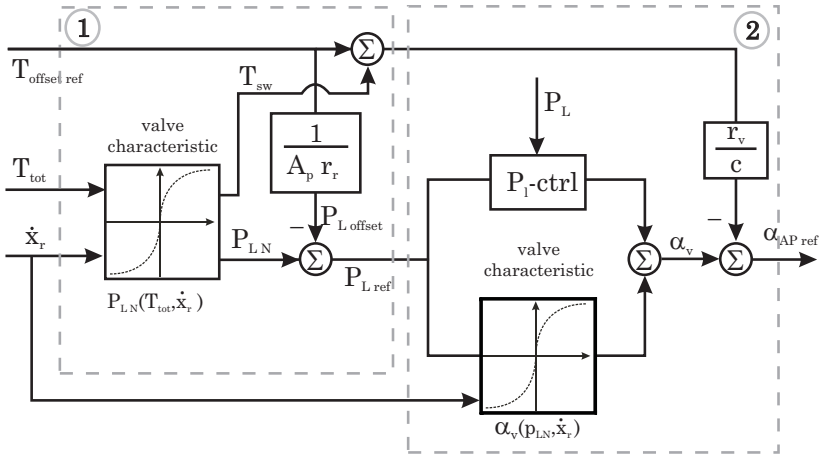

Figure 5.28 *Regulator structure of the offset torque control. The first part of the controller generates the load pressure reference; the second part generates the reference angle to the active pinion.*

The second part of the controller, marked 2 in Figure 5.28, has to fulfill requests regarding generated assisting torque or load pressure. The static characteristics of the valve are also used to calculate how the valve should be displaced in order to generate the commanded assisting torque. Parallel to this function is a closed-loop controller of the load pressure to compensate for deviation between implemented valve characteristics and actual valve characteristics defined by the hardware. The result from this controller is a commanded total actuation of the valve, α_v, in order to generate the required pressure. One part of the commanded actuation angel is generated by the steering wheel torque, since the size of the steering wheel torque is given by T_{tot} and T_{offset},

$T_{sw} = T^*_{sw} + T_{offset}$. The remaining part of the commanded actuation angle, α_v, has to be generated by the active pinion, α_{AP}.

In Figure 5.29, the actuation of the active pinion is plotted as a function of total torque and offset torque. As seen in the graph, the actuation angel is non-linear close to zero total torque and limits out to a constant value for higher values of total torque. The value that the angle limits out to is the pure mechanical deflection generated by the active pinion actuation angle, Equation 5.9. This is due to the fact that the normal load pressure, p_{L_N}, is dominant over the required change in load pressure, due to the offset torque, $p_{L_{offset}}$.

$$\alpha_{AP}(T_{tot} = 60) \approx \frac{T_{offset}}{C} \tag{5.9}$$

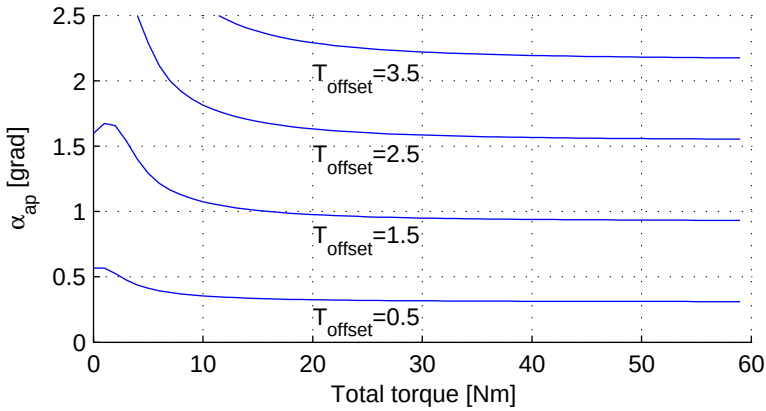

Figure 5.29 *Actuation of the active pinion as a function of total torque, T_{tot} and T_{offset}. Load flow $q = 0$, T_{tot} =60 Nm represents a normal load pressure of $P_{LN} = 8.2\ MPa$.*

Parts of the offset torque controller are also used in the virtual boost curve generation. The difference between the controllers is the first part, which is changed to generate a different characteristic, see Figure 5.30. The characteristic is implemented in the same way as in the offset torque controller. The steering wheel torque and load pressure are functions of the total torque. The specified characteristic gives the load pressure reference and the torque to be generated on the steering wheel.

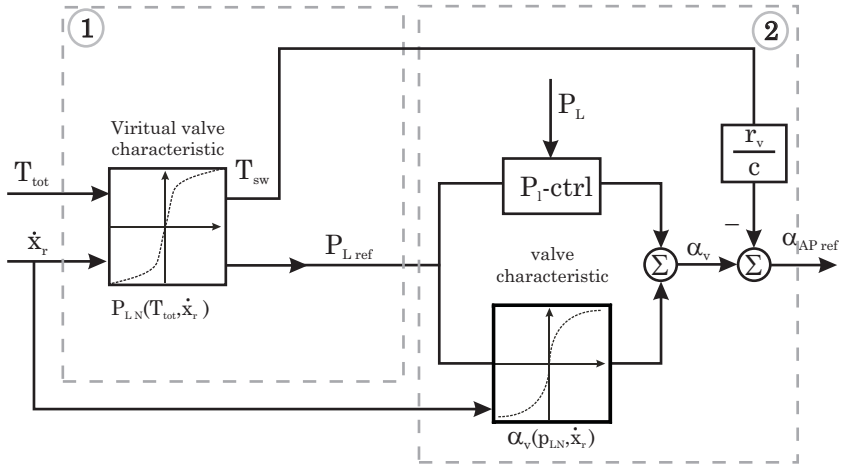

Figure 5.30 *Virtual boost curve controller uses the second part from the offset torque controller to calculate the actuation of the active pinion.*

Results from measurements of offset torque control

In order to reduce the influence of static friction in the load cylinder, small steering inputs are applied to the steering wheel with a much higher frequency than the commanded offset torque request, compare to dithering in a servo valve application. By filtering the generated steering wheel torque, it is possible to establish the results that represent a mean value of the torque applied to the steering wheel. Figure 5.31 shows the results of such a test; in Figure 5.32, the results are filtered, which creates a mean value of the steering wheel torque. Figure 5.33 shows the displacement of the pilot motor, which is translated to the actuation angle of the valve via the excenter and the inclined grow. The figure shows both unfiltered and filtered measurements. The disturbance is partly due to imperfection in the mapping, but mostly due to the backlash between the inclined grow and the pin mounted on the pinion. In Figures 5.34 and 5.35, two other cases are displayed. The measurements show that the concept and controller are working. However, the prototype can be improved especially regarding the backlash problem in the inclined grow.

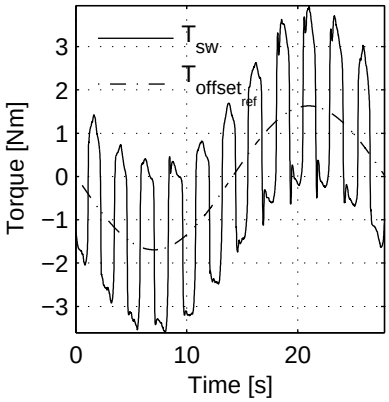

Figure 5.31 *Results from the offset torque control. Small steering inputs are applied to reduce the influence of static friction.*

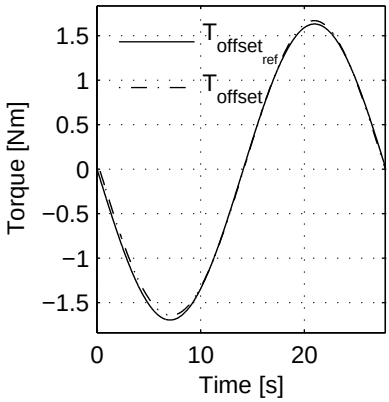

Figure 5.32 *Filtered results from the offset torque control, showing the mean value of the applied steering wheel torque.*

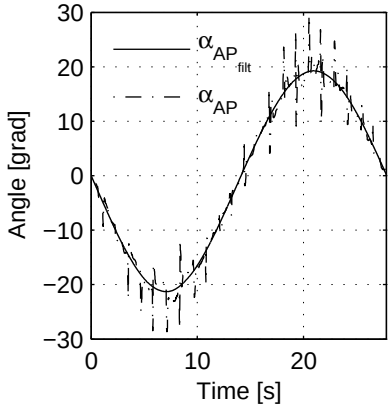

Figure 5.33 *Measurement of the actuation angle of the active pinion. Note that the measurement is on the pilot motor and not on the actual valve displacement.*

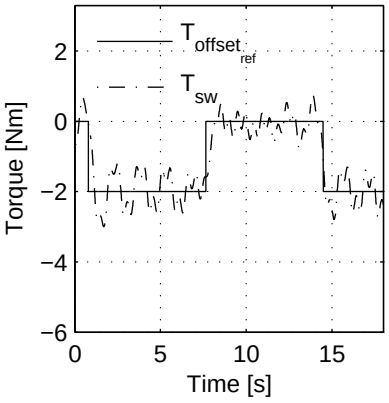

Figure 5.34 *Results from the offset torque control. Small steering inputs are applied to reduce the influence of static friction.*

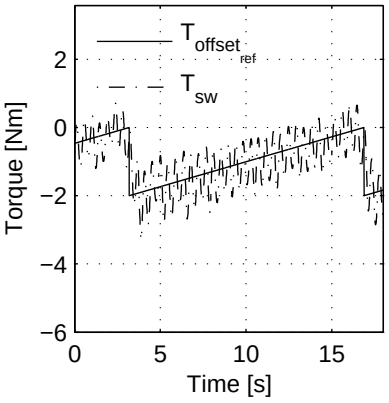

Figure 5.35 *Filtered results from the offset torque control, showing the mean value of the applied steering wheel torque.*

5.4.3 Sensor requirements and function mapping

The active pinion requires different sensors to enable functions. Requirements differ between functions. The need for sensors has been mentioned briefly in the section about controller design above and in the discussion regarding fail safe. The different sensors that can be utilized in the concept are listed below.

- Pilot motor position sensor
- Steering wheel sensor
- Pressure sensor
  - Load pressure
  - Pump pressure
- Torque sensor

The *pilot motor position sensor* is a necessary sensor and has to be utilized independent of implemented functions to keep track of the pilot motor, which is a closed loop system in itself. Also, it is to be used during calibration together with the pump pressure sensor or the load pressure sensor. The *pump pressure sensor* is not used in the active control of the active pinion, but is useful for calibration and fault detection. The steering wheel sensor is used in position control, and is normally installed in the vehicle, which means that it can be utilized by the active pinion. The requirements on the position sensor depend on the positioning requirements of the parking pilot system.

There are three different ways to establish the total torque of the offset torque control:

1. Load pressure sensor and pilot motor sensor
2. Load pressure sensor and steering wheel torque sensor
3. Steering wheel torque sensor and pilot motor sensor

All of these can be used in the active control of the active pinion and to establish the total torque. However, the *load pressure sensor* is not preferred when a wide range in pressure has to be covered if the offset torque is to be utilized in the entire working envelope. This is due to the exponential behavior of the pressure characteristic, which will lead to low resolution in the low torque region. On the other hand, the offset actuation of the offset torque is linear to the actuation angle in the upper region of the total torque, see Figure 5.29. Based on the figure, the pressure sensor would only need high resolution in the lower region between 0-25 Nm, which relates to a load pressure of 0-3.5 MPa. This could be even lower if the resolution of the offset torque could be compromised at higher offset torque commands. The *steering wheel torque sensor* is more suitable as it will give equal resolution in the working envelope. In Table 5.1, some of the implementation stages are listed with descriptions and related control methods. In the table, the sensor requirements are also listed.

Implementation stage	Customer function	Customer function description	Control variable	Required sensor for active pinion control		
				Steering wheel angle sensor	Load pressure sensor	Steering column torque sensor
1	Parking Pilot	Comfort function that conducts semi-automatic rearward parallel parking manoeuvres. Steering control is done by the function.	Steering wheel angle	√		
2	Lane Keeping Assist	Comfort function that eases lane position control during highway driving by superimposing an offset torque that guides the driver into an appropriate lane position.	Offset Steering column torque	√	√	
3	Emergency Lane Assist	Active safety function that superimposes a guiding torque during collision situations with oncoming traffic, where the subject vehicle is changing lanes unintentionally.	Offset Steering column torque	√	√	
4	Active yaw Control with torque feedback	Active safety function that superimposes a guiding torque during large body sideslip angle conditions in order to guide the driver into a stable state of driving.	Offset Steering column torque	√	√	
5	Torque Reference control	Comfort function that filters out any unwanted torque disturbance in the steering column within the actuator bandwidth.	Steering column torque control	√	√	√

Table 5.1 *Implementation stages for the active pinion concept.*

6

Discussion and Conclusion

Even though hydraulic power steering systems have been a proven technology for decades, there are still problems to be solved, most concerning quality issues. In this thesis, two predominant problems have been studied, hydraulic lag and the chattering phenomena.

As stated in the paper [2] and briefly in this thesis, chapter 4.2.2, hydraulic lag, also mentioned as dynamic catch-up, is a result of under-dimensioned pump flow and, therefore, a sizing issue. The main problem with the sizing of the system is the introduction of the ECA, which expands during pressurization, thereby reducing the effective flow entering the valve. In order to solve the sizing problem, the expansion characteristic of the ECA has to be known when sizing the system. This is not always possible as the ECA is usually introduced and tuned late in the design process to minimize sound emission from the system.

In order to obtain an optimal solution to the problem, there has to be an iterative process involving most of the components in the system. However, this is not a realistic solution unless a dynamic model of the sound characteristic of the complete system including installation is available. The most feasible solution to minimize the problem with hydraulic lag is to specify ECA requirements regarding the expansion ratio during the design process, which can be used in dynamic simulation, thereby defining the sizing of the ingoing components.

The second problem is the chattering phenomena, which like the hydraulic lag is a dynamic problem. The chattering phenomena is on the other hand also a control problem related to the internal closed loop. In paper [I] and in this thesis, chapter 4.1, the problem is described in detailed, where it is shown with the help of linear models and how tolerances affect the stability margin of the system. The problem occurs when the desired static characteristic is in conflict with the stability margin of the system. In order to avoid the problem,

the desired characteristic should be dynamically evaluated and the variation in valve tolerances taken into account. If the outcome of the evaluation is negative the solution could either result in change in the characteristic or demands on tighter tolerances.

The cases mentioned above are both related to an existing platform or vehicle model, which has eased the modeling of the external forces and inertia loads. In the preliminary design of the power steering system, these load forces are essential for the sizing and evaluation of stability but might not be available as measurements. In order to perform a preliminary design of the power steering unit, a simulation model of the vehicle generating the external forces is needed. In paper [III], a vehicle model is used together with a dynamic power steering model to generate accurate tie-rod forces acting on the steering rack. These could work as a substitute for real life measurements in the preliminary design and sizing of a power steering unit. In this paper, the friction in the steering rack was also evaluated; it was shown that the friction force in the steering rack is strongly dependent on the system pressure, which has to be included in the model.

The active pinion has played an important part in this project and is a modular way to enhance the functionality of the traditional hydraulic power steering units. The basic dimensioning and layout of the system would not only work for a standard power steering system but also for the active pinion solution. In paper [VI], the requirements regarding the active pinion concept are evaluated. It was found that the basic system layout of a traditional HPAS unit will also fit the requirements set by the automatic parking system. Even the layout of the valve can be the same; however, this may not be the optimal solution considering the increased flexibility given by the active concept, which could for example be used for increasing the assistance at lower speeds.

Using the active pinion for offset torque control has been one of the key features of the active pinion concept and was the first function that was proven in both simulation, [IV], and hardware tests, [V]. The reason to implement offset torque is to enable the possibility to haptically communicate with the driver, thereby guiding, warning and assisting the driver in different driving situation. The function using the offset torque could either be for comfort or for active safety. The controller of the offset torque uses knowledge of the valve characteristic as a feed-forward link in the pressure controller and a weak closed loop controller to compensate for mismatch in the mapping of the valve characteristic. The offset torque controller needs to know the load pressure in the cylinder, but only in the lower pressure region when it compensates for non-linearity. In the upper pressure region, the load pressure is dominant over the applied torque and a more or less open loop controller can be used for the offset torque control.

Apart from the offset torque control, a positioning controller has been applied. This is to meet the demand for autonomous steering functions such as an automatic parking system. Due to the fact that the valve is non-linear in its characteristic, a gain scheduling controller is needed. The model presented in

the thesis, Chapter 4.1, and paper [I], has been used to design the controller. Positioning control has proven effective in the test rig and is presented both in this thesis, Chapter 5.4.1 and in papers [5] and [6].

The Active Pinion concept opens up new possibilities to include more functionality in traditional power steering system without any major changes in the overall system layout. The enhanced functionality could be used for new active safety features, as well as comfort functions to support and ease the driver during different driving scenarios. The Active Pinion concept uses the built-in power of the HPAS system without installing additional high torque motors. The pilot motor can be small when it only has to overcome the friction within the valve. The technology of the Active Pinion concept could be seen as an add-on to a present HPAS system and be used in cars as well as heavy trucks.

7
Outlook

The prototype used in this project is a modified valve from a traditional Hydraulic Power Assisted Steering, HPAS, system; this was to speed up the process and make it possible to perform the necessary modifications in-house. By doing this, it has been possible to show that the Active Pinion can be used as a modular add-on to a traditional HPAS unit. However, the drawback is that the hardware design of the prototype is not the optimal solution, but the best solution at this time. In order to mechanically improve the concept, the actuation of the valve should avoid axial movement, which would significantly reduce the friction problem and enable the possibility for a small pilot motor. Another way of reducing the friction problem is to change the design of the seals and adapt them to the axial motion. Play is also an issue related to the usage of a valve from a traditional valve unit.

In the thesis two different control methods, positioning control and offset control, were designed and evaluated; a third method mentioned was the Free Torque Control, FTC. The FTC concept has not been evaluated, thereby making it a natural next step in future work. In order to do so, a control strategy has to be designed and tested.

In this thesis,the testing of the concept has been performed in the power steering test rig, which means that no real vehicle testing has been performed. To complete the evaluation of the concept, vehicle testing should be one of the next steps. The last prototype designed was prepared for vehicle tests and is equipped with a flexible installation of the pilot motor in order to adapt to different packing scenarios. The housing of the valve is also prepared for pressure sensors, A-port, B-port and P-port, which makes it possible to use the original rack and lines and still have the necessary sensors. The torque sensor is still mounted on the torsion bar of the valve.

Even though the vehicles mentioned in this thesis are cars, the largest breakthrough in technology has been in truck. Today, trucks use HPAS systems; however, most do not use the rack and pinion solution, but rather integral

power assisted steering gear systems. However, these systems use the same type of valve unit and actuation as the HPAS system described in this thesis. Prototype steering gear for trucks on the market that aim towards the same functionality as the ACTIVE PINION concept use add-on electric torque motors with a size comparable to an EPAS system for cars on top of the integral power assisted steering gear. With the ACTIVE PINION concept, the power available in the hydraulic system can be used.

8

Review of papers

The papers included in this thesis cover both hydraulic power steering systems in general and the novel approach to enhance the functionality of the power steering systems. The order of the papers is not chronological, but rather organized by their contents. The first three papers, [I–III], concern power steering system problems and simulation. The last three papers, [IV–VI], concern the active pinion concept and different methods of control.

Paper I

Robust Design of a Power Steering System with Emphasis on Chattering Phenomena

In the first paper, a linear model is used to explain and investigate the chattering effect occurring in power steering systems. Chattering is experienced as noise and vibration in the steering system occurs and when the steering system is activated by the driver or when the system is driven by the load, aligning torque. Chattering is a problem, which is a result of bad system layout with regards of system stability. The problem can reduce the performance of the system but is mainly a quality problem from the users point-of-view. In this paper, the phenomena is investigated with the help of a linear model of the system, where the stability margin for different characteristic of the system is analyzed.

Paper II

Modeling and Simulation of a Conventional Hydraulic Power Steering System for Passenger Cars

The second paper investigates the catch-up effect that occurs in power steering systems. Catch-up effect is when the hydraulic assistance fades away and the driver and has to rely on manual torque applied to the steering wheel to perform steering maneuvers; thus significantly less assistance is provided. This can lead to disaster if it occurs in a critical situation for the driver. The catch-up effect can be divided into two types, one static and one dynamic. Both are a result of insufficient flow delivered to the valve; however, the dynamic effect is due to volumetric expansion in the supply line. In this paper, both simulation and measurements of dynamic catch-up are presented. The simulation model is used to further study the compressibility effect in the supply line, which includes an Expansion Chamber Attenuator, ECA.

Paper III

Modeling and Simulation of a Conventional Hydraulic Power Steering System for Passenger Cars

In the third paper, a non-linear model of a hydraulic power steering system is presented. The model is described in detail regarding modeling of the included components. This model is validated in two steps, one regarding the static characteristics, boost curve, and the other based on driving scenario measurements. Also included in this paper is a vehicle model; this model is validated with the help of measurements based on a driving scenario. The purpose of this model is to calculate in co-simulation with the HPAS model, the loads acting on the steering rack during driving, which is a great advantage when the HPAS system simulation is to be executed with realistic loads.

Paper IV

Active Pinion - A Cost Effective Solution for Enabling Steering Intervention in Road Vehicles

The fourth paper introduces the active pinion concept, which is a modification of a traditional hydraulic power steering system to achieve increased functionality. The enhancement in functionality consists of the possibility to add or retract offset torque to the steering wheel to make it possible to intervene in the driver's actions. The reason for intervening is to assist the driver in his/her effort in keeping the car in the correct lane, also used in the Lane Keeping Assist, LKA, system. This system is a new type of active safety feature, which

could be introduced in future cars. The basic idea behind the LKA system is introduced, as well as the mechanical concept regarding the active pinion. A control structure is also introduced and tested in a simulated environment.

Paper V

Increased Hydraulic Power Assisted Steering Functionality Using the Active Pinion Concept

Paper number five presents the control strategies for position control and offset torque control of the active pinion concept included are test results carried out in the hardware in the loop test rig. The main focus in this paper is the positioning control for the automatic parking system where test results from the offset torque control are also displayed.

Paper VI

Parking System Demands on the Steering Actuator

In the last paper, requirements on the actuator from the parking system and how the actuator's performance translates into parking maneuver performance are studied. The parking system has been installed in a test rig and in a demonstrator car. The performance on the active pinion system is analyzed and related to the requirements from the parking system especially when it comes to rate limitation. The active pinion can be seen as a modular add onto a traditional power steering unit already dimensioned to meet the overall requirements for the vehicle. The basic system layout will set the performance limit of the active pinion system. In the paper, the active pinion concept performance is evaluated in order to see if the modular approach is valid without any further changes in overall system dimensioning.

References

[1] Bleckmann H., Fennel H., Gräber J. and Seibert W., "Traction control system with teves abs mark ii," in *SAE International Congress and Exposition*, no. 860506, Februari 1986.

[2] Wilfert K., "Entwicklungsmöglichkeiten im automobilbau," *ATZ Automobiltechnische Zeitschrift*, **75**:273–278, 1973.

[3] Donges E., "Conceptual framework for active safety in road traffic," *Vehicle System Dynamics*, **32**(2):113 – 128, 1999. Adaptive cruise control (ACC);.

[4] Tingvall C., Krafft M., Kullgren A. and Lie A., "The effectiveness of esp (electronic stability programme) in reducing real life accidents," in *The 18th International Technical Conference on the Enhanced Safety of Vehicles (ESV)*, no. 261–O, Nagoya, Japan, May 2003.

[5] van Zanten A., "Bosch esp systems: 5 years of experience," in *SAE Automotive Dynamics and Stability Conference*, no. 2000–01–1633, Troy, Michigan, USA, May 2000.

[6] Sferco R., Page Y., Coz J.Y.L. and Fay P.A., "Potential effectiveness of electronic stability programs (esp) - what european field studies tell us," in *17th ESV Conference*, no. 2001-S2-O-327, Amsterdam, Netherlands, 2001.

[7] *Federal Motor Vehicle Safety Standard (FMVSS) No. 126, Electronic Stability Control Systems*, Preliminary regulatory impact analysis, Office of Regulatory Analysis and Evaluation, National Center for Statistics and Analysis, National Highway Traffic Safety Administration NHTSA, U.S. Department Of Transportation, August 2006.

[8] Kreiss J.P., Schüler L. and Langwieder K., "The effectiveness of primary safety features in passenger cars in germany," in *19th International Technical Conference on the Enhanced Safety of Vehicles*, no. 05-0145-O, NHTSA, Washington DC, USA, June 2005.

[9] Uhler W., Scherl M. and Lichtenberg B., "Driving course prediction using distance sensor data," in *SAE International Congress and Exposition*, no. 1999–01–1234, Detroit, Michigan, USA, March 1999.

[10] Koehn P., "Active steering - the bmw approach towards modern steering technology," in *World Congress & Exhibition*, no. 2004–01–1105, SAE, Detroit, Mi, USA, March 2004.

[11] köhn P., Pauly A., R.Fleck, M.Pischinger and Richter T., *Die Aktivlenkung das fahrdynamische lenksysteme des neuen 5er*, chap. Aktivlenkung, ATZ/MTZ Extra: Der neue BMW 5er, August 2003. In German.

[12] Ackermann J. and Buente T., "Yaw disturbance attenuation by robust decoupling of car steering," *Control Engineering Practice*, **5**(8):1131 – 1136, 1997.

[13] Ackermann J., "Active steering for better safety, handling and comfort," in *Proceedings of Advances in Vehicle Control and Safety*, pp. 1–10, Amiens, France, July 1-3 1998.

[14] Ackermann J., Brünte T. and Odenthal O., "Advantages of acrive steering for vehicle dynamics control," in *32nd International Symposium of Automotive Technology and Automation*, no. 99ME013, pp. 263–270, Vienna, Italy, 1999.

[15] Franke U., Mehring S., Suissa A. and Hahn S., "The daimler-benz steering assistant- a spin-off from autonomous driving," in *Intelligent Vehicles '94 Symposium*, pp. 120–124, Paris, France, October 1994.

[16] Pohl J. and Ekmark J., "Development of a haptic intervention system for unintended lane departure," in *SAE World Congress & Exhibition*, Detroit, MI, USA,, March 2003.

[17] Dominke P. and Ruck G., "Electric power steering - the first step on the way to 'steer by wire' ," in *SAE International Congress and Exposition*, no. 1999–01–0401, SAE, Detriot, MI, USA, March 1999.

[18] Breitfeld C., Foag W., Guldner J., Müller S., Schmidt W. and Vielwerth G., "Actuator principles for integrated chassis control system - a comarison," in *3rd International Fluid Power Conference*, vol. 1, pp. 399–418, Aachen, Germany, March 2002, ISBN 3–8265–9900–4. 42V.

[19] Davis F.W., "Hydraulic steering mechanism," in *US Patent US1790620*, United States Patent Office, Waltham, Massachusetts, USA, 27 January 1931.

[20] Davis F.W., "Auxiliary power steering gear," in *US Patent US1874248*, United States Patent Office, Waltham, Massachusetts, USA, 30 August 1932.

[21] Ulrich H., Böcker M. and Kett R., "Simulationen zur optimierung von servolenksystemen," in *1. Internationales Fluidtechnishes Kolloquium in Aachen, 1 IFK*, pp. 411–432, 1998.

[22] Segel L., "On the lateral stability and control of the automobile as influenced by thedynamics of the steering system," in *Journal of Engineering for Industry*, pp. 283–95, August 1966.

[23] Jaksch F.O., "Driver-vehicle interaction with respect to steering controllability." in *SAE Preprints*, no. 790740, p. 40, 1979.

[24] Adams F.J., "Power steering 'road feel'." in *SAE Technical Paper Series*, no. 830998, Dearborn, MI, USA, 1983.

[25] Norman K.D., "Object evaluation of on-centre handling preformance," in *SAE International Congress and Exhibition*, no. 840069, Detroit, Michigan, USA, February 27-March 2 1984.

[26] Liu A. and Chang S., "Force feedback in a stationary driving simulator," *Proceedings of the IEEE International Conference on Systems, Man and Cybernetics*, **2**:1711 – 1716, 1995.

[27] Backhaus R., "Die servolectric von zf," *ATZ Automobiltechnische Zeitschrift*, **100**(9):636 –, 1998.

[28] Heisler H., *Advanced vehicle technology*, Butterworth-Heinemann, 2nd edn., 2002, ISBN 0-7506-5131-8.

[29] Merritt H.E., *Hydraulic Control Systems*, no. ISBN 0–471–59617–5, John Wiley & Sons, New York, 1967.

[30] Nishimura S. and Matsunaga T., "Analysis of response lag in hydraulic power steering system," in *JSAE Review*, vol. 21 Issiue 1, pp. 41–46, January 2000.

[31] Chang S., Byeong J. and Je D., "Development of electronic-controlled power steering system," in *SAE International Congress & Exposition*, no. 981117, Detroit, MI, USA, February 1998.

[32] Baxter J. and Dyer G.P., "Bishop variatronic power steering system," in *International Congress and Exposition*, no. 880708, SAE, Detroit, Michigan, USA, March 1988.

[33] Herkommer R., "Ways toward energy saving in hydraulic steering system," in *3rd International Fluid Power Conference, IFK02*, vol. 1, pp. 465–474, Aachen, Germany, March 2002, ISBN 3–8265–9900–4.

[34] Tokumoto Y., "Development of energy-saving pump for hydraulic power steering," in *JSAE Review 18*, no. JSAE–9733729, pp. 310–313, 1997.

[35] Bootz A., Zarth R., Kolbeck K. and Beck S., "Evolutionary energy saving concepts for hydraulic power steering systems," in *5th International Fluid Power Conference ů Aachen*, 2006.

[36] Lauth H.J., Webert D., Agner I. and Brunsch B., "Reduced power consumption in power steering, active chassis, transmission system and engine oil pumps," in *The 8th Scandinavian International Conference on Fluid Power, SICFP03*, Tampere, Finland, May 2003.

[37] Suzuki K., Inaguma Y., Haga K. and Nakayama T., "Integrated electro-hydraulic power steering system with low electric energy consumption," in *SAE International Congress and Exposition*, no. 950580, Detroit, Michigan, USA, February 27–March 2 1995.

[38] Inaguma Y., Suzuki K. and Haga K., "An energy saving techique in an electro-hydraulic power steering ehps system," in *SAE International Congress and Exposition*, no. 960934, 1996.

[39] Bootz A., *Konzept eines Energiesparenden Elektrohydraulischen Closed-Center-Lenksystems Für Pkw mit hoher lenkleistung*, Ph.D. thesis, Technischen Universität Darmstadt, Darmstadt Germany, 2004.

[40] Bootz A., Brander M. and Stoffel B., "efficiency analysis of hydraulic power steering system," in *The Eighth Scandinavian International Conference on Fluid Power, SICFP'03*, Tampere, Finland, May 2003.

[41] Pollmeier K. and Poppe F., "Steering valve arrangement for a power steering mechanism," in *Patent:EP1528999*, patent applicant: Toyota Motorsport gmbh, 11 May 2005.

[42] Birsching J.E., "Two dimentional modeling of a rotary power steering valve," in *SAE International Congress and Exposition*, no. 1999–01–0396, 1–4 March 1999.

[43] Box M., "A new method of constraint optimization and a comparison with other methods," *Computer Journal*, **8**:42–52, 1965.

[44] Andersson J., *Multiobjective Optimization in Engineering Design - Applications to Fluid Power Systems*, Ph.D. thesis, Linköping University, 2001.

[45] Mavris D.N. and DeLaurentis D.A., "A probabilistic approach for examining aircraft concept feasibility and viability," *Aircraft Design*, **3**(2):79 – 101, 2000.

[46] Hultén J., *Drum break squeal*, Ph.D. thesis, Chalmers University of Technology, November 1998.

[47] HOPSAN, hopsan*, a Simulation Package, User's Guide*, Tech. Rep. LiTH–IKP–R–704, Divistion of Fluid and Mechanical Engineering System, Department of Mechanical Engineering, Linköping University, Linköping, Sweden, 1998.

[48] Neureder U., "Modellierung und simulation des lenkstranges fur die untersuchung der lenkungsunruhe," *ATZ Automobiltechnische Zeitschrift*, **103**(3):216 –, 2001.

[49] Neureder U., "Investigation into steering wheel nibble," *Proceedings of the Institution of Mechanical Engineers, Part D: Journal of Automobile Engineering*, **216**(4):267 – 277, 2002.

[50] Larsson J., *Interoperability in Modeling and Simulation*, Ph.D. thesis, Linköping University, 2003.

[51] Jang B. and Karnopp D., "Simulation of vehicle and power steering dynamics using tire model parameters matched to whole vehicle experimental results," *Vehicle System Dynamics*, **33**(2):121 – 133, 2000.

[52] Cheli F., Sabbioni E., Leo E. and Zuin A., "a semi-physical model of a hydraulic power steering system for vehicle dynamics sysmulations," in *8th Biennial ASME Conference on Engineering Systems Design and Analysis, ESDA2006*, no. ESDA2006-95591, Torino, italy, July 2006.

[53] Switkes J.P., Rossetter E.J., Coe I.A. and Gerdes J.C., "Handwheel force feedback for lanekeeping assistance: Combined dynamics and stability," in *2004 International Symposium on Advanced Vehicle Control*, 2004.

[54] Switkes J.P., Coe I.A. and Gerdes J.C., "Using mems accelerometers to improve automobile handwheel state estimation for force feedback," *American Society of Mechanical Engineers, Dynamic Systems and Control Division (Publication) DSC*, **73**(2 PART B):1271 – 1278, 2004.

[55] von Groll M., Mueller S., Meister T. and Tracht R., "Disturbance compensation with a torque controllable steering system," *Vehicle System Dynamics*, **44**(4):327–338, April 2006 2006.

[56] Pilutti T. and Ulsoy G., "On-line identification of driver state for lanekeeping," in *1995 American Control Conference*, vol. 1, pp. 678–681, Seattle, WA, USA, June 1995.

[57] Tan H.S., Rajamani R. and Zhang W.B., "Demonstration of an automated highway platoon system," in *1998 American Control Conference*, vol. 3, pp. 1823–1827, 1998.

[58] Naranjo J.E., Gonzalez C., Garcia R., De Pedro T. and Haber R.E., "Power-steering control architecture for automatic driving," *IEEE Transactions on Intelligent Transportation Systems*, **6**(4):406 – 415, 2005.

[59] Bauer H., *Driving-Safety Systems*, Robert Bosch GmbH, Stuttgart, Germany, 2nd edn., 1999, ISBN 0–7680–0511–6.

[60] Furui N., Miyakoshi H., Noda M. and Miyauchi K., "Development of a scanning laser radar for acc," in *SAE International Congress and Exposition*, no. 980615, Detroit, Michigan, USA, February 1998.

[61] Eidehall A., Pohl J. and Gustafsson F., "Combined road prediction and target tracking in collision avoidance," in *IEEE Intelligent Vehicles Symposium*, pp. 619–624, 2004.

[62] Eidehall A., *Tracking and threat assessment for automotive collision avoidance*, Linköping studies in science and technology. dissertations. no. 1066, Linköpings universitet, Linköping, Sweden, Dec 2006.

[63] Ryding E. and Öhlund E., *Lane Keeping Aid – A Driver Support System for Cars*, Master's thesis ISRN:LITH-ISY-EX-3207-2002, ISY, Linköping University, Linköping University, Sweden, April 2002. Swedish.

[64] Pohl J., Sethson M., Degerman P. and Larsson J., "A semi-automated parallel parking system for passenger cars," *Proceedings of the Institution of Mechanical Engineers, Part D: Journal of Automobile Engineering*, **220**:53 – 65, 2006. In press.

[65] Dick W. and Holle M., *Entwicklung einer Überlagerungslenkung*, vol. 105, chap. Lenksysteme, ATZ, May 2003. In German.

[66] Rieger W., *Aktivlenkung für aktive Sicherheit*, chap. Lenkung, ATZ/MTZ Extra: System Partners, May 2003. In German.

[67] Krus P. and Gunnarsson S., "Adaptive control of a hydraulic crane using on-line identification." in *the Third Scandinavian International Conference on Fluid Power*, Linköping, Sweden, 1993.

[68] Webpage, Jan 2007. *http* : $//flumes.ikp.liu.se/staff/marro/$.